Ohio University



# CGER

Center for Geotechnical and Environmental Research

# TRAFFIC NOISE BARRIER
# OVERLAP GAP DESIGN

FINAL REPORT

By

Lloyd A. Herman
Assistant Professor, Civil Engineering
Ohio University

Craig M. Clum
Research Assistant, Civil Engineering
Ohio University



OHIO RESEARCH INSTITUTE
FOR
TRANSPORTATION AND THE ENVIRONMENT

OHIO DEPARTMENT OF TRANSPORTATION
FEDERAL HIGHWAY ADMINISTRATION



January 1998

| 1. Report No. | 2. Government Accession No. | 3. Recipient's Catalog No. |
|---|---|---|
| FHWA/OH-98/007 | | |

| 4. Title and Subtitle | 5. Report Date |
|---|---|
| TRAFFIC NOISE BARRIER OVERLAP GAP DESIGN | January, 1998 |
| | 6. Performing Organization Code |
| 7. Author(s) | 8. Performing Organization Report No. |
| Lloyd A. Herman, Craig M. Clum | 10. Work Unit No. (TRAIS) |
| 9. Performing Organization Name and Address | 11. Contract or Grant No. |
| Ohio University<br>Department of Civil Engineering<br>Athens, OH 45701-2979 | State Job No. 14665(0) |
| | 13. Type of Report and Period Covered |
| | Final Report |
| 12. Sponsoring Agency Name and Address | 14. Sponsoring Agency Code |
| Ohio Department of Transportation<br>25 S. Front St.<br>Columbus, OH 43215 | |

15. Supplementary Notes

Prepared in cooperation with the U.S. Department of Transportation, Federal Highway Administration

16. Abstract

Sound propagation through the gap produced by two parallel vertical barriers with overlapped ends was formulated for traffic noise sources. The method accounts for sound propagated from vehicle source positions for a maximum of ten roadway lanes. Six receiver regions were considered based on potential receiver locations with respect to a gap. The analysis identified both source and receiver regions according to the mechanisms which influence noise propagation in the vicinity of an overlap gap which can result in: direct rays, diffracted rays from the top edge of one barrier, diffracted rays from the top edge of both barriers, rays reflected between the barriers and rays that are both reflected and diffracted.

The derived method was implemented in the computer simulation model Gap Analysis Program (GAP). Field measurements for up to 30 receiver positions from four overlap gaps were compared with the uncalibrated predictions made using GAP. The equivalent continuous levels, A-weighted, were overpredicted by 2-3 dB. When the analysis was based on an octave band characterization of the source, the mean overprediction was reduced to less than 1 dB.

GAP is intended to aid the noise barrier designer by modeling the effect of varying the overlap gap geometry or the incorporation of sound absorbing materials to user selected portions of the barrier surfaces that form the overlap gap.

| 17. Key Words | 18. Distribution Statement |
|---|---|
| Traffic noise barrier; barrier overlap gaps | No Restrictions. This document is available to the public through the National Technical Information Service, Springfield, Virginia 22161 |

| 19. Security Classif. (of this report) | 20. Security Classif. (of this page) | 21. No. of Pages | 22. Price |
|---|---|---|---|
| Unclassified | Unclassified | | |

## ACKNOWLEDGMENTS

The authors would like to thank the many students who were involved in the project. Todd Eilerman assisted with site selection process in the initial phase of the project. John Betzing, Srikanth Seshadri, and Roger Earwood were members of the field measurement team. Matt Ambroziak and Mark Johnston spent many hours analyzing video to provide traffic data to correlate with the field measurements.

The authors acknowledge the efforts of Fred Calef of the Institute for Local Government Administration and Rural Development for developing locator maps for the Cincinnati sites. Dinesh Dhamija from the Department of Industrial Technology provided support in answering technical questions about programming in Visual Basic. The advice of Grant Anderson of Harris Miller Miller and Hanson, Inc. was helpful in developing the theory for the segmentation of roadways.

## TABLE OF CONTENTS

## LIST OF FIGURES

## LIST OF TABLES

Table Page

## NOTATIONS

A-weighting network: An electronic filter in a sound level meter which approximates under defined conditions the frequency response of the human ear. The A-weighting network is most commonly used.

Absorption coefficient: Ratio of sound absorbing effectiveness, at a specific frequency. The ratio is an indication of the amount of acoustic energy absorbed by a material relative to the amount of acoustic energy incident on the material.

Decibels (dB): A unit of logarithmic measure based on ratios of power-related quantities, thereby compressing a wide range of amplitude values into a small set of numbers.

Diffraction: The deflection of a sound wave caused by an obstruction or by nonhomogeneity in a medium or between media.

Direct propagation: The transmission of sound waves from source to receiver with no obstructions located in the path.

Double diffraction: The deflection of a sound wave caused by two obstructions (e.g. noise barriers) located in the path between source and receiver.

Far barrier: The noise barrier in an overlap barrier configuration which is located farthest from the residential community or closest to the highway.

Frequency: The number of cyclical variations (periods) unit of time. Expressed in cycles per second (cps) also denoted as Hertz (Hz).

Hertz (Hz): The unit of frequency measurement, representing cycles per second.

$L_{Aeq}$ : Equivalent continuous sound pressure level. The steady A-weighted sound level which would produce the same A-weighted sound energy over a stated period of time as a specified time-varying sound. $L_{Aeq}(h)$ is the $L_{Aeq}$ for a one hour period.

Multiple reflected rays (MRR): Sound waves which propagate directly to a receiver after reflecting off of the overlap barriers.

Multiple reflected diffracted rays (MRDR): Sound waves which propagate to a receiver by diffracting over the top of the near barrier after reflecting off of the overlap barriers.

Near barrier: The noise barrier in an overlap barrier configuration which is located nearest to the residential community or protected area.

Octave: Two frequencies are an octave apart if the ratio of the higher frequency to the lower frequency is two.

Octave (frequency) bands: Frequency ranges in which the upper limit of each band is twice the lower limit.

Propagation: The transmission of acoustic energy through air from a noise source to a receiver.

REMEL: Reference Energy Mean Emission Level. The statistical mean of acoustic energy emitted by a vehicle class as measured at a reference distance perpendicular to the centerline of the vehicle path.

Receiver: One or more observation points at which sound is measured or evaluated. The effect of sound on an individual receiver is usually evaluated by measurements near the ear or close to the body.

Simple diffraction: The deflection of a sound wave caused by a single obstruction (e.g. noise barrier) located in the path between source and receiver.

Sound pressure level: The ratio, expressed in decibels, of mean-square sound pressure to a reference mean-square pressure which by convention has been selected to be equal to the assumed threshold of hearing.

Source: An object (ex. traffic) which radiates sound energy.

Spectral, spectrum: Description, for a function of time, of the resolution of a signal into components, each of different frequency and usually different amplitude and phase.

Wavelength: For a periodic wave in an isotropic medium, the perpendicular distance between two wave-fronts in which the displacements have a difference in phase of one complete period.

NOTE : Unless indicated otherwise, all sound pressure levels referenced in this report are the equivalent continuous A-frequency weighted sound pressure levels.

# 1. INTRODUCTION

Noise barriers are constructed between a noise source and the receiver of the noise to reduce noise levels at the receiver. The direct path of the noise from the source to the receiver can be effectively blocked by choosing a barrier material with sufficient density. To reach the receiver, noise from the source must follow a bent or diffracted path over the top of the barrier, which reduces the intensity of the noise.

Noise barrier effectiveness can be compromised by discontinuities in the noise barrier. Therefore, traffic noise barrier designers try to avoid openings in noise barriers. However, site conditions may require the presence of discontinuities or gaps in the noise barriers. Noise barriers that are constructed on fill sections along roadways are typically placed at the top of the slope near the roadway shoulder. On the other hand, noise barriers constructed in cut sections are typically placed at the top of the cut. The transition between fill and cut sections is accomplished by changing the horizontal alignment of the barrier. To provide drainage in the transition zones, gaps are often provided where the horizontal alignment is changed. Further, there are times when transportation agencies wish to provide access to right-of-way areas that are located on the residential side of noise barriers. Other changes in the horizontal or vertical alignment of roadways may also necessitate gaps in noise barriers. Gaps created by overlapped barrier sections are not only found in Ohio, but throughout the nation and in other countries.

In order to reduce the negative effect of gaps on noise barrier performance, designers typically overlap barriers at gap areas. This blocks line-of-sight propagation for most propagation paths. The amount of overlap is often selected to reduce the levels of noise flanking around the

ends of the barriers to the point that the noise diffracting over the top of the barrier becomes the dominant noise at the receiver. This strategy has led to rule-of-thumb guidelines such as a 2:1 ratio of overlap length to overlap width. The distance that the barriers extend past each other is known as the overlap length. The overlap width is the perpendicular distance between the two barriers.

The convention that will be adopted is to designate the barrier closest to the roadway as the far barrier. Similarly, the noise barrier located nearest the residential or protected area is termed the near barrier. Figure 1 illustrates the main components of a typical noise barrier overlap gap.

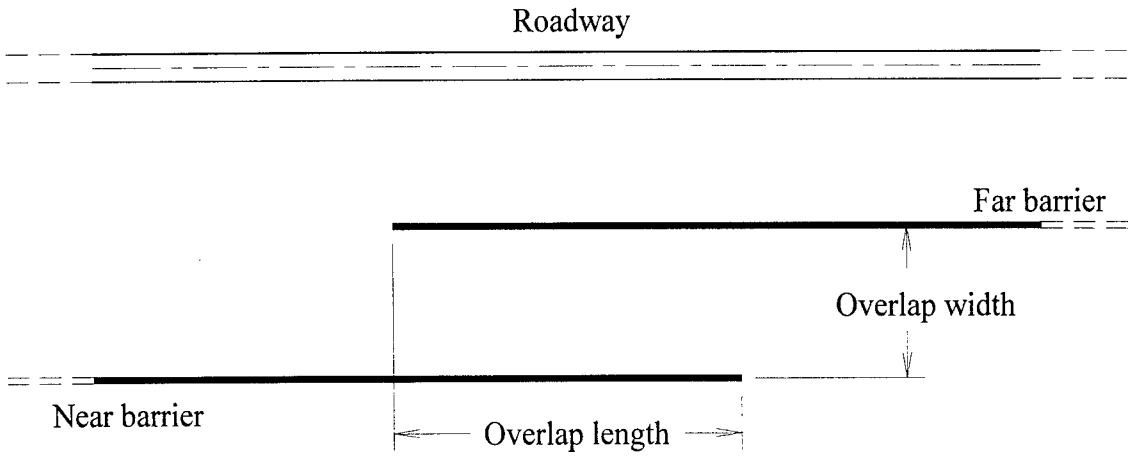


Figure 1 Typical noise barrier overlap gap

At a particular noise barrier site located in southwestern Ohio, north of Cincinnati on Interstate 71, a total of 12 overlap gaps have been incorporated into the barrier's design. A preliminary investigation of these noise barriers showed that overlap gaps contributed to the

degradation of the barrier insertion loss [Herman, Clum, and Finney 1997]. This finding was revealed through two independent sources. First, many residents complained about the overlap gaps being ineffective at reducing the traffic noise. Second, acoustical measurements performed at two overlap gap sites revealed that up to 4-5 dB of degradation existed. This loss affected approximately 30 to 50 homes in the overlap gap area. The results of one overlap gap measurement site from this study are shown in Figure 2 and 3.

Based on this finding, further research was warranted to study the effect of overlap gaps on the surrounding area. Existing noise models and proposed revisions to noise models do not account for these effects. Consequently, the Federal Highway Administration (FHWA) and the Ohio Department of Transportation (ODOT) found it important to fund a study of noise barrier overlap gaps to provide a solution to the problem. The culmination of this research is the development of the computer model discussed in this report. The model is useful in analyzing sound wave reflections found to occur between overlapped barrier sections. Its purpose is to provide a design tool for engineers to help select the appropriate overlap length to width ratio to minimize the gap's effect on the noise environment. Also, the model was developed to allow the user to evaluate the effect of incorporating absorptive panels on varying horizontal and vertical sections of the overlap gap to control detrimental reflections.

The material covered in this report will include a literature review of past work performed on overlap gaps. Next, the analysis theory will be presented and all fundamental equations that will be used to examine an overlap gap site will be derived. The computer model and the steps required to produce the model will be covered in order to give the reader an understanding of the development of the program. In order to validate and calibrate the resulting model, actual field

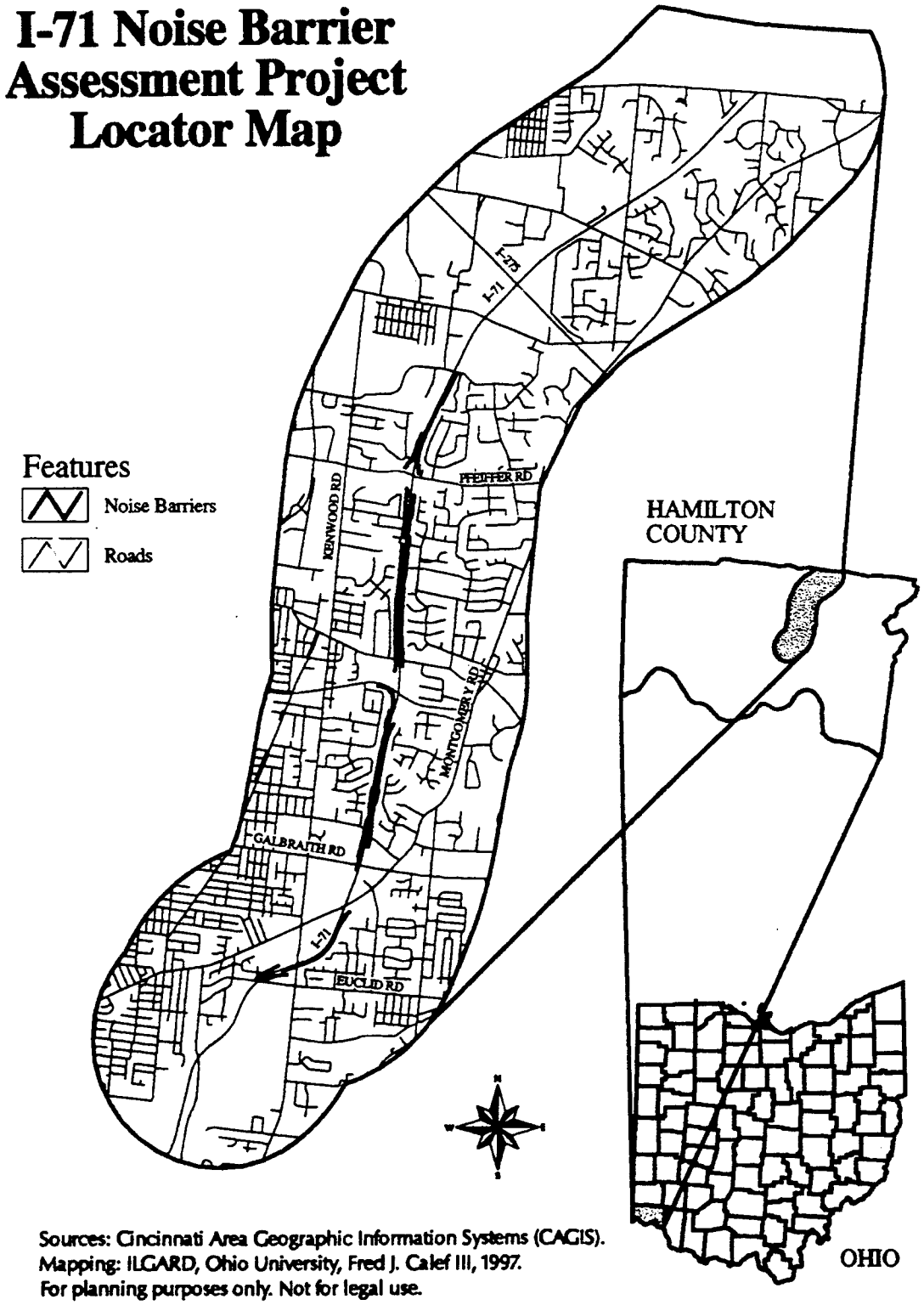


Figure 2. Overlap gap study area locator map

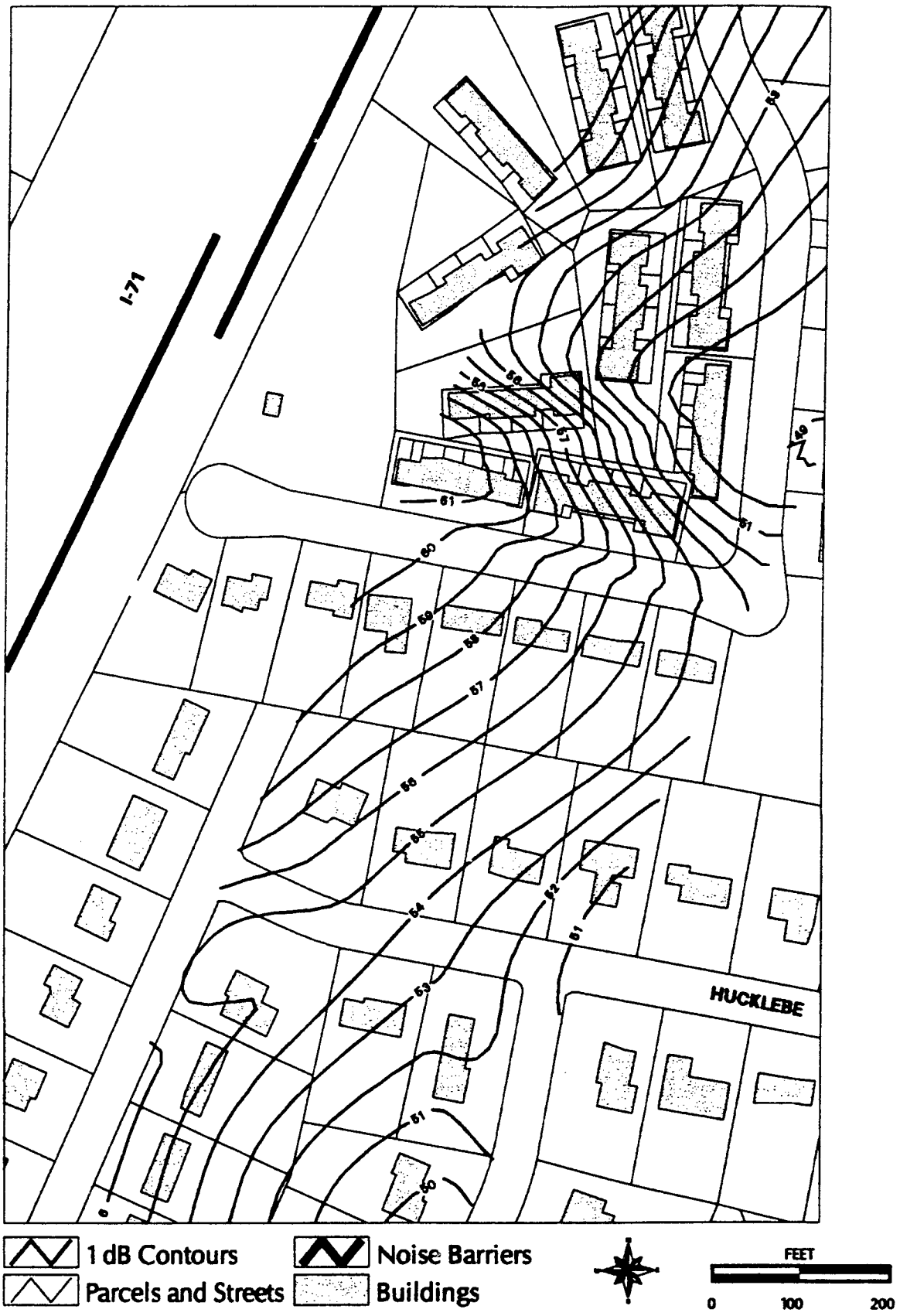


Figure 3. Overlap gap measurement site

data must be collected and analyzed. The field study that was performed to accomplish this objective will be outlined in detail. Finally, results of this research shall be provided and conclusions will be drawn.

## 2. RESEARCH OBJECTIVES

The objectives of this research on traffic noise barrier overlap gaps are as follows:

1. Survey the 12 overlap barrier gaps at the Cincinnati noise barrier site, identify factors which affect noise propagation through each, and select a minimum of five gaps for study.
2. Perform sound pressure level measurements to characterize the acoustical sound field in overlap gap areas.
3. Identify the factors that currently degrade barrier performance in gap areas.
4. Develop an acoustical model to predict noise propagation through barrier gaps.
5. Validate the acoustical model using data acquired from field measurements.
6. Develop an overlap gap design procedure, based on noise propagation modeling, that can be incorporated in the ODOT noise barrier design process to improve noise barrier effectiveness in gap areas.

# 3. LITERATURE REVIEW

The literature review on overlap gaps revealed that limited work has been done in this area. Many sources referred to overlap gaps and their use, but few actually attempted to analyze the propagation of sound through the gap. Also, the basis for current design standards could not be identified. The results of the literature review demonstrate the need for the research performed in this project.

The main reason to install an overlap gap is to provide access for maintenance to the residential or protected side of the barrier. Different designs other than overlap gaps can be employed to ensure that access is furnished [Bowlby 1992]. First, local streets found behind the noise barrier can be used to gain access to right-of-way land. However, many residential areas do not lend themselves to this type of access. If this alternative is used, a gate would need to be installed in the right-of-way fence, if one exists, in order to get equipment to the barriers. Another method is the installation of doors in the noise barrier. Doors must be of an appropriate material to prevent high transmission losses. A door must fit relatively airtight so as to insure the acoustical integrity of the barrier. The use of doors for access has been limited due primarily to aesthetic concerns. Fire hose access was also addressed but this can usually be provided by designing holes in the barrier with removable plugs at locations where fire hydrants are found.

If overlap gaps are used, the design of the overlap gap ratio (the ratio between the overlap length to width) must be performed. Sources are not consistent in recommending the necessary overlap gap ratios. Early work shows that it had not been determined how far the overlap must be extended [Cohn 1981]. Other publications state that an overlap ratio of two to one should be

used [Simpson 1976] while others recommend a minimum ratio of three to one to ensure that the noise environment is not adversely affected [OECD 1995]. However, little scientific basis for these recommended ratios could be found. The overlap ratios that are presently used for design are primarily rule-of-thumb guidelines.

The primary problem with installing an overlap gap in an otherwise continuous noise barrier is the introduction of reflective sound waves. By overlapping the near and far wall a sufficient distance, the line-of-sight is broken between the traffic and most receivers. Therefore, the majority of direct rays are eliminated. However, reflected rays exist regardless of the length of the overlap. In recent research, it has been determined that these reflected rays may be responsible for increased noise levels in communities near the overlapped noise barriers [Herman, Clum, and Finney 1997]. Absorptive treatment is commonly used on parallel noise barriers to prevent reflections from causing an insertion loss degradation. A potential method to attenuate detrimental reflections is to install absorptive panels on the inside of the overlap gap.

Research has been conducted to study the effectiveness of using absorptive panels to minimize reflections at overlap gap sites [Hatano 1980]. Two gaps were installed with different absorptive treatments to investigate the acoustical performance of the absorptive panels in overlap gaps. At one site in which the overlap length was 7.32 m (24 ft) and the overlap width was 3.05 m (10ft), the application of absorbing cladding resulted in a reduction of sound levels in the range of 3.2 - 3.9 dBA at receivers near the gap. This is an appreciable amount which lowered the noise at a nearby residence to levels which would have existed had the overlap gap not existed. The second site had similar results but will not be discussed since reflections due to an overhead pedestrian bridge complicated the evaluation. Even though the gaps studied in this

project had greater overlap dimensions, Hatano's research provided promising findings for the application of absorptive panels to other overlap gaps.

Considerable development has been done on a model to analyze the reflections propagated at overlap gap sites [Lee et al. 1990]. The model, known as the Barrier Overlap Analysis Procedure (BOAP), was designed for overlaps gaps that accommodated service roads and highway entrance and exit ramps. BOAP could also analyze gaps that were installed for maintenance access. Analyses performed by BOAP showed that an insertion loss degradation similar to that measured by Hatano existed at overlap gap sites.

The development of BOAP was useful as a guide to establish the varying mechanisms influencing propagation that affected receivers at an overlap gap site. However, there are shortcomings in the program that the model in this report effectively manages. First, the overlapped noise barriers input into BOAP are required to be of equal height. Next, absorptive barriers are not directly modeled in BOAP. Rather, the sound level is adjusted by replacing the reference energy mean emission level (REMEL) for each class of vehicles with a reflection dependent term. Finally, BOAP is not capable of analyzing receivers in front of the near wall.

Other literature, while not directly linked to the overlap gap problem, does relate to the phenomenon of sound wave reflections between barrier walls. Previous work performed on the multiple reflection problem with parallel noise barriers proved valuable in the development of the model theory [Bowlby and Cohn 1986]. This research was useful in presenting the fundamentals of image theory and the determination of image existence. Also, the method used in calculating image distances and image angles for parallel barriers could be applied to overlap gap sites after considerable modification. Another publication generated from this same research was helpful in developing a method of dealing with the loss of energy upon each reflection,

which was applied to the absorptive treatment theory [Bowlby and Cohn 1983]. This paper was also helpful in establishing the inputs that were necessary for the Gap Analysis Program (GAP) developed in this report.

In summary, while problems associated with noise barrier overlap gaps have been recognized, little work has been done to model traffic noise propagation through the gaps. BOAP resulted in substantial progress but is limited in its range of application, its specification of noise barrier heights, and its placement of absorptive treatment. Consequently, no comprehensive analytical tools exist to predict the noise levels caused by the propagation of reflected sound waves through noise barrier overlap gaps.

# 4. THEORETICAL DEVELOPMENT OF THE MODEL

Noise prediction models used on Federal Aid projects must conform to FHWA equations [Federal Highway Administration 1982]. The theoretical development of the GAP model complies with the assumptions and principles embodied in the FHWA Highway Traffic Noise Prediction Model [Barry and Reagan 1978]. The equations developed in this model were utilized in the highway noise computer prediction model STAMINA 2.0 [Bowlby, Higgins, and Reagan 1982]. Current work is being performed on the development of a new computer prediction model, FHWA Traffic Noise Model (FHWA-TNM) [Anderson and Menge 1995], which will replace the current STAMINA 2.0 program. At the time of this research, STAMINA 2.0 is still the primary computer program in use today for highway noise prediction modeling.

TNM was designed to improve upon some of the shortcomings that existed in STAMINA 2.0. These shortcomings included the lack of parallel barrier reflections and a poor ground attenuation formulation, among others. Many of these problems exist when performing an analysis on an entire noise barrier project with multiple receivers spread throughout a large area.

An analysis by either STAMINA 2.0 or TNM could involve the modeling of several kilometers of roadways and barriers with receivers located up to a kilometer in distance from the barriers. The issue of analyzing noise barrier overlap gaps is a much more localized analysis. A typical overlap gap study may consist of a 1 km roadway and barrier length with receivers located a maximum of 50-75 meters away from the noise barrier on the residential side of the barrier. The benefits of using TNM can only be realized on large scale projects. On small scale studies comparable in size to overlap gap analyses, the results from STAMINA 2.0 and TNM

will be similar. Therefore, the equations applied in STAMINA 2.0 have been used in the development of this model.

## 4.1. FHWA Highway Traffic Noise Prediction Equation

In any noise analysis, the primary issues of concern are the source, path, and receiver. The source is the object that creates the noise. In highway applications, the source is most often a vehicle. However, one vehicle can generate noise due to many varied mechanisms such as tire-pavement interaction noise, engine noise, wind noise, and exhaust noise. The source is made up of these individual vehicles and can vary from one vehicle on a one-lane road up to thousands of vehicles traveling on a multilane, divided highway.

The path is the area over which sound waves travel in their course from source to receiver. Typically, the path can contain some or all of the following: pavement, grass median strips, median barriers, gravel or paved shoulders, right-of-way land, noise barriers, earth berms, and lawns. The path also is made up of the atmosphere through which the sound waves are transmitted. As a sound wave proceeds along its path, the noise level is attenuated, or reduced, from its original source level to the level experienced at the receiver.

The receiver is the object that is subject to the noise created by the source. The most common receivers are humans. When conducting noise measurements, the receiver is a calibrated microphone placed on top of a tripod. Receivers are typically modeled behind a noise barrier in locations where high outdoor activity exists. It is these locations that are targeted for noise reduction when constructing highway noise barriers.

Traffic noise is attenuated by many mechanisms as it travels from source to receiver. These mechanisms can include some or all of the following:

1. Geometric spreading
2. Atmospheric attenuation
3. Ground attenuation
4. Barrier attenuation

As sound waves travel outward from the source, the area over which the waves travel increases. The farther the waves are from its source, the lower the intensity of the sound. This phenomenon is known as geometric spreading. Receivers at long distances from a source benefit from this mechanism for noise reduction.

The propagation of sound waves through air brings forth the next attenuation mechanism, atmospheric attenuation. Air is made up of primarily oxygen, nitrogen, and water vapor. As sound waves travel through this medium, energy is dissipated by the air molecules. Atmospheric attenuation is only significant at long distances.

The third mechanism is the interaction of sound waves with the ground over which they travel. This attenuation occurs due to factors such as the geometry of the propagation path, the soil conditions, and the wavelength of the sound waves. This mechanism is highly complex and often difficult to characterize.

The final mechanism occurs when sound waves travel over objects located between the source and receiver. As sound waves travel over objects, diffraction, or a bending of the sound waves, occurs. This diffraction causes a decrease in the intensity of the sound waves. The phenomenon is termed barrier attenuation when the object responsible for the diffraction is a noise barrier. Barrier attenuation will be discussed more thoroughly later in this chapter.

The basic equation that governs over the computation of a noise level at a given receiver due to a source composed of one class of vehicles on a single roadway is as follows:

$$L_{eq}(h)_i = (\overline{L_o})_{Ei} + 10\log\left(\frac{N_i \pi D_o}{S_i T}\right) + 10\log\left(\frac{D_o}{D}\right)^{1+\alpha} + 10\log\left(\frac{\psi_\alpha(\phi_1, \phi_2)}{\pi}\right) - \Delta_{Bi} \qquad (1)$$

where

$L_{eq}(h)_i$ is the hourly equivalent continuous sound level of the *i*th class of vehicles.

$(\overline{L_o})_{Ei}$ is the reference energy mean emission level of the *i*th class of vehicles.

$N_i$ is the number of vehicles in the *i*th class passing a specified point during a specified time period (1 hour).

$D$ is the perpendicular distance, in meters, from the centerline of the traffic lane to the observer.

$D_o$ is the reference distance at which the emission levels are measured. In the FHWA model, $D_o$ is 15 meters.

$S_i$ is the average speed of the *i*th class of vehicles and is measured in kilometers per hour (km/h).

$T$ is the time period over which the equivalent sound level is computed (1 hour).

$\alpha$ is a site parameter whose value depends on site conditions that effect ground attenuation.

$\psi$ is a symbol representing a function used for segment adjustments.

$\Delta_{Bi}$ is the attenuation provided by shielding due to a noise barrier for the *i*th class of vehicles.

The derivation of this equation is a complicated procedure which requires a thorough understanding of the principles of acoustics. It is not the purpose of this study to present its mathematical development. The reader should refer to the FHWA Highway Traffic Noise Prediction Model [Barry and Reagan 1978] for a complete derivation of this fundamental

equation. A brief overview of the equation will be provided to acquaint the reader with the main issues involved.

The fundamental equation enables the calculation of the noise level at a single receiver protected by a noise barrier due to a source consisting of a single class of vehicles on one roadway. The individual terms of Equation 1 will be discussed to relate each term's purpose and significance. The following list describes each term's function in the equation:

1. Equivalent continuous sound level
2. Reference energy mean emission level
3. Traffic flow adjustment
4. Distance adjustment
5. Finite roadway adjustment
6. Barrier attenuation adjustment

It should be noted that sound intensity and sound pressure are expressed in units based upon a logarithmic scale. Therefore, the base 10 logarithmic terms multiplied by a factor of 10 preceding each term converts the sound energy into a sound level, which has the units of decibels (dB).

The first term in the equation, $L_{eq}(h)_i$, is known as the equivalent continuous sound level at a receiver for the *i*th class of vehicles. This level is a time-weighted average of the acoustic energy over a period of time. It is equal to the time-varying acoustic energy that is present over the same period of time. The period of time that is most commonly used is one hour. This is indicated by the $(h)$ which represents an hourly equivalent continuous sound level.

The second term, $(\overline{L_o})_{Ei}$, is the reference energy mean emission level (REMEL) of the *i*th class of vehicles, in units of decibels (dB). Vehicles are divided into three classes based on similar acoustical characteristics:

1. Automobiles (A): vehicles with two axles and four wheels
2. Medium Trucks (MT): vehicles having two axles and six wheels
3. Heavy Trucks (HT): vehicles having three or more axles

Each class of vehicles emits noise at varying levels depending on speed. Research has been conducted to measure the sound levels that each class of vehicles produces depending on the speed of the vehicle [Reagan 1978]. The REMEL for each class of vehicles can be found by inputting the speed of the vehicle of a respective class, S in km/h, into the following empirical equations:

$$(\overline{L_o})_{EA} = 38.1\ \log(S) - 2.4 \tag{2}$$

$$(\overline{L_o})_{EMT} = 33.9\ \log(S) + 16.4 \tag{3}$$

$$(\overline{L_o})_{EHT} = 24.6\ \log(S) + 38.5 \tag{4}$$

These reference levels are for a single vehicle traveling at constant speed on level terrain at a reference distance of 15 meters. The vehicle is assumed to be traveling on an infinitely long roadway. The remaining terms act as adjustments to account for different source, path and receiver conditions.

The first of these adjustments, $10\log\left(\frac{N_i \pi D_o}{S_i T}\right)$, is known as the traffic flow adjustment. Equations 2-4 provide only the noise levels for a single vehicle at the source. However, traffic flows typically consist of several hundred vehicles passing a given point in a short period of time. This adjustment accounts for the number of vehicles that are present in the

*i*th class of vehicles on a particular lane or roadway. The time period, $T$, is usually one hour in most highway noise applications.

The distance adjustment, $10\log\left(\frac{D_o}{D}\right)^{1+\alpha}$, accounts for receivers located farther from the source than the reference distance of 15 meters. Since the REMELs are used to calculate noise levels assuming the receiver is positioned at this reference distance, an adjustment must be made for receivers located at greater distances. As the distance between the source and receiver increases, the sound level decreases due to the phenomenon of geometric spreading discussed earlier in this chapter.

The REMEL calculation assumes that the highway is infinitely long. Due to the fact that no road is infinitely long, the REMELs need to be modified to reduce the sound level that is actually being produced on the finite highway. The finite roadway adjustment, $10\log\left(\frac{\psi_\alpha(\phi_1,\phi_2)}{\pi}\right)$, makes the correction for this assumption. Figure 4 shows an example of the finite roadway adjustment concept. The angle, $\phi_1$, is measured from the perpendicular from the receiver to the roadway to the left end of the roadway. Similarly, $\phi_2$ is measured from the perpendicular from the receiver to the roadway to the right end of the roadway. The ends of the roadway are defined arbitrarily but an approximation of a roadway length of one kilometer is usually adequate. These angles are input into the proper function to arrive at the finite roadway adjustment.

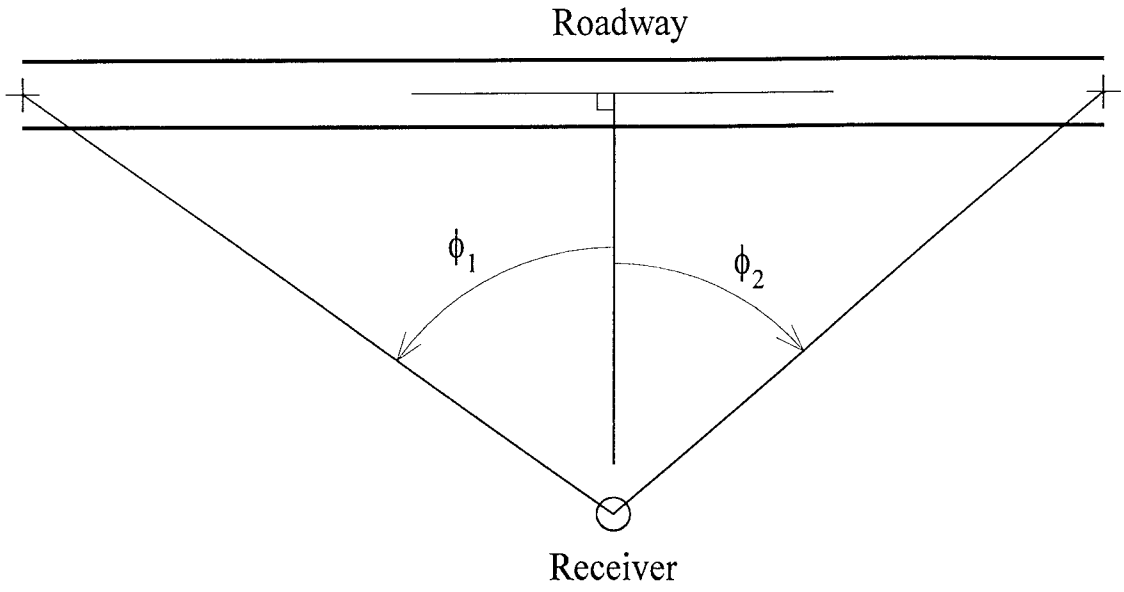


Figure 4. Finite roadway adjustment

The preceding adjustments have all been straightforward corrections that are applied to the reference emission levels. If a noise barrier does not exist in the path between source and receiver, the noise level calculation for the *i*th class of vehicles on one lane or roadway would be complete. If a noise barrier is present, the prediction process becomes a much more difficult task.

### 4.1.1. Barrier Attenuation Adjustment

Sound attenuation can occur whenever an object made from a dense material is placed in the path between the source and receiver. The object must be of sufficient height to break the line of sight between source and receiver. These objects can consist of noise barriers (i.e. constructed walls), earth berms, dense woods, buildings, etc. This discussion will be limited to

noise barriers since overlap gaps are constructed from noise barriers and other shielding mechanisms rarely exist at an overlap gap site.

There are certain design characteristics that must be considered to ensure a barrier's optimum performance. The barrier must be sufficiently long so that the receiver is protected from edge diffraction. Edge diffraction, also known as side flanking, is the propagation of sound waves around the ends of a noise barrier. If a barrier is extended a reasonable distance past any potential receiver, side flanking has minimal effect on the noise level. Also, the noise barrier must be a solid material of adequate density with no cracks to prevent noise from transmitting directly through the barrier.

The effectiveness of a noise barrier depends directly on its length and its orientation with respect to the source and receiver. The following equation [Kurze and Anderson 1971] is an expansion of the last term of Equation 1:

$$\Delta_{Bi} = 10 \log \left[ \frac{1}{\phi_R - \phi_L} \right] \int_{\phi_L}^{\phi_R} 10^{\frac{-\Delta i}{10}} d\phi \qquad (5)$$

where

$\Delta_{Bi}$ is the attenuation provided by the barrier for the *i*th class of vehicles.

$\phi_R, \phi_L$ are angles that establish the relationship between the barrier and the observer measured from the receiver to the right and left ends of the barrier, similar to the finite roadway adjustment.

$$\Delta_i = \begin{cases} 0 & N_i \le -0.1916 - 0.0635\varepsilon \\ 5(1+0.6\varepsilon) + 20\log\dfrac{\sqrt{2\pi|N_o|_i\cos\phi}}{\tan\sqrt{2\pi|N_o|_i\cos\phi}} & (-0.1916 - 0.0635\varepsilon) < N_i \le 0 \\ 5(1+0.6\varepsilon) + 20\log\dfrac{\sqrt{2\pi|N_o|_i\cos\phi}}{\tanh\sqrt{2\pi|N_o|_i\cos\phi}} & 0 < N_i \le 5.03 \\ 20(1+0.15\varepsilon) & N_i \ge 5.03 \end{cases} \quad (6)$$

where

$\Delta_i$ is the point source attenuation for the $i$th class of vehicles.

$N_i = (N_o)_i \cos\phi$

$\varepsilon$ is a barrier shape parameter, 0 for a freestanding wall.

$N_o$ is the Fresnel number determined along the perpendicular line between the source and receiver.

$N_{oi}$ is the Fresnel number of the $i$th class of vehicles determined along the perpendicular line between the source and receiver.

The Fresnel number is characterized by the following:

$$N_o = 2\left(\frac{\delta_o}{\lambda}\right) \quad (7)$$

where

$\delta_o$ is the path-length difference measured along the perpendicular line between the source and receiver.

$\lambda$ is the wavelength of the sound wave radiated by the source.

The path-length difference is a critical component in the preceding equation in considering the barrier attenuation at a receiver. The path-length difference is the difference in length between the path for a wave that is diffracted by the top edge of a barrier and a wave that propagates directly from the source to the receiver. A graphical presentation of the path length

difference is shown in Figure 5. It is crucial that the barrier be constructed so that the line of sight between source and receiver is broken. If the line of sight is not broken, no barrier attenuation can occur and consequently, the barrier is ineffective. Once the line of sight is broken, further increases in the path length difference will result in greater attenuation due to increased diffraction of the sound wave.

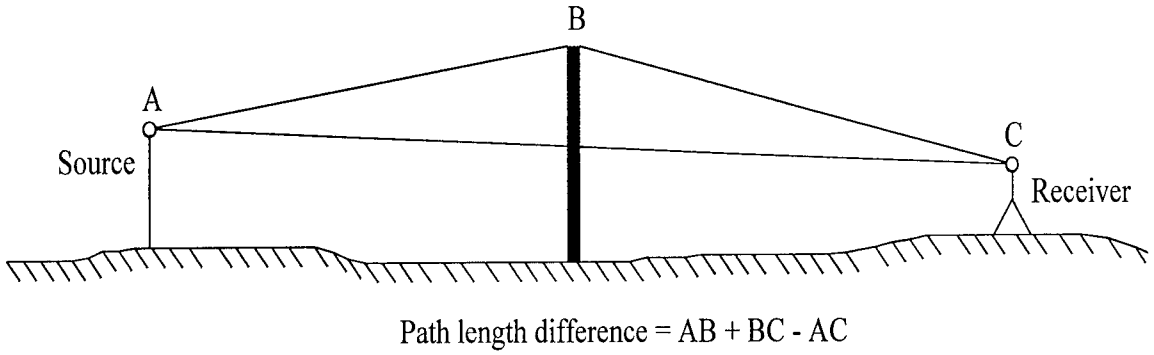


Figure 5. Path length difference

### 4.1.2. Summation of Contributing Noise Levels

In the previous discussion, all variables in the equations dealt with values from only one class of vehicles. Therefore, Equation 1 will only give the noise level at a receiver produced by one class of vehicles. However, the FHWA model generally considers three classes of vehicles for typical traffic flows. All three classes must be summed by logarithmic addition to arrive at the noise level from a single lane or roadway.

Since most highways consist of many lanes, another iteration must be performed to calculate the total noise level at a receiver. All noise contributions from each lane of traffic must be analyzed in each of the three classes of vehicles. Therefore, a high number of iterations can result in calculating the noise level at one receiver. This is a time consuming process to perform by hand. Consequently, all but the most trivial noise studies are performed using a computer model.

## 4.2. Propagation of Sound Waves at an Overlap Gap Site

The previous section accounted for the calculation of noise levels due to a flow of traffic on a finite roadway. However, the path over which a sound wave travels to reach a receiver was not fully covered. It was assumed that all sound waves passed over the top of a noise barrier before reaching the receiver. This is correct if the receiver is located behind a single, continuous noise barrier of sufficient length. However, the introduction of a break, such as an overlap gap, in an otherwise continuous barrier permits noise to propagate to the receiver in many different ways.

The possible paths through which noise may propagate to a receiver at an overlap gap site are influenced by the following mechanisms:

1. Direct propagation
2. Simple diffraction
3. Double diffraction
4. Multiple reflected rays (MRR)
5. Multiple reflected diffracted rays (MRDR)

Not all the terms of the noise prediction equation apply to each of these mechanisms influencing propagation. In some cases additional terms must be added to Equation 1 to arrive at the proper

predicted noise level. Figures 6-7 illustrate the five different mechanisms that can contribute to the noise level at an overlap gap receiver.

Direct propagation of a sound wave does not involve any barrier attenuation. The sound wave travels directly to the receiver from the source. This path of propagation is responsible for producing the highest sound levels at a receiver. Direct propagation occurs when the line of sight between the source and receiver is not broken by a noise barrier. Since barrier attenuation can account for significant reduction in noise levels, direct propagation should be avoided whenever possible.

The most common mechanism influencing propagation is simple diffraction. Simple diffraction occurs when sound waves from a source are diffracted to the receiver by a noise barrier. Diffraction is the bending of a sound wave as it passes over the top edge of a noise barrier. A sound wave must strike a noise barrier relatively close to its top edge to be diffracted to the receiver. If it does not strike the barrier edge, the wave will reflect off of the barrier or pass freely over the top. In either case, the sound wave will not reach the receiver and consequently, will have no effect on the receiver's noise level.

Double diffraction is a specialized case of simple diffraction. Double diffraction occurs when two barriers are placed relatively close to each other. As sound waves strike the edge of the first barrier, some will be diffracted to the edge of the second barrier. This second barrier will then diffract the waves to the receiver. Although double diffraction does result in a higher reduction of sound energy than a single wall, predicting its attenuation is not easily performed. Since double diffraction only constitutes a small part of the mechanisms influencing propagation of noise to the overlap gap receivers and cannot degrade barrier performance, its effect will be neglected. To further ensure a conservative approach where double barriers exist, an analysis of

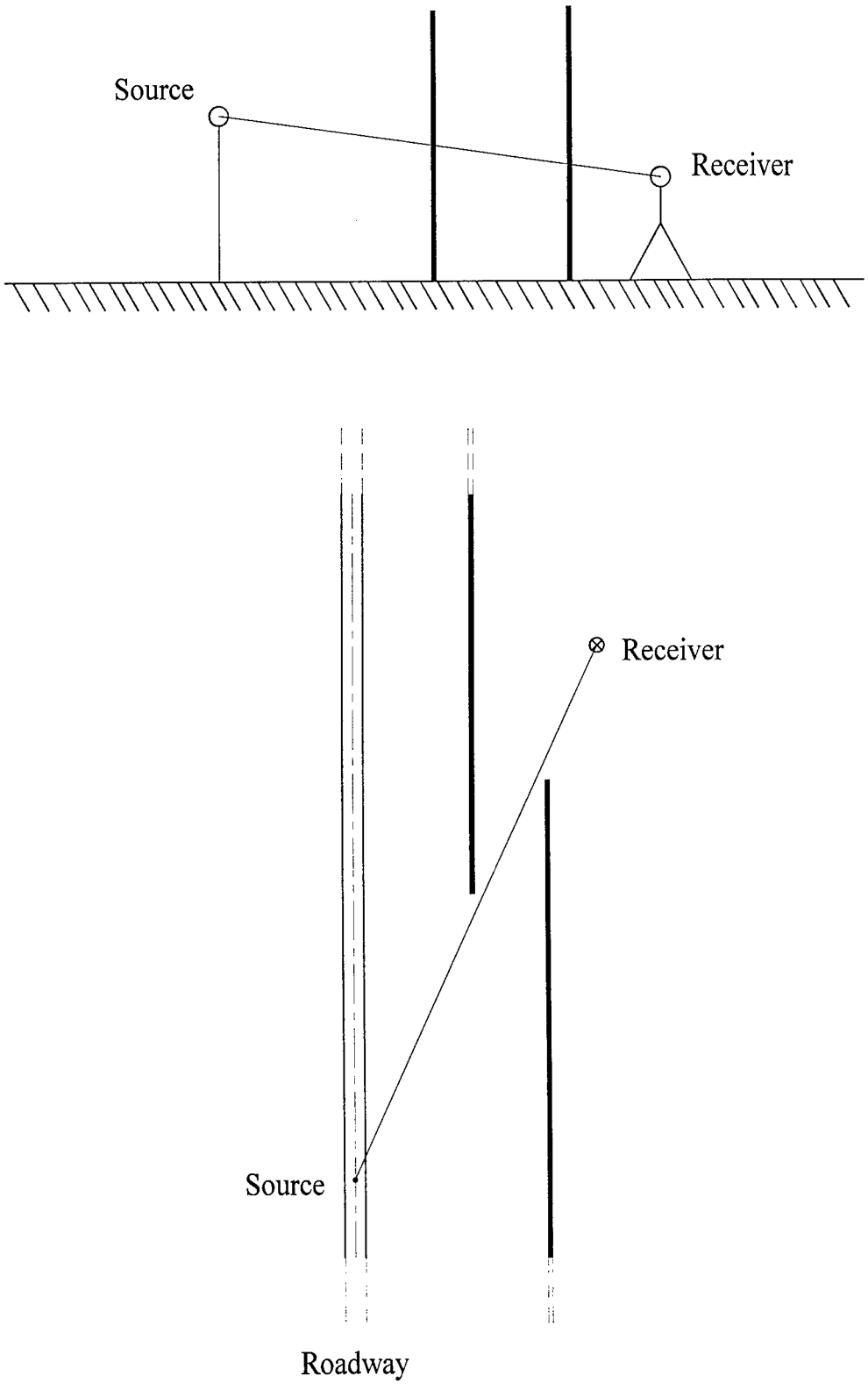


Figure 6. Direct propagation

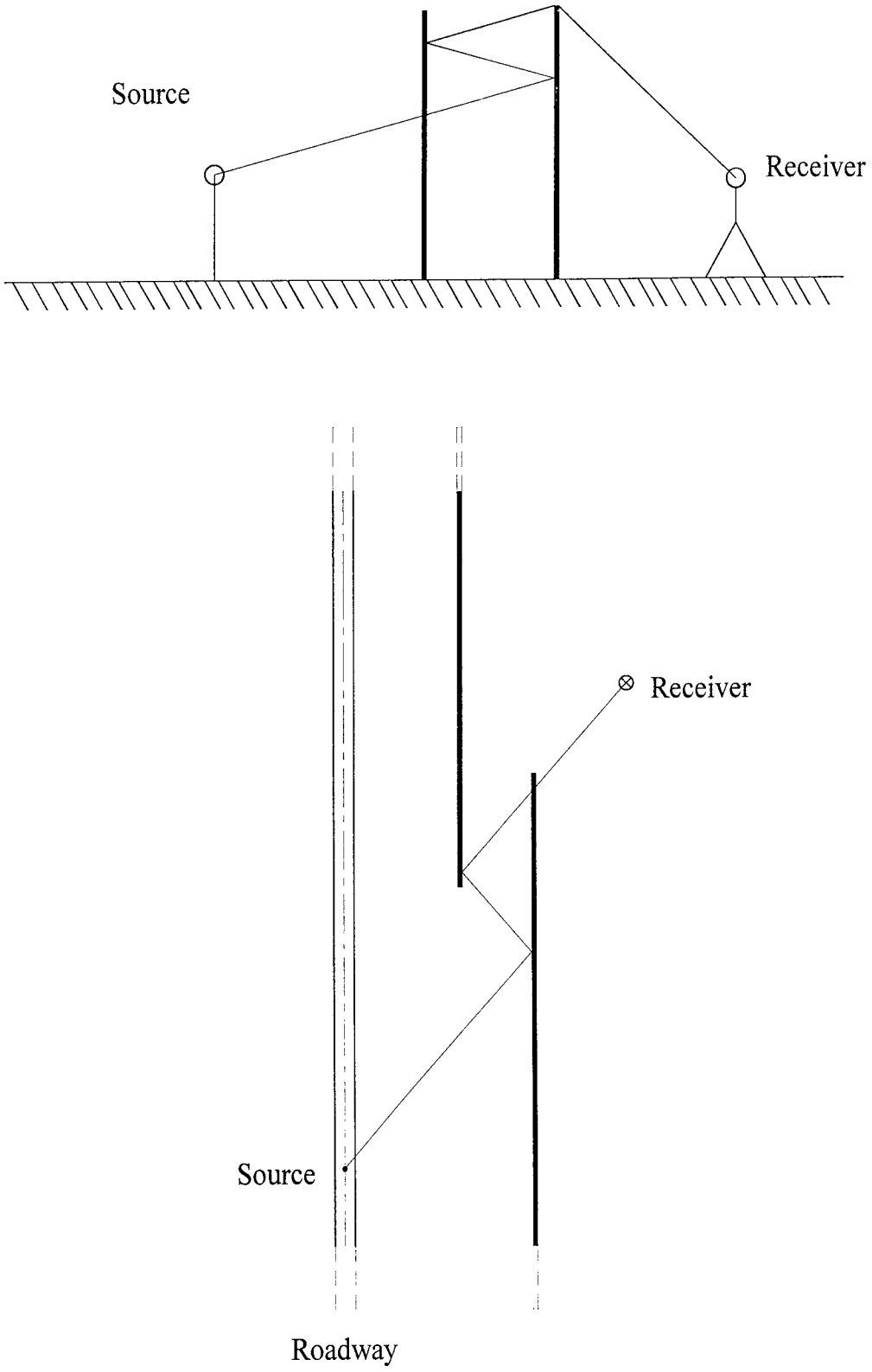


Figure 7. Multiple reflected diffracted rays

the path length differences for each barrier will be performed. The barrier which produces the greatest path length difference will be used to compute the barrier attenuation due to diffraction.

The last two mechanisms deal with sound waves that are reflected off one or more noise barriers before reaching the receiver. The first mechanism, multiple reflected rays (MRR), are sound waves reflected off of noise barriers which reach the receiver without being diffracted over the top of a noise barrier. It is a special case of direct propagation. As with direct propagation, no barrier attenuation occurs. However, with each reflection, a certain amount of the wave's energy is lost. Also, a MRR must travel greater distances than a direct ray to reach the receiver. For these reasons, MRR cause less noise level increases than direct rays when originating from the same source.

The final mechanism which influences propagation, multiple reflected diffracted rays (MRDR), is similar to MRR. Whereas a MRR is a special case of direct propagation, a MRDR is a special case of simple diffraction. A MRDR is also reflected off one or more noise barriers. However, after the final reflection, a MRDR is diffracted over the top edge of a noise barrier to a receiver. MRDR experience a loss of energy from the reflections with the barriers and also through diffraction. Because of the added barrier attenuation, MRDR have less effect on overall noise levels than do MRR.

All receivers are subject to sound waves from the source which are influenced by at least one of these propagation mechanisms. In many cases, several mechanisms exist at a single receiver. A receiver's location at the overlap gap site is the determining factor as to how many mechanisms influencing propagation contribute to its total noise level.

## 4.3. Overlap Gap Receiver Locations

There are many locations where a receiver can be positioned at an overlap gap site. As discussed in the previous section, this positioning determines which sound waves influenced by propagation mechanisms reach a receiver. In order to be adversely influenced by an overlap gap, a receiver must be located in one of the six zones shown in Figure 8. Any receivers outside of these zones can be analyzed using standard traffic noise prediction methods.

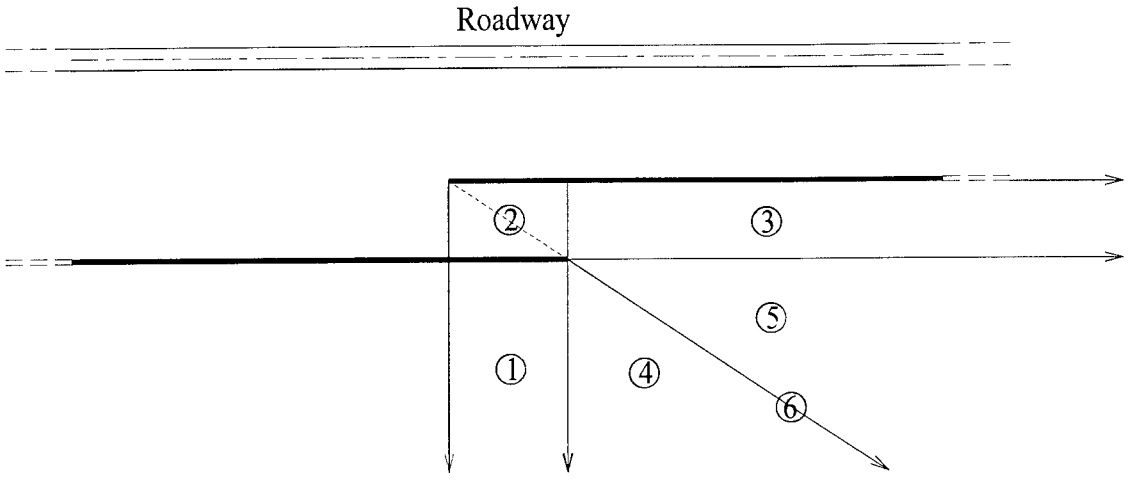


Note: Case 6 is located on the line drawn between the ends of the far and near barriers.

Figure 8. Overlap gap receiver locations

Different zones are established based on the geometry of the overlap gap. The size of each of these zones can vary from site to site, depending on the design of the gap. Based on the zone in which a receiver is located, different mechanisms of propagation may influence the receiver. A complete listing of receiver locations and the possible propagation mechanisms can be found in Table 1. At this point, receivers in zone 1 will be termed Case 1 receivers.

Similarly, receivers from zone 2 will be classified as Case 2 receivers, and so on. Each case will be covered fully in the next section regarding its susceptibility to these mechanisms which influence propagation.

Table 1. Propagation mechanisms which influence overlap gap receivers

| | Receiver case | | | | | |
|---|---|---|---|---|---|---|
| | 1 | 2 | 3 | 4 | 5 | 6 |
| *Propagation mechanism* | | | | | | |
| Direct propagation | | X | X | | X | |
| Simple diffraction | X | X | X | X | X | X |
| Double diffraction | X | | | X | | |
| Multiple reflected rays (MRR) | X | X | X | X | X | X |
| Multiple reflected diffracted rays (MRDR) | X | | | X | X | X |

### 4.4. Determination of Source Regions

Receivers can be located in six different zones, as shown in Figure 8. For each receiver case, certain sections of the source or roadway may be located in a position where different mechanisms influence the propagation of noise. Depending on the orientation of the receiver with respect to the roadway and overlap gap, these source regions can vary greatly in size. An analysis must be performed to establish these source regions for each receiver.

The first step in this analysis is to find the zone in which the receiver is located. This is done by comparing the coordinates of the receiver with the endpoints of both the near and far barriers. After the receiver case is determined, the angular relationships between the receiver with the ends of the barriers and roadways can be investigated for source region existence.

This investigation primarily consists of calculating many angles from the perpendicular from the receiver to the roadway to critical endpoints of the overlap gap geometry. These endpoints may consist of the following:

1. Left end of the roadway, as determined by the user
2. Overlap end of the near barrier (the barrier nearest to the community)
3. Overlap end of the far barrier (the barrier farthest from the community)
4. Intersection of perpendicular line from the overlap end of the far barrier with the roadway
5. Right end of the roadway, as determined by the user

These endpoints are all used when analyzing Case 1, 4, 5, and 6 receivers. Cases 2 and 3 do not require the use of the overlap end of the near barrier since these receivers are located in front of the near barrier.

All of these endpoints are easily identified except for the fourth endpoint, which requires some clarification to demonstrate its importance. The intersection of the perpendicular line from the overlap end of the far barrier with the roadway is the boundary point for reflections. As shown in Figure 9, to the right of this point, no reflective path from the source to the receiver can exist due to the fact that the angle of incidence with the near barrier would cause any sound wave originating to the right of this point to reflect away from the overlap gap. Any sound wave traveling at a sufficient angle emitted from a source to the left of this point could freely enter the overlap gap.

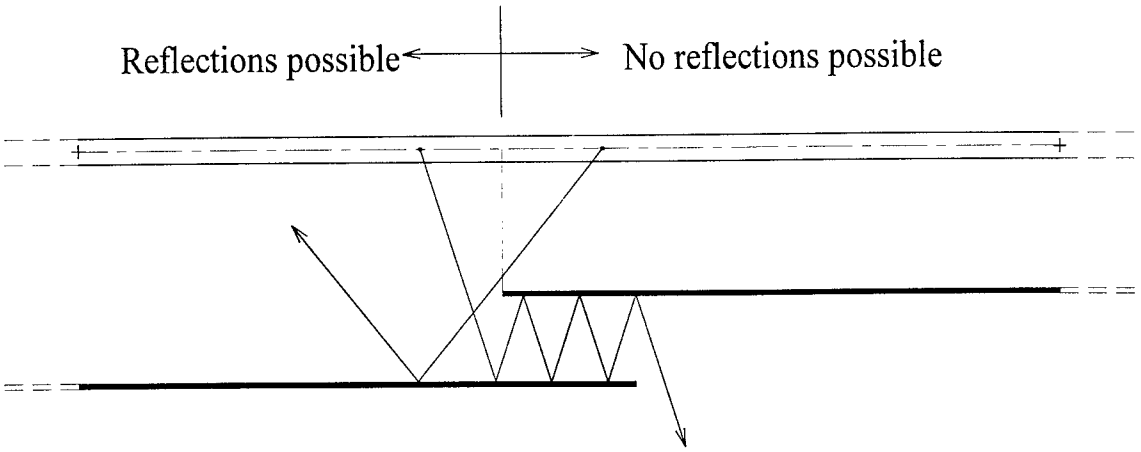


Figure 9. Reflective source endpoint

The formulation of the equations to calculate these angular relationships will not be presented. However, the graphical illustration of this process can be seen in Figures 10-11. This procedure must be performed for each roadway as the angles from the receiver to the ends of the roadway change with each roadway-receiver pair.

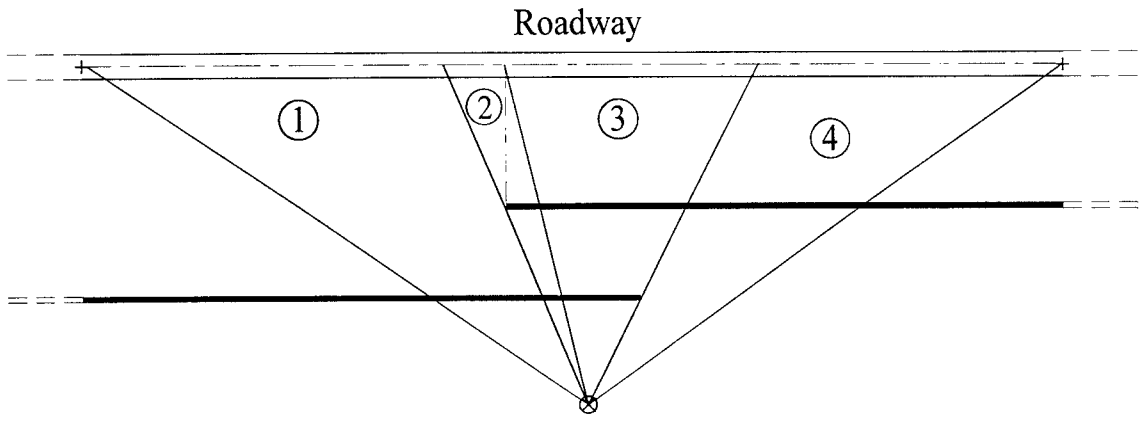


Figure 10. Case 1 source regions

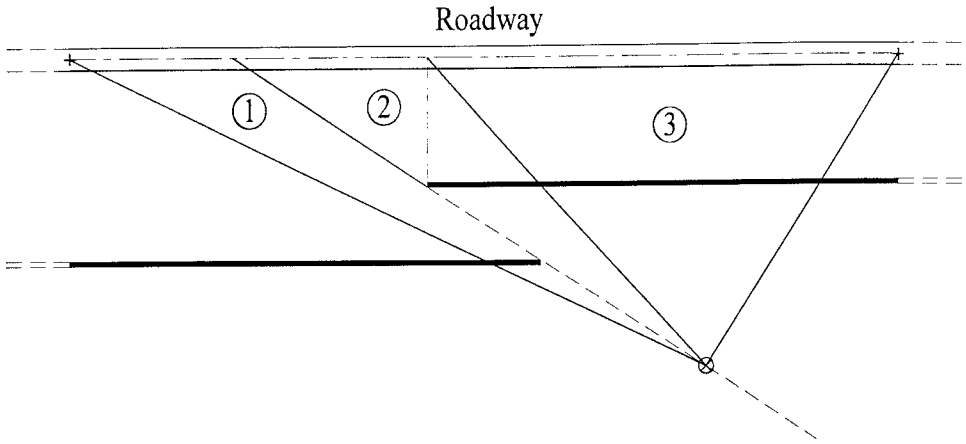


Figure 11. Case 6 source regions

By identifying these various source regions for each case, the source has been divided from one source into several small sub-sources. This division of sources enables the proper computation of the noise levels since each sub-source may be influenced by different mechanisms of propagation. Table 2 details the mechanisms which influence propagation that may exist within each receiver's sub-source regions.

Table 2. Sub-source propagation mechanisms for each receiver case

| | Receiver case | | | | | | | |
|---|---|---|---|---|---|---|---|---|
| | 1 | 2 | 3 | 4a | 4b | 4c | 5 | 6 |
| *Sub-source propagation mechanisms* | | | | | | | | |
| ***Region 1*** | | | | | | | | |
| Direct propagation | | X | X | | | | | |
| Simple diffraction | X | | | X | X | X | X | X |

| | | | | | | | | |
|---|---|---|---|---|---|---|---|---|
| Double diffraction | | | | | | | | |
| Multiple reflected rays (MRR) | | X | X | X | X | X | X | X |
| Multiple reflected diffracted rays (MRDR) | X | | | X | X | X | X | X |
| ***Region 2*** | | | | | | | | |
| Direct propagation | | | | | | | X | |
| Simple diffraction | | X | X | | | | | X |
| Double diffraction | X | | | X | X | X | | |
| Multiple reflected rays (MRR) | | X | X | X | X | X | X | X |
| Multiple reflected diffracted rays (MRDR) | X | | | X | X | X | X | X |
| ***Region 3*** | | | | | | | | |
| Direct propagation | | | | | | | | |
| Simple diffraction | | X | X | X | | X | X | X |
| Double diffraction | X | | | | X | | | |
| Multiple reflected rays (MRR) | | | | X | | | X | |
| Multiple reflected diffracted rays (MRDR) | | | | X | | | X | |
| ***Region 4*** | | | | | | | | |
| Direct propagation | | NA | NA | | | NA | | NA |
| Simple diffraction | X | NA | NA | X | X | NA | X | NA |
| Double diffraction | | NA | NA | | | NA | | NA |
| Multiple reflected rays (MRR) | | NA | NA | | | NA | | NA |
| Multiple reflected diffracted rays (MRDR) | NA | NA | | | | NA | | NA |

## 4.5. Segmentation of Roadway Source

The division of each roadway source into sub-sources to analyze different mechanisms influencing propagation creates a problem with the computation of noise levels. The fundamental noise equation's finite roadway adjustment is based on the angles from the receiver to the ends of the roadway as shown in Figure 4. The sub-sources no longer contain these necessary angles.

In the division of the original source, the angles to the boundaries of each region are calculated. Each pair of angles defining the region can be considered to be the angles necessary for input into the finite roadway adjustment. The noise levels from each sub-source are calculated separately and the results are summed to give the total noise level for each receiver.

## 4.6. Derivation of Reflective Propagation Mechanisms

The main research for the modeling of overlap gaps focuses on the development of the theory necessary to determine the noise level contributions from reflected sound waves. These reflected waves may reach the receiver by direct reflection or by diffracted reflection as discussed in preceding sections. The analysis of the remaining mechanisms influencing propagation (direct propagation, simple diffraction, and double diffraction) is a straightforward process. Direct propagation results in the sound level at a receiver generated by a source, neglecting any barrier attenuation. Simple diffraction can be calculated using Equation 1. Double diffraction is essentially the same as simple diffraction, using the barrier which generates the largest path length difference for input into the barrier attenuation algorithm.

This discussion will concentrate on the mechanisms of MRR and MRDR. Before these mechanisms can be derived, a basic introduction into image ray theory must first be presented.

### 4.6.1. Image Ray Analysis

A sound wave strikes a barrier at a certain angle from the perpendicular to the barrier, known as the angle of incidence. The wave reflects off at the same angle on the other side of the perpendicular, known as the angle of reflection. This concept is fundamental to the principles of geometrical ray acoustics. However, the computation of reflected sound energy is more complex. It should be noted that all reflections considered in the model are assumed to be specular. This means that upon striking a surface, sound energy is not scattered.

A vehicle traveling on a highway can be considered to be emitting sound waves from a point if the distance between the vehicle and receiver is at least twice the greatest dimension of the vehicle or greater than the wavelength of the lowest frequency sound wave emitted from a vehicle. Rarely is a receiver located less than this distance from the source.

From any given point along the roadway, there is only one path that a ray can take to reach a potential receiver. This path is characterized by the ray's horizontal and vertical angles with respect to the source. If a vehicle is stationary, the determination of these angles for the ray is trivial. However, traffic noise modeling involves the analysis of moving vehicles.

As an individual vehicle approaches a receiver, the instantaneous noise level increases until the vehicle is at a position closest to the receiver, after which the instantaneous noise level falls off. Equation 1 allows the modeling of the same phenomenon for numerous vehicles of different classes traveling on many roadways. This assembling of individual vehicles causes a problem in that the point from which a sound wave is emitted can no longer be identified. A

well-defined point responsible for the emission of the sound wave must be specified in order to determine whether or not the path of the sound wave is valid.

As described previously, the roadway was divided into sub-sources in order to define the zones from which different mechanisms affecting propagation originated. This procedure will be repeated, but to a much greater extent, in order to attain short roadway segments that approach the dimensions of a single vehicle or smaller. Each of these segments represents a portion of the total energy contained in the sound source. The reflective mechanisms influencing propagation from each of these segments can be analyzed and summed to attain their total contribution to the noise level.

Through this segmentation process, a particular source region may be divided into several hundred segments. Each individual segment's horizontal and vertical propagation angles are calculated from the mid-angle point of the segment. This mid-angle point approximates the location of the energy centroid of the segment.

Testing was performed to determine the validity of using the mid-angle point for calculating the segment's horizontal and vertical propagation angles. As the length of the segment approaches zero, the mid-angle approximation becomes more accurate. The accuracy of the method is maximized by dividing the roadways into many equal-angle sub-segments to minimize each segment's length. An expert in the acoustics field was consulted to verify that the mid-angle is the appropriate location at which reflection angles may be calculated to represent the total energy of a segment [Anderson 1996].

With this point being defined, rays from each segment can be individually analyzed and summed over the length of the source region. The division of a source region into segments is demonstrated in Figure 12.

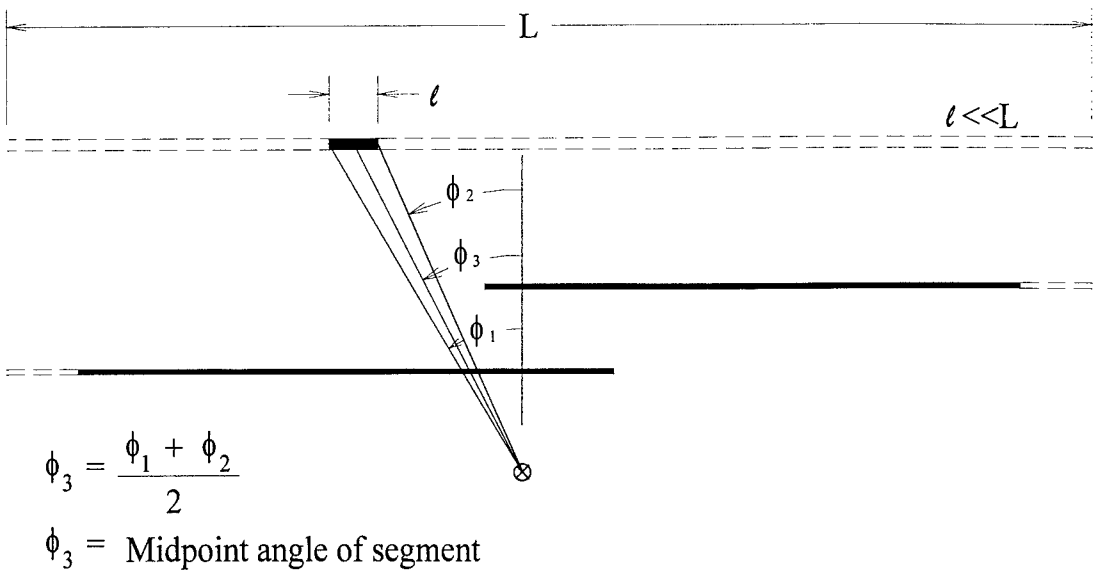


Figure 12. Source region segmentation

From any given segment in a valid source region, it is possible for a number of rays to reach a given receiver. However, as stated previously, for each segment there are required horizontal and vertical angles from which a ray must be emitted from the source to reach the receiver. Rays not traveling at these angles will either pass by the receiver or fail to enter the overlap gap altogether. Each ray must be analyzed to determine if it can reach the receiver.

Although all rays (direct, diffracted, and/or reflected) originate from the source location, ray tracing can be used to graphically illustrate the location from which the ray appears to originate, known as the image source. Image sources allow the necessary angles to be calculated more readily without compromising the physical principles involved. Figure 13 illustrates an example of the image source concept.

With every reflection that occurs, the perpendicular distance that a ray must travel increases by an amount equal to the length of the perpendicular component of the ray's reflected path between the actual source and receiver. By creating an image source at a distance equal to this component beyond the actual source, the same horizontal propagation angle can be used in drawing the image ray. The same holds true for the vertical propagation angle. By illustrating the process using image rays and sources, the geometrical relationships defining the propagation angles and distances can be established more easily. This is especially true for image rays that are comprised of many reflections.

This process is required for each reflective mechanism, MRR and MRDR. Since the geometrical relationships between source and receiver change depending on the receiver's location, separate equations defining the propagation path are needed for each receiver case. The ensuing discussions will focus on the determination of these necessary equations. The equations are required for implementing the theory into the model. Since thousands of rays are analyzed for any given receiver and the results are coded for computer implementation, the equations will be presented using index notation.

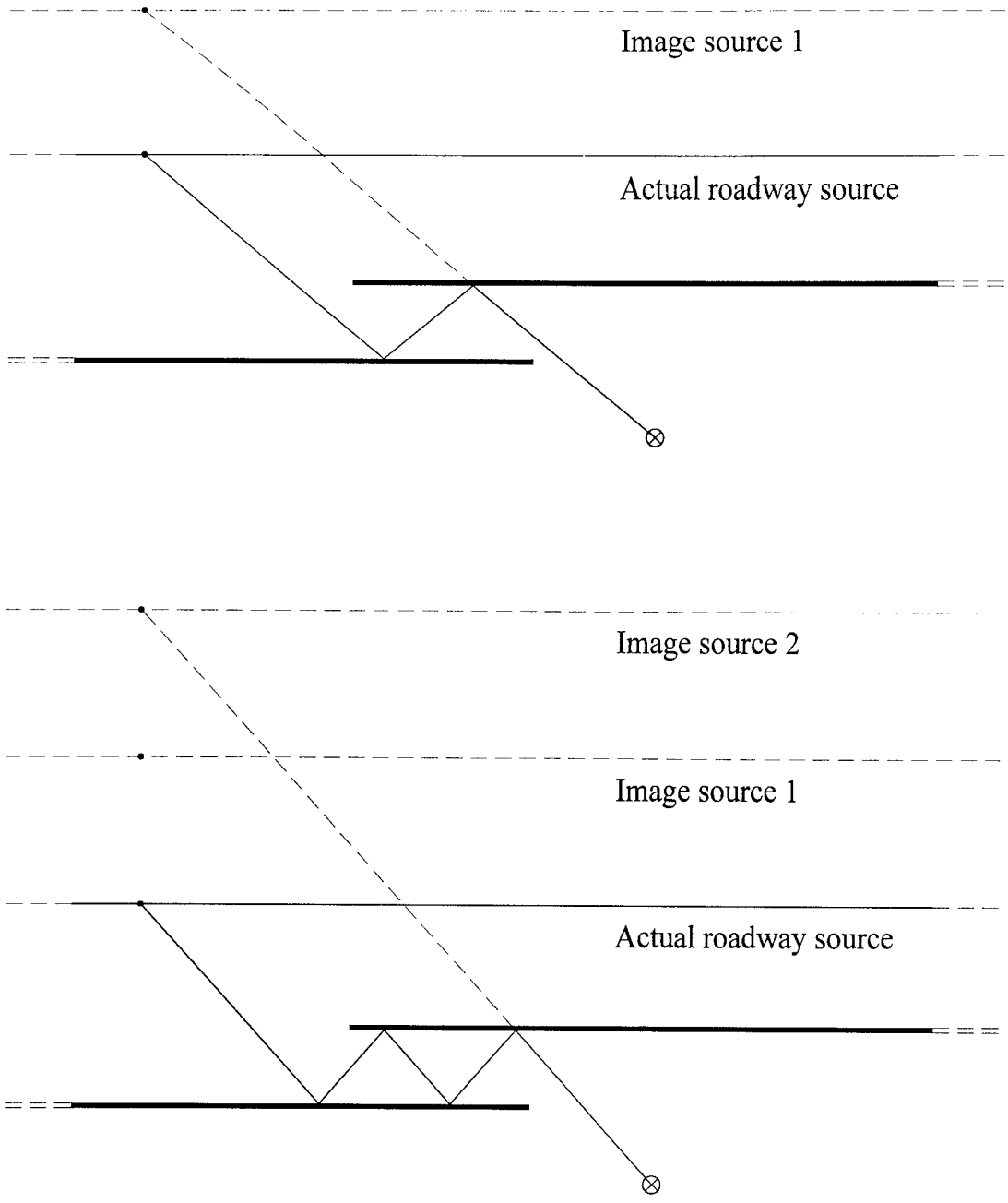


Figure 13. Image source concept

### 4.6.2. Case 1 MRDR: Horizontal Propagation

With each reflection, the perpendicular distance between the image source and the receiver increases. This horizontal distance, known as the image source distance, is determined for Case 1 MDRR by the following equations. Figure 14 shows a graphical representation of the problem.

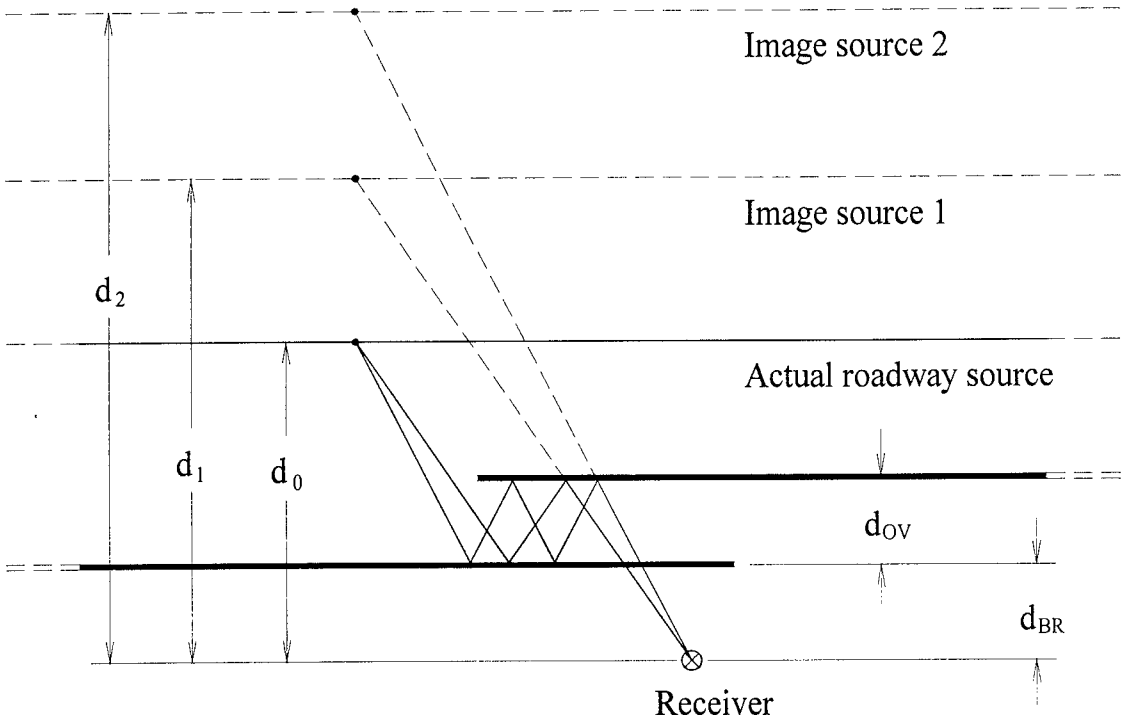


Figure 14. Horizontal propagation of Case 1 MRDR

$$d_1 = d_0 + (2 \times d_{OV})$$

$$d_2 = d_0 + (4 \times d_{OV})$$

$$d_i = d_0 + (2 \times i) d_{OV} \tag{8}$$

where

$d_i$ perpendicular distance from the $i$th image source to the receiver.

$d_0$ perpendicular distance from the roadway source to the receiver.

$d_{OV}$ overlap gap width.

The development of the vertical propagation of Case 1 MRDR requires that the horizontal perpendicular distance be computed from the image source to the respective barrier off which each reflection occurs. Equation 9 is the result of this procedure.

$$\text{Image source 1} \begin{cases} \text{Reflection 1} : Dist_{11} = d_0 - d_{BR} \\ \text{Reflection 2} : Dist_{12} = d_0 - d_{BR} + d_{OV} \end{cases}$$

$$\text{Image source 2} \begin{cases} \text{Reflection 1} : Dist_{21} = d_0 - d_{BR} \\ \text{Reflection 2} : Dist_{22} = d_0 - d_{BR} + d_{OV} \\ \text{Reflection 3} : Dist_{23} = d_0 - d_{BR} + 2d_{OV} \\ \text{Reflection 4} : Dist_{24} = d_0 - d_{BR} + 3d_{OV} \end{cases}$$

$$Dist_{ij} = d_0 - d_{BR} + (j-1) d_{OV} \tag{9}$$

where

$Dist_{ij}$ perpendicular distance from the $i$th image source to the $j$th reflection.

$d_0$ perpendicular distance from the roadway source to the receiver.

$d_{BR}$ perpendicular distance from the near barrier to the receiver.

$d_{OV}$ overlap gap width.

### 4.6.3. Case 1 MRDR: Vertical Propagation

Similar to the horizontal propagation of Case 1 MRDR, the height of each reflection increases before the ray is diffracted over the near barrier to the receiver. Figure 15 shows the vertical propagation of the image ray for two source images. The derivation of the equation to calculate the vertical propagation angle follows:

$$\tan\theta_1 = \frac{Z_N - Z_S}{d_1 - d_{BR}}$$

$$\tan\theta_2 = \frac{Z_N - Z_S}{d_2 - d_{BR}}$$

$$\tan\theta_i = \frac{Z_N - Z_S}{d_i - d_{BR}} \qquad (10)$$

where

$\theta_i$ vertical angle of the $i$th image ray from the horizontal.

$Z_N$ elevation of the top of the near barrier.

$Z_S$ elevation of the source (vehicle-class dependent).

$d_i$ perpendicular distance from the $i$th image source to the receiver, as determined from Equation 8.

$d_{BR}$ perpendicular distance from the near barrier to the receiver.

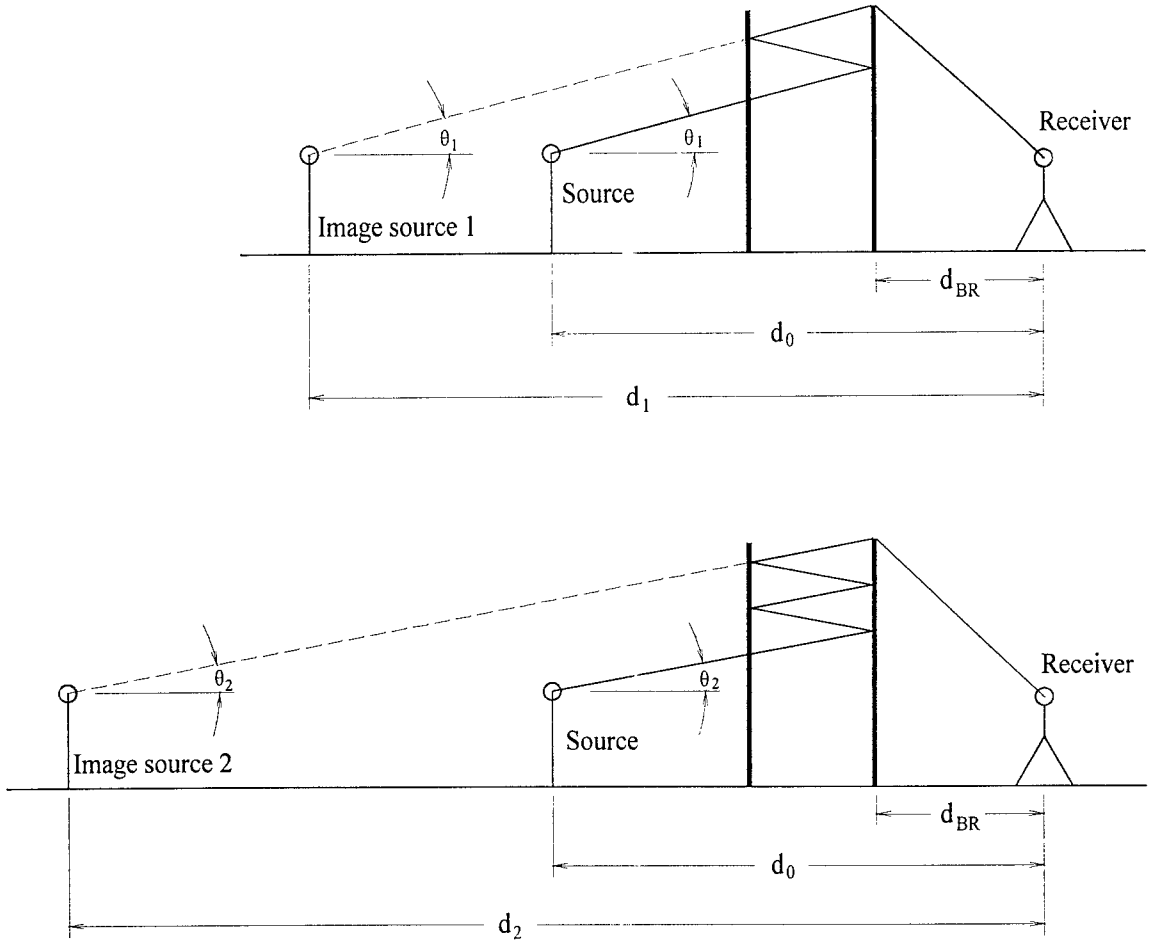


Figure 15. Vertical propagation of Case 1 MRDR

Equation 10 allows the vertical propagation angle of each ray to be computed. However, it is of greater interest to be able to compute the elevation of the ray every time it strikes a barrier and is reflected or diffracted. This will make it possible to verify whether or not a ray is capable of successfully propagating to a receiver. Also, by determining the elevation of each reflection, a specific absorption coefficient may be assigned to each reflection to model the effect of

absorptive treatment. Given Equation 10, the height of each reflection relative to the source, $H_{ij}$, can be determined by the following:

$$\tan\theta_i = \frac{Z_N - Z_S}{d_i - d_{BR}} \tag{10}$$

$$\tan\theta_i = \frac{H_{ij}}{Dist_{ij}} \tag{11}$$

Combining Equations 10 and 11, the height of each reflection relative to the source is:

$$H_{ij} = (Z_N - Z_S)\left(\frac{Dist_{ij}}{d_i - d_{BR}}\right) \tag{12}$$

Since the user-inputs to the model will be based on elevations relative to some arbitrary datum, not necessarily the source, it would be more useful for Equation 12 to be generalized to give the elevation of each reflection.

$$Z_{Rij} = (Z_N - Z_S)\left(\frac{Dist_{ij}}{d_i - d_{BR}}\right) + Z_S \tag{13}$$

where

$Z_{Rij}$ elevation of the $j$th reflection from the $i$th image source.

$Z_N$ elevation of the top of the near barrier.

$Z_S$ elevation of the source (vehicle-class dependent).

$Dist_{ij}$ perpendicular distance from the $i$th image source to the $j$th reflection, as determined from Equation 9

$d_i$ perpendicular distance from the $i$th image source to the receiver, as determined from Equation 8.

$d_{BR}$ perpendicular distance from the near barrier to the receiver.

### 4.6.4. Case 2 MRR: Horizontal Propagation (even-numbered reflections)

Case 2 MRR differ significantly from Case 1 MRDR. The primary reason the difference exists is the location of the receiver. Case 1 receivers are located behind the near barrier wall. These receivers are protected from direct reflected rays. Consequently, all sound waves that contribute to a Case 1 receiver's noise level must be diffracted by either the near or far barrier, or both.

Case 2 receivers are located in front of the near barrier but behind the far barrier. Because of their location, these receivers are susceptible to direct rays. All reflected rays that contribute to a Case 2 receiver's noise level are not diffracted over a noise barrier. Other rays can influence a Case 2 receiver through simple diffraction, but this discussion focuses only on those rays that are reflected within an overlap gap region. None of the reflected rays will be diffracted.

The analysis of Case 2 receivers brings forward another complication that did not exist in Case 1. Case 1 MRDR (due to the geometry of the barrier, roadways, and receivers) always consist of an even number of reflections. This implies that an equal number of reflections occur on both near and far barriers before a sound wave reaches a receiver.

Case 2 MRR can be made up of odd or even-numbered reflections, again depending on the geometry of the components. A ray can reach a receiver by reflecting off of both barriers an equal number of times (even-numbered reflections) or by reflecting off of the near barrier one more time than the far barrier (odd-numbered reflections). This requires the derivation of solutions to two different problems. With even-numbered reflections, the image source is

located beyond the actual roadway source, as was the situation with Case 1 MRDR. However, with odd-numbered reflections, the image source is actually located behind the receiver. This section will deal with the determination of the equations necessary to find the horizontal distances of even-numbered reflections.

The following work, along with Figure 16, is the derivation of the horizontal propagation of even-numbered Case 2 MRR.

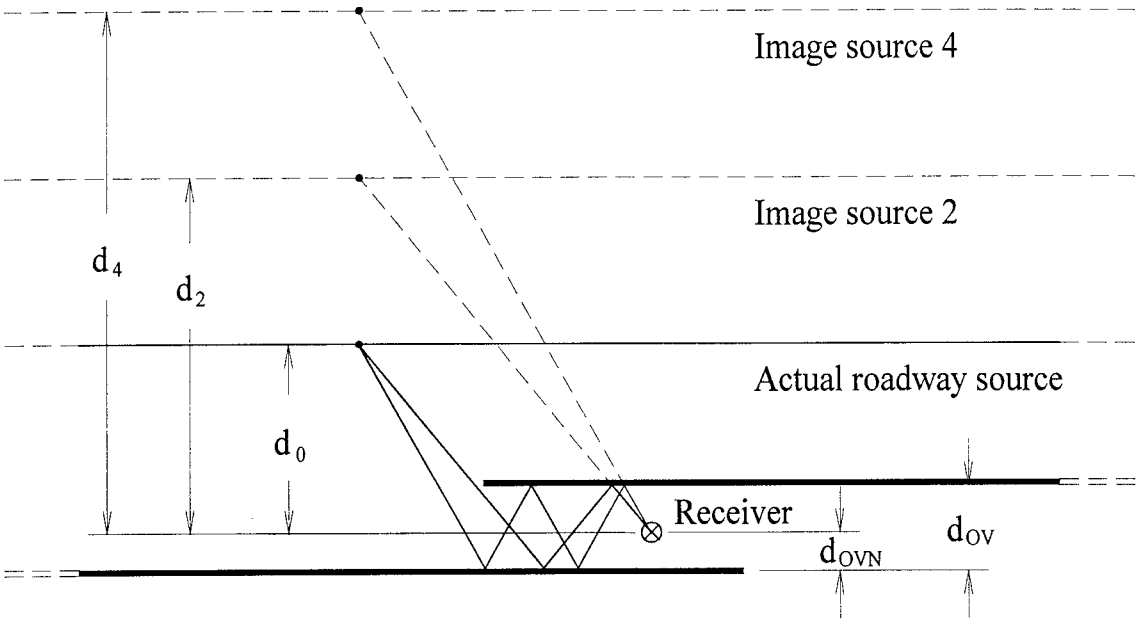


Figure 16. Horizontal propagation of even-numbered Case 2 MRR

$$d_2 = d_0 + (2 \times d_{OV})$$

$$d_4 = d_0 + (4 \times d_{OV})$$

$$d_i = d_0 + i(d_{OV}) \qquad \text{for } i = 2,\ 4,\ 6,\ \ldots \tag{V}$$

where

$d_i$ perpendicular distance from the $i$th image source to the receiver, for $i = 2, 4, 6, ...$

$d_0$ perpendicular distance from the roadway source to the receiver.

$d_{OV}$ overlap gap width.

Inspection of Equation 14 shows that it is basically the same formulation as Equation 8, except for the change in indices. This is essential for the development of Case 2 MRR, as mentioned before, because the location of the image source and all subsequent governing equations depends on whether the image ray has an even or odd number of reflections.

As with Case 1 MRDR, it is helpful to establish the horizontal perpendicular distance from the image source to each reflection for every image ray since it will be needed to determine the vertical propagation of the image ray.

$$\text{Image source 2} \begin{cases} \text{Reflection 1} : Dist_{21} = d_0 + d_{OVN} \\ \text{Reflection 2} : Dist_{22} = d_0 + d_{OVN} + d_{OV} \end{cases}$$

$$\text{Image source 4} \begin{cases} \text{Reflection 1} : Dist_{41} = d_0 + d_{OVN} \\ \text{Reflection 2} : Dist_{42} = d_0 + d_{OVN} + d_{OV} \\ \text{Reflection 3} : Dist_{43} = d_0 + d_{OVN} + 2d_{OV} \\ \text{Reflection 4} : Dist_{44} = d_0 + d_{OVN} + 3d_{OV} \end{cases}$$

$$Dist_{ij} = d_0 + d_{OVN} + (j-1)d_{OV} \qquad \text{for } i = 2,\ 4,\ 6,\ ... \tag{15}$$

where

$Dist_{ij}$ perpendicular distance from the $i$th image source to the $j$th reflection, for $i = 2, 4, 6, ...$

$d_0$ perpendicular distance from the roadway source to the receiver.

$d_{OVN}$ perpendicular distance from the receiver to the near barrier.

$d_{OV}$ overlap gap width.

### 4.6.5. Case 2 MRR: Horizontal Propagation (odd-numbered reflections)

The determination of the horizontal propagation of odd-numbered Case 2 MRR is significantly different than that of even-numbered Case 2 MRR. The main difference, as mentioned in the previous section, is the location of the image source. The image source for odd-numbered Case 2 MRR is positioned behind the receiver and the near barrier. It is located somewhere on the residential side of the noise barriers. This can initially be difficult to understand, but Figure 17 helps clarify the geometrical relationships that are involved.

The determination of the horizontal perpendicular distance from the image source to the receiver will be performed in a manner similar to before.

$$d_1 = d_0 + (2 \times d_{OVN})$$

$$d_3 = d_0 + (2 \times d_{OVN}) + (2 \times d_{OV})$$

$$d_5 = d_0 + (2 \times d_{OVN}) + (4 \times d_{OV})$$

$$d_i = d_0 + (2 \times d_{OVN}) + (i-1)d_{OV} \qquad \text{for } i = 1,\ 3,\ 5,\ \ldots \tag{16}$$

where

$d_i$ perpendicular distance from the $i$th image source to the receiver, for $i = 1, 3, 5, \ldots$

$d_0$ perpendicular distance from the roadway source to the receiver.

$d_{OVN}$ perpendicular distance from the receiver to the near barrier.

$d_{OV}$ overlap gap width.

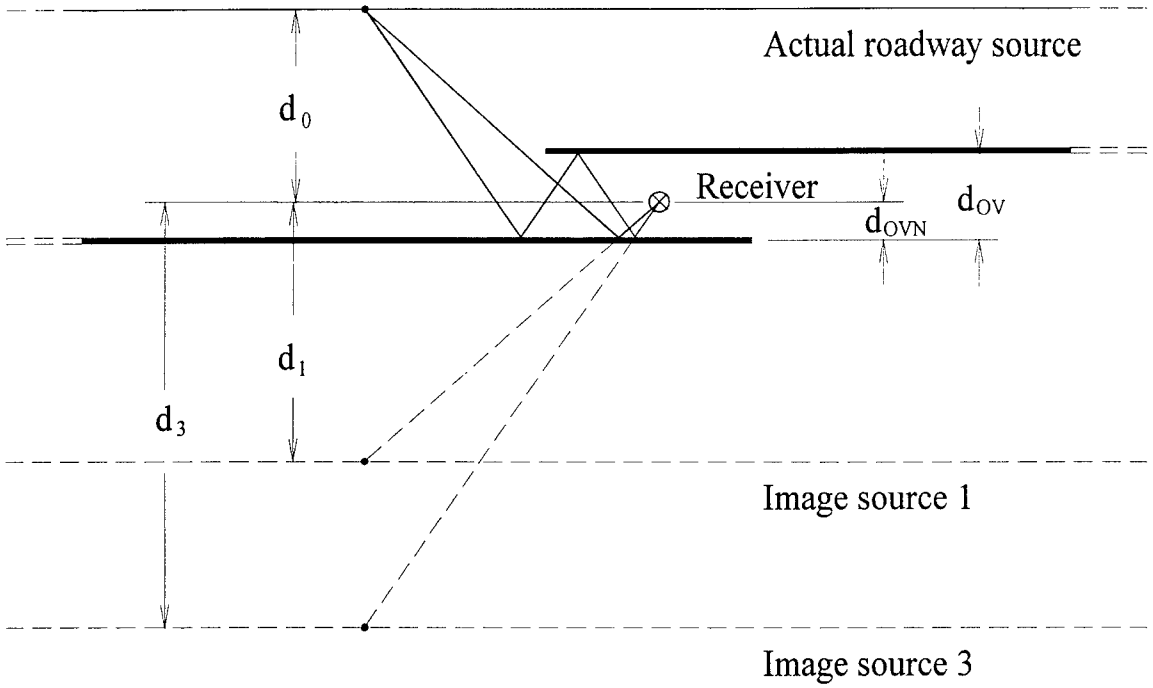


Figure 17. Horizontal propagation of odd-numbered Case 2 MRR

The determination of the intermediate horizontal distances from the image source to the receiver can be found using the same formulation as used for the even-numbered situation. Two image sources have been checked to demonstrate that the same relationships hold true.

$$\text{Image source 1} \left\{ \begin{array}{l} \text{Reflection 1} : Dist_{11} = d_0 + d_{OVN} \end{array} \right.$$

$$\text{Image source 3} \left\{ \begin{array}{l} \text{Reflection 1} : Dist_{31} = d_0 + d_{OVN} \\ \text{Reflection 2} : Dist_{32} = d_0 + d_{OVN} + d_{OV} \\ \text{Reflection 3} : Dist_{33} = d_0 + d_{OVN} + 2d_{OV} \end{array} \right.$$

$$Dist_{ij} = d_0 + d_{OVN} + (j-1)d_{OV} \qquad \text{for } i = 1,\ 3,\ 5,\ \ldots \tag{15}$$

where

$Dist_{ij}$ perpendicular distance from the $i$th image source to the $j$th reflection, for $i = 1, 3, 5, ...$

$d_0$ perpendicular distance from the roadway source to the receiver.

$d_{OVN}$ perpendicular distance from the receiver to the near barrier.

$d_{OV}$ overlap gap width.

### 4.6.6. Case 2 MRR: Vertical Propagation (even-numbered reflections)

Just as the horizontal propagation of Case 2 MRR varied depending on whether the total number of reflections were odd or even, so does the vertical propagation. The variation in the vertical propagation are a result of the differences in the horizontal computations. The odd and even-numbered vertical propagation discussion of Case 2 receivers could be combined. However, to eliminate any confusion that might result, the two conditions have been kept separate.

The vertical propagation angle of the image ray from the image source to the receiver is defined below. Figure 18 is a graphical illustration of the vertical propagation of the even-numbered Case 2 MRR.

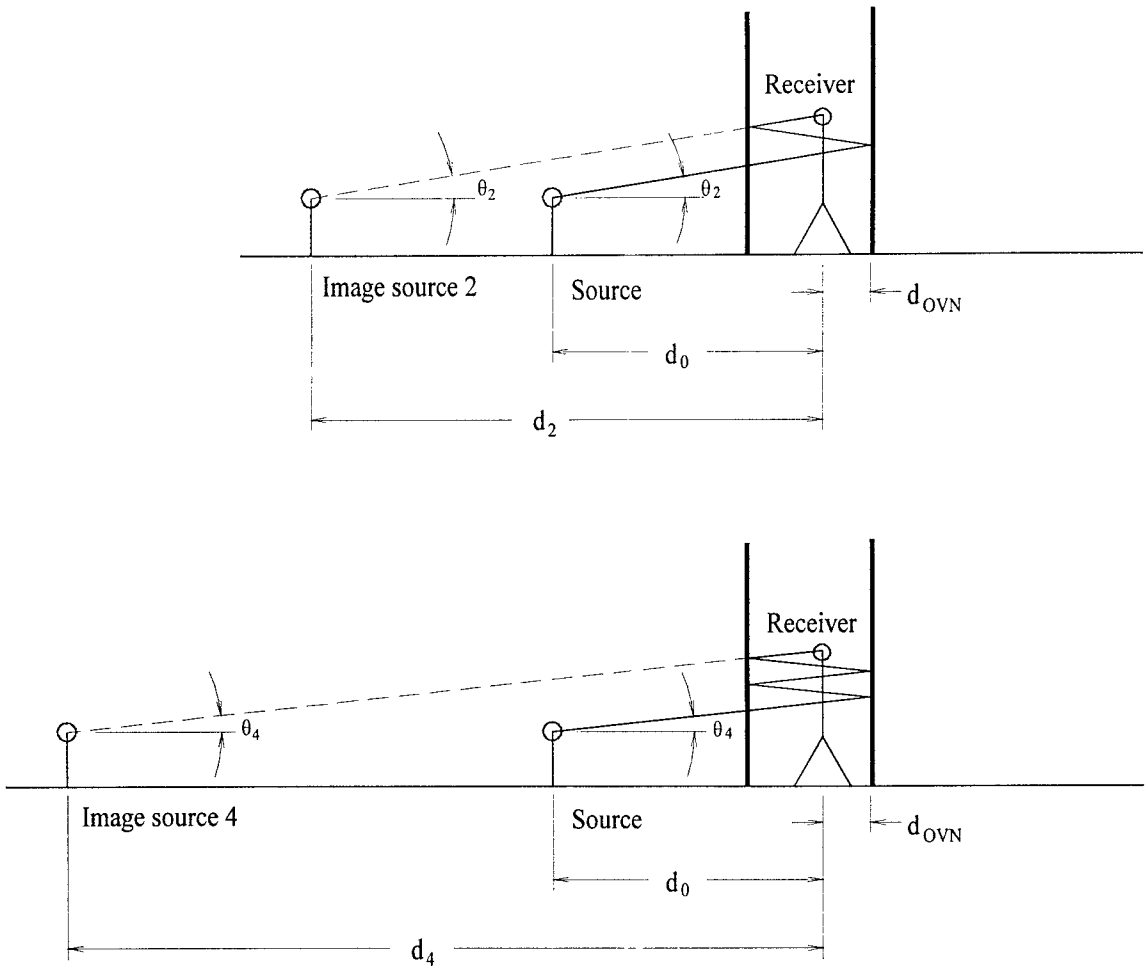


Figure 18. Vertical propagation of even-numbered Case 2 MRR

$$\tan\theta_2 = \frac{Z_R - Z_S}{d_2}$$

$$\tan\theta_4 = \frac{Z_R - Z_S}{d_4}$$

$$\tan\theta_i = \frac{Z_R - Z_S}{d_i} \qquad \text{for } i = 2,\ 4,\ 6,\ \ldots \tag{17}$$

where

$\theta_i$ vertical angle of the $i$th image ray from the horizontal, for $i = 2, 4, 6, ...$

$Z_R$ elevation of the receiver.

$Z_S$ elevation of the source (vehicle-class dependent).

$d_i$ perpendicular distance from the $i$th image source to the receiver, as determined from Equation 14, for $i = 2, 4, 6, ...$

Similar to previous cases, Equation 17 will be manipulated to provide an equation that enables the determination of the elevation of each reflection.

$$\tan\theta_i = \frac{Z_R - Z_S}{d_i} \tag{17}$$

$$\tan\theta_i = \frac{H_{ij}}{Dist_{ij}} \tag{18}$$

Combining Equations 17 and 18, the height of each reflection relative to the source, $H_{ij}$, is:

$$H_{ij} = (Z_R - Z_S)\left(\frac{Dist_{ij}}{d_i}\right) \qquad \text{for } i = 2,\ 4,\ 6,\ ... \tag{19}$$

Equation 19 is modified to give Equation 20, which allows the calculation of the elevation of each reflection from the $i$th image source:

$$Z_{Rij} = (Z_R - Z_S)\left(\frac{Dist_{ij}}{d_i}\right) + Z_S \qquad \text{for } i = 2,\ 4,\ 6,\ ... \tag{20}$$

where

$Z_{Rij}$ elevation of the $j$th reflection from the $i$th image source, for $i = 2, 4, 6, ...$

$Z_R$ elevation of the receiver.

$Z_S$ elevation of the source (vehicle-class dependent).

$Dist_{ij}$ perpendicular distance from the $i$th image source to the $j$th reflection, as determined from Equation 15, for $i = 2, 4, 6, ...$

$d_i$ perpendicular distance from the $i$th image source to the receiver, as determined from Equation 14, for $i = 2, 4, 6, ...$

### 4.6.7. Case 2 MRR: Vertical Propagation (odd-numbered reflections)

The vertical propagation angle is derived in the work that follows. Figure 19 displays the graphical concepts involved in the derivation of the vertical propagation of the odd-numbered Case 2 MRR.

$$\tan\theta_1 = \frac{Z_R - Z_S}{d_1}$$

$$\tan\theta_3 = \frac{Z_R - Z_S}{d_3}$$

$$\tan\theta_i = \frac{Z_R - Z_S}{d_i} \qquad \text{for } i = 1,\ 3,\ 5,\ \ldots \tag{21}$$

where

$\theta_i$ vertical angle of the $i$th image ray from the horizontal, for $i = 1, 3, 5, ...$

$Z_R$ elevation of the receiver.

$Z_S$ elevation of the source (vehicle-class dependent).

$d_i$ perpendicular distance from the $i$th image source to the receiver, as

determined from Equation 16, for $i = 1, 3, 5, \ldots$

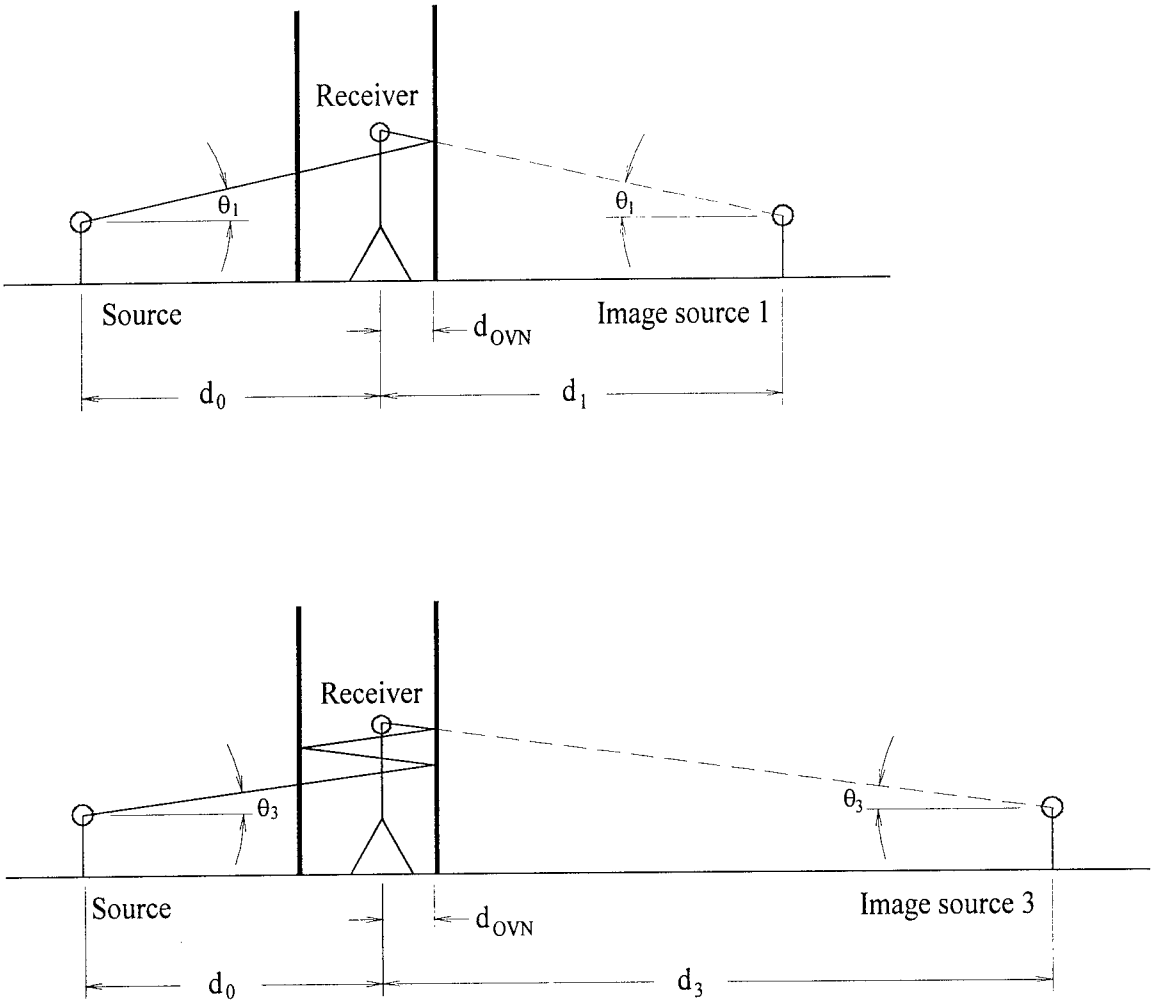


Figure 19. Vertical propagation of odd-numbered Case 2 MRR

Equation 21 will now be transformed into a form that will make it possible to calculate the elevation of each reflection.

$$\tan\theta_i = \frac{Z_R - Z_S}{d_i} \tag{21}$$

$$\tan\theta_i = \frac{H_{ij}}{Dist_{ij}} \tag{22}$$

Combining Equations 21 and 22, the height of each reflection relative to the source is:

$$H_{ij} = (Z_R - Z_S)\left(\frac{Dist_{ij}}{d_i}\right) \qquad \text{for } i = 1,\ 3,\ 5,\ \ldots \tag{23}$$

Equation 24 is used to calculate the elevation of each reflection for the $i$th image source.

$$Z_{Rij} = (Z_R - Z_S)\left(\frac{Dist_{ij}}{d_i}\right) + Z_S \qquad \text{for } i = 1,\ 3,\ 5,\ \ldots \tag{24}$$

where

$Z_{Rij}$ elevation of the $j$th reflection from the $i$th image source, for $i = 1, 3, 5, \ldots$

$Z_R$ elevation of the receiver.

$Z_S$ elevation of the source (vehicle-class dependent).

$Dist_{ij}$ perpendicular distance from the $i$th image source to the $j$th reflection, as determined from Equation 15, for $i = 1, 3, 5, \ldots$

$d_i$ perpendicular distance from the $i$th image source to the receiver, as determined from Equation 16, for $i = 1, 3, 5, \ldots$

### 4.6.8. Case 3 MRR: Horizontal and Vertical Propagation

The derivation of Case 3 MRR theory follows the same steps as Case 2 MRR. Consequently, the work will not be repeated here. Reference is given to the preceding sections on Case 2 MRR. All equations and discussions are valid for both odd and even- numbered Case 3 MRR, including horizontal and vertical propagation. The only difference between Case 2 and Case 3 receivers is that Case 3 receivers are located past the overlap gap while receivers from Case 2 are located within the bounds of the overlap.

There are checks that must be performed to verify whether or not it is possible for a ray to reach a receiver. This is the step where the calculation of noise levels for Case 2 and Case 3 receivers differs. Case 3 requires one more check than Case 2 due to the fact that it is located outside of the bounds of the overlap gap. The discussion on these checks is located later in this chapter under the section entitled "Image Ray Existence Checks".

### 4.6.9. Cases 4, 5, and 6 MRR and MRDR : Horizontal Propagation

The horizontal propagation of Case 4, 5, and 6 MRR and MRDR is identical to that of Case 1 MRDR. For a full discussion on its development, the section covering Case 1 MRDR horizontal propagation should be consulted. The final equations from this section will be repeated here. Refer to Figure 14 as needed.

Equation 8 defines the horizontal perpendicular distance from the *i*th image source to the receiver.

$$d_i = d_0 + (2 \times i)dov \tag{8}$$

where

$d_i$ perpendicular distance from the *i*th image source to the receiver.

$d_0$ perpendicular distance from the roadway source to the receiver.

$dov$ overlap gap width.

To find the horizontal distance from the image source to each reflection for Case 4, 5, and 6 receivers, Equation 9 should be utilized.

$$Dist_{ij} = d_0 - d_{BR} + (j-1)dov \tag{9}$$

where

$Dist_{ij}$ perpendicular distance from the $i$th image source to the $j$th reflection.

$d_0$ perpendicular distance from the roadway source to the receiver.

$d_{BR}$ perpendicular distance from the near barrier to the receiver.

$d_{OV}$ overlap gap width.

### 4.6.10. Cases 4, 5, and 6 MRDR : Vertical Propagation

As with horizontal propagation, the vertical propagation for Case 4, 5, and 6 MRDR is analogous to that of Case 1 MRDR. Again, the reader is given reference to the section on Case 1 MRDR vertical propagation and Figure 15 for a full derivation of the following equations.

The vertical angle of the image ray from the $i$th image source referenced to the horizontal is given in Equation 10.

$$\tan\theta_i = \frac{Z_N - Z_S}{d_i - d_{BR}} \tag{10}$$

where

$\theta_i$ vertical angle of the $i$th image ray from the horizontal.

$Z_N$ elevation of the top of the near barrier.

$Z_S$ elevation of the source (vehicle-class dependent).

$d_i$ perpendicular distance from the $i$th image source to the receiver, as determined from Equation 8.

$d_{BR}$ perpendicular distance from the near barrier to the receiver.

The elevation of the jth reflection of the image ray from the ith image source is determined by Equation 13.

$$Z_{Rij} = (Z_N - Z_S)\left(\frac{Dist_{ij}}{d_i - d_{BR}}\right) + Z_S \tag{13}$$

where

$Z_{Rij}$ elevation of the $j$th reflection from the $i$th image source.

$Z_N$ elevation of the top of the near barrier.

$Z_S$ elevation of the source (vehicle-class dependent).

$Dist_{ij}$ perpendicular distance from the $i$th image source to the $j$th reflection, as determined from Equation 9.

$d_i$ perpendicular distance from the $i$th image source to the receiver, as determined from Equation 8.

$d_{BR}$ perpendicular distance from the near barrier to the receiver.

### 4.6.11. Cases 4, 5, and 6 MRR : Vertical Propagation

The vertical propagation of Case 4, 5, and 6 MRR is different than that of Case 4, 5, and 6 MRDR. Whereas MRDR are diffracted to the receiver by the near barrier, MRR are not diffracted but are propagated at a constant vertical angle from source to receiver. Due to this fact, the vertical propagation angle will change as will the formulation to determine the elevation of each reflection. Figure 20 shows the vertical propagation of Case 4, 5, and 6 MRR image rays.

$$\tan\theta_1 = \frac{Z_R - Z_S}{d_1}$$

$$\tan\theta_2 = \frac{Z_R - Z_S}{d_2}$$

$$\tan\theta_i = \frac{Z_R - Z_S}{d_i} \tag{25}$$

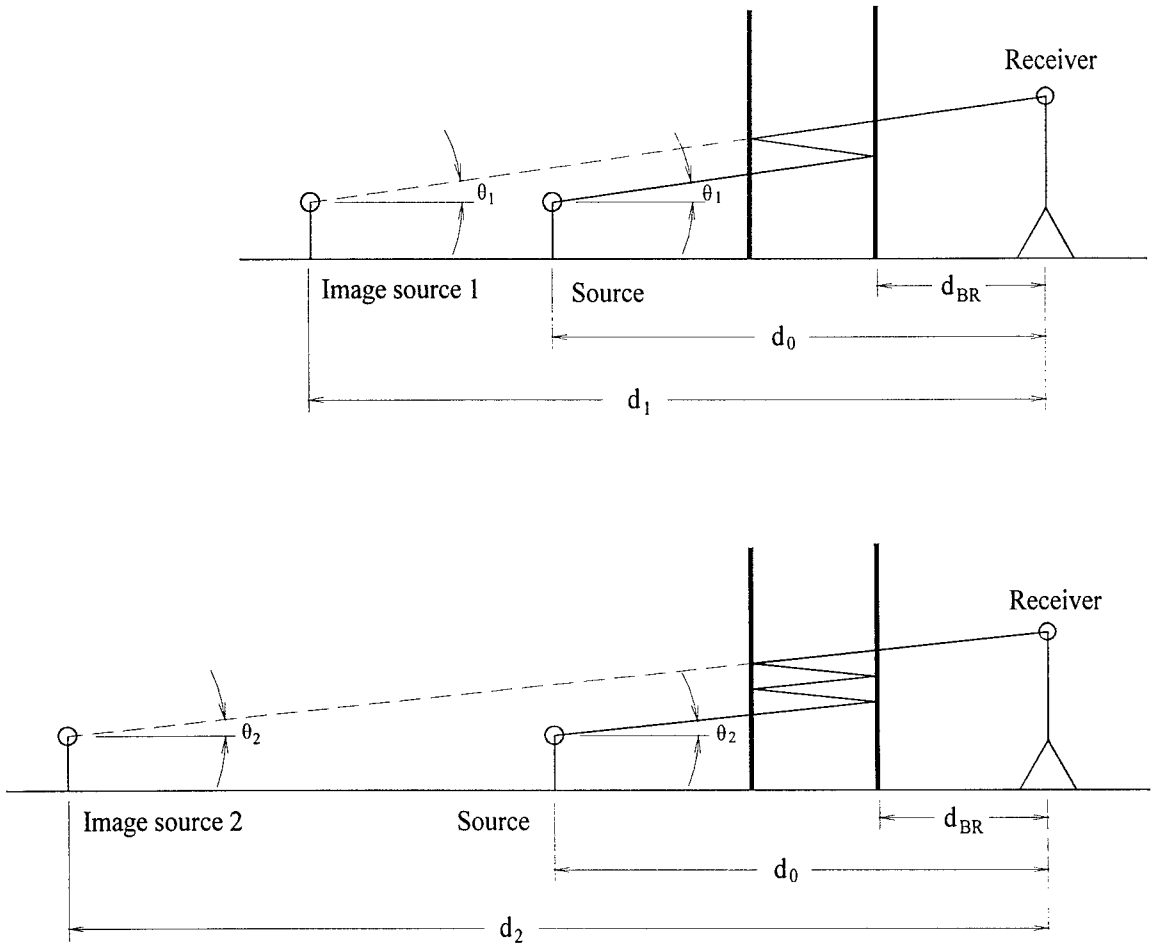


Figure 20. Vertical propagation of Case 4, 5, and 6 MRR

where

$\theta_i$ vertical angle of the *i*th image ray from the horizontal.

$Z_R$ elevation of the receiver.

$Z_S$ elevation of the source (vehicle-class dependent).

$d_i$ perpendicular distance from the *i*th image source to the receiver, as determined from Equation 8.

Equation 25 is used to calculate the vertical angle from the horizontal for the *i*th image ray. As in previous discussions, it is of greater interest to use the result of Equation 25 to develop an equation that will compute the elevation of each reflection. The necessary equations are derived as follows:

$$\tan\theta_i = \frac{Z_R - Z_S}{d_i} \tag{25}$$

$$\tan\theta_i = \frac{H_{ij}}{Dist_{ij}} \tag{11}$$

Combining (25) and (11), the height of each reflection relative to the source is:

$$H_{ij} = (Z_R - Z_S)\left(\frac{Dist_{ij}}{d_i}\right) \tag{26}$$

In order to determine the elevation of each reflection, Equation 26 must be modified to give the following result:

$$Z_{Rij} = (Z_R - Z_S)\left(\frac{Dist_{ij}}{d_i}\right) + Z_S \tag{27}$$

where

$Z_{Rij}$ elevation of the *j*th reflection from the *i*th image source.

$Z_R$ elevation of the receiver.

$Z_S$ elevation of the source (vehicle-class dependent).

$Dist_{ij}$ perpendicular distance from the *i*th image source to the *j*th reflection, as determined from Equation 9.

$d_i$ perpendicular distance from the *i*th image source to the receiver, as determined from Equation 8.

## 4.7. Image Ray Existence Checks

The derivation of reflective mechanisms affecting propagation in the preceding sections outlined the technique to establish the propagation parameters of horizontal and vertical angles of the image ray and the perpendicular distance from image source to receiver. These parameters must be analyzed to determine whether or not an image ray can successfully reach the receiver by this defined path. Checks are performed at critical points of the path to verify that the ray is reflected the number of times required. These checks will be based on the location of source and receiver with respect to the overlapped barriers. The following discussions will cover the derivation of all necessary horizontal and vertical propagation checks. However, before the checks can be described the technique used to determine if an image ray is MRDR or MRR must be explained.

### 4.7.1. Determination of Image Ray as MRDR or MRR

Before covering the image ray checks, it is necessary to establish the image ray as MRDR or MRR. This is required to define the vertical propagation path of the ray. Whereas the horizontal propagation is the same for both MRDR and MRR, the vertical path differs greatly. MRDR are diffracted over the top of the near barrier to the receiver while MRR follow a reflected path to the receiver with no diffraction. By distinguishing a ray as MRDR or MRR, the noise prediction equation can be modified to include barrier attenuation for MRDR or to omit this attenuation for MRR. This determination need only be performed for Case 4, 5, and 6 receivers as Case 1 receivers can only be influenced by MRDR while Case 2 and 3 receivers are only subject to MRR.

The determination of an image ray as MRDR or MRR is based on the path of the ray from the last reflection to the receiver. If the near barrier is located in this path, the ray will have to be diffracted over the near barrier to reach the receiver. If the near barrier is not located in the path, the ray can propagate directly to the receiver after the last reflection off of the far barrier. Figure 21 shows an example where the ray of the first image source is a MRDR while the second image source produces a MRR.

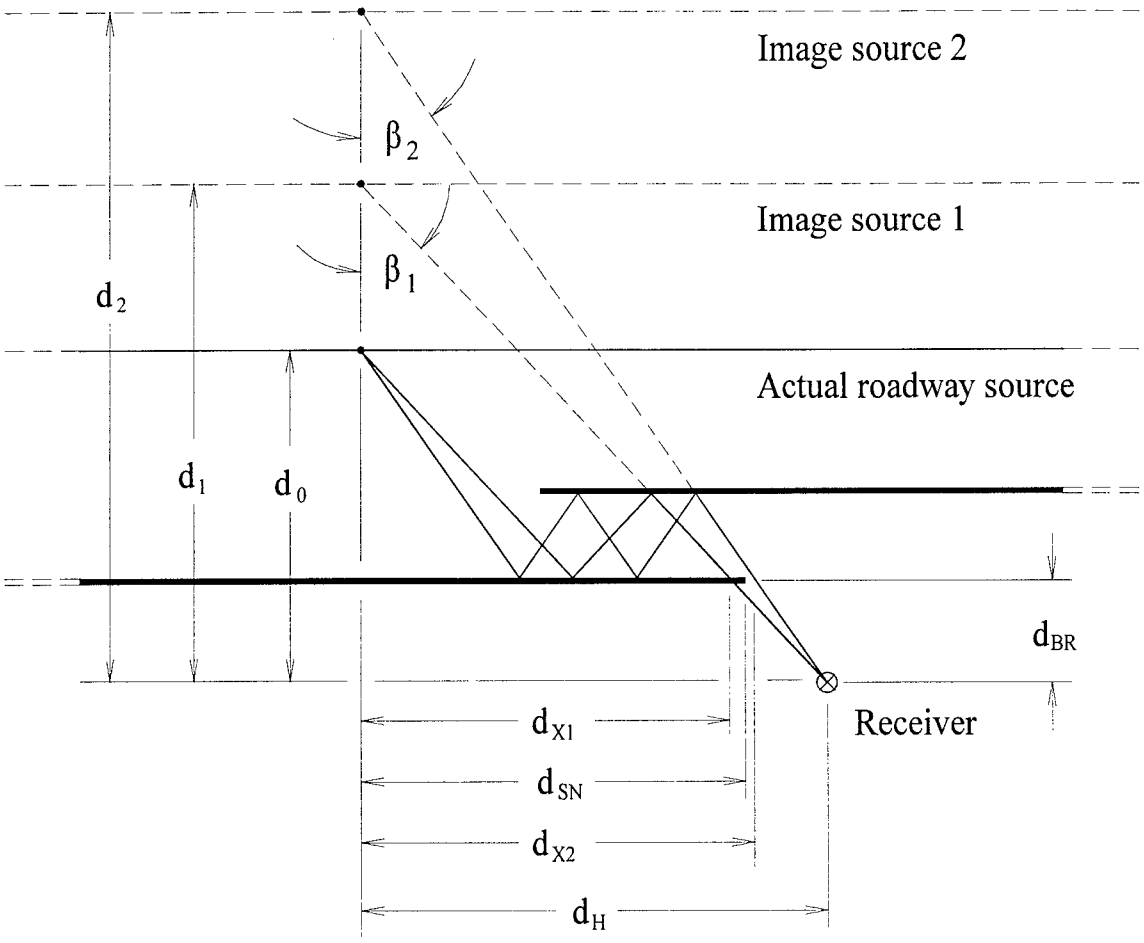


Figure 21. Determination of image ray type

The conditions that determine the image ray's reflective type are as follows:

$$\text{If } d_{Xi} > d_{SN} \quad \Rightarrow \quad \text{image ray is MRR}$$

$$\text{If } d_{Xi} < d_{SN} \quad \Rightarrow \quad \text{image ray is MRDR}$$

To determine the above variables, the following relationships are established:

$$\tan \beta_i = \frac{d_H}{d_i} \tag{28}$$

$$\tan \beta_i = \frac{d_{Xi}}{d_i - d_{BR}} \tag{29}$$

where

$\beta_i$ angle to the $i$th image ray from the perpendicular.

$d_H$ parallel distance from the receiver to the source.

$d_i$ perpendicular distance from the $i$th image source to the receiver.

$d_{Xi}$ parallel distance from the $i$th image source to the point where the $i$th image ray breaks the plane of the near barrier.

$d_{SN}$ parallel distance from the $i$th image source to the overlap end of the near barrier.

$d_{BR}$ perpendicular distance from the near barrier to the receiver.

Combining Equations 28 and 29,

$$d_{Xi} = d_H\left(\frac{d_i - d_{BR}}{d_i}\right) \tag{30}$$

$$d_{SN} = X_{\text{OVERLAP END OF NEAR BARRIER}} - X_{\text{IMAGE SOURCE}} \tag{31}$$

### 4.7.2. Far Barrier Entrance Check

The image ray must first be investigated to ensure that enough clearance exists for the ray to pass by the far barrier and enter the overlap gap. If sufficient clearance does not exist, the ray will be reflected from the highway side of the far wall and will not contribute to the sound level at the receiver. Figure 22 illustrates the relationships that must be considered in this check. All receivers, Cases 1-6, are subject to this analysis.

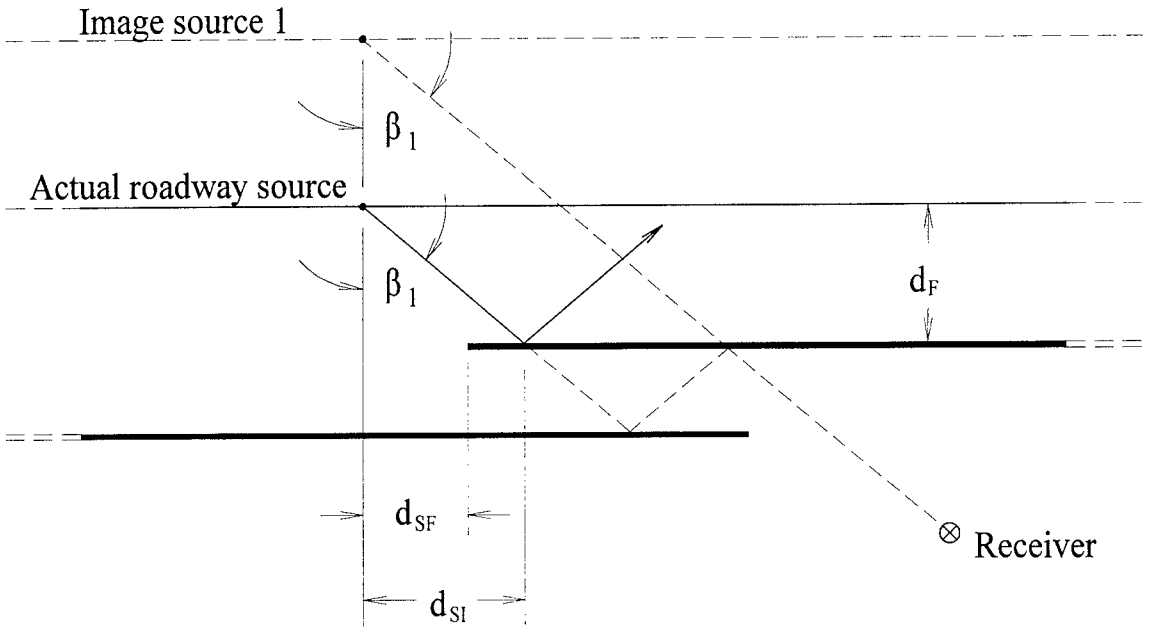


Figure 22. Far barrier entrance check

The check that determines if an image ray exists based on the above criteria is summarized below:

If $d_{SI} > d_{SF}$ $\Rightarrow$ image ray cannot enter the overlap gap

If $d_{SI} < d_{SF}$ $\Rightarrow$ image ray can enter the overlap gap

$$d_{SI} = d_F(\tan\beta_i) \tag{32}$$

$$d_{SF} = X_{\text{OVERLAP END OF FAR BARRIER}} - X_{\text{IMAGE SOURCE}} \tag{33}$$

where

$d_{SI}$ parallel distance from the $i$th image source to the point where the $i$th image ray first breaks the plane of the far barrier.

$d_F$ perpendicular distance from the roadway source to the far barrier.

$\beta_i$ angle to the $i$th image ray from the perpendicular.

$d_{SF}$ parallel distance from the $i$th image source to the overlap end of the far barrier.

### 4.7.3. Far Barrier First-Reflection Check

If the image ray passes the far barrier entrance check, it is subjected to the far barrier first-reflection check. Many image rays strike the near barrier at distances far from the overlap gap. Consequently, these reflected rays may not encounter the far barrier and may not contribute to the sound level at the receiver. These checks are necessary for all receivers in Cases 1,4, 5, and 6. Receivers in Case 2 and 3 regions are subject to this test for image rays composed of two or more reflections. The physical representation of this check is shown in Figure 23.

The following statements highlight the analysis of the far barrier first-reflection check.

If $d_{SJ} > d_{SF}$ $\Rightarrow$ image ray will be reflected off the far barrier

If $d_{SJ} < d_{SF}$ $\Rightarrow$ image ray will not be reflected off the far barrier

$$d_{SJ} = (d_F + 2d_{OV})(\tan\beta_i) \tag{34}$$

$$d_{SF} = X_{\text{OVERLAP END OF FAR BARRIER}} - X_{\text{IMAGE SOURCE}} \tag{35}$$

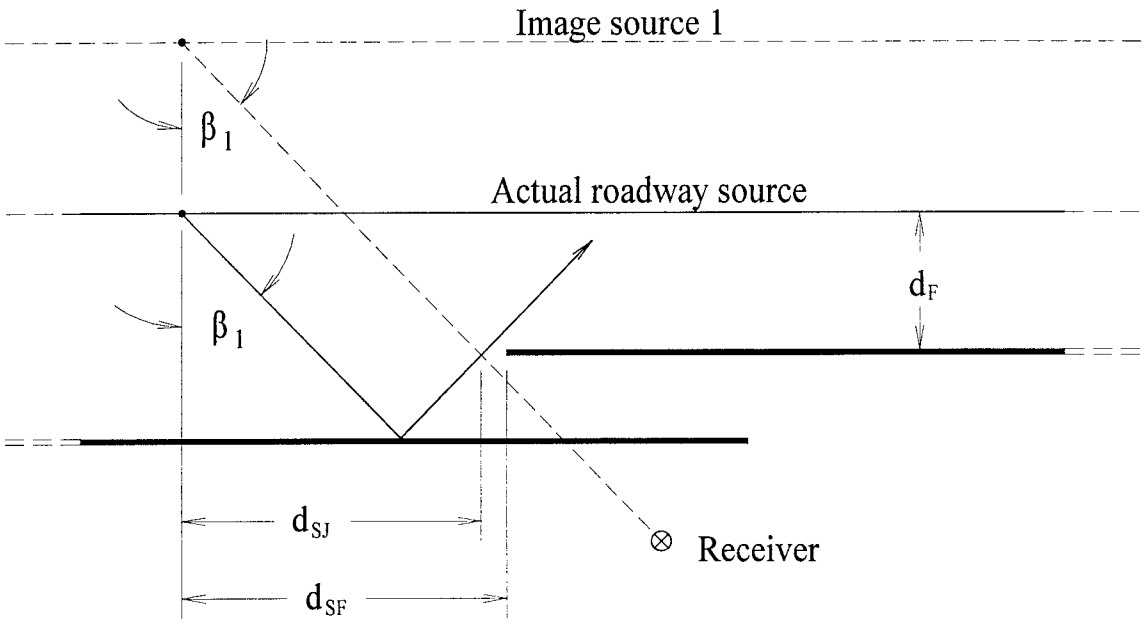


Figure 23. Far barrier first-reflection check

where

$d_{SJ}$ parallel distance from the $i$th image source to the point where the reflected ray from the first reflection of the $i$th image ray breaks the plane of the far barrier.

$d_F$ perpendicular distance from the roadway source to the far barrier.

$d_{OV}$ overlap gap width.

$\beta_i$ angle to the $i$th image ray from the perpendicular.

$d_{SF}$ parallel distance from the $i$th image source to the overlap end of the far barrier.

### 4.7.4. Near Barrier Next-To-Last-Reflection Check

Tests must also be conducted to verify that each image ray is properly reflected off the near barrier if the ray has successfully passed the two previous far barrier checks. As a ray propagates through the overlap gap, it can be subjected to many reflections before reaching a receiver. However, an image ray may never reach a potential receiver if the near wall is not of sufficient overlap length. This investigation checks each applicable image ray to answer the question: Is the near barrier long enough to reflect the next-to-last-reflection of the *i*th image ray to the far barrier? This analysis is shown graphically in Figure 24. Image rays influencing receivers in Cases 1, 4, 5, and 6 as well as Case 2 and 3 receivers subjected to rays composed of even-numbered reflections are tested for compliance with this check.

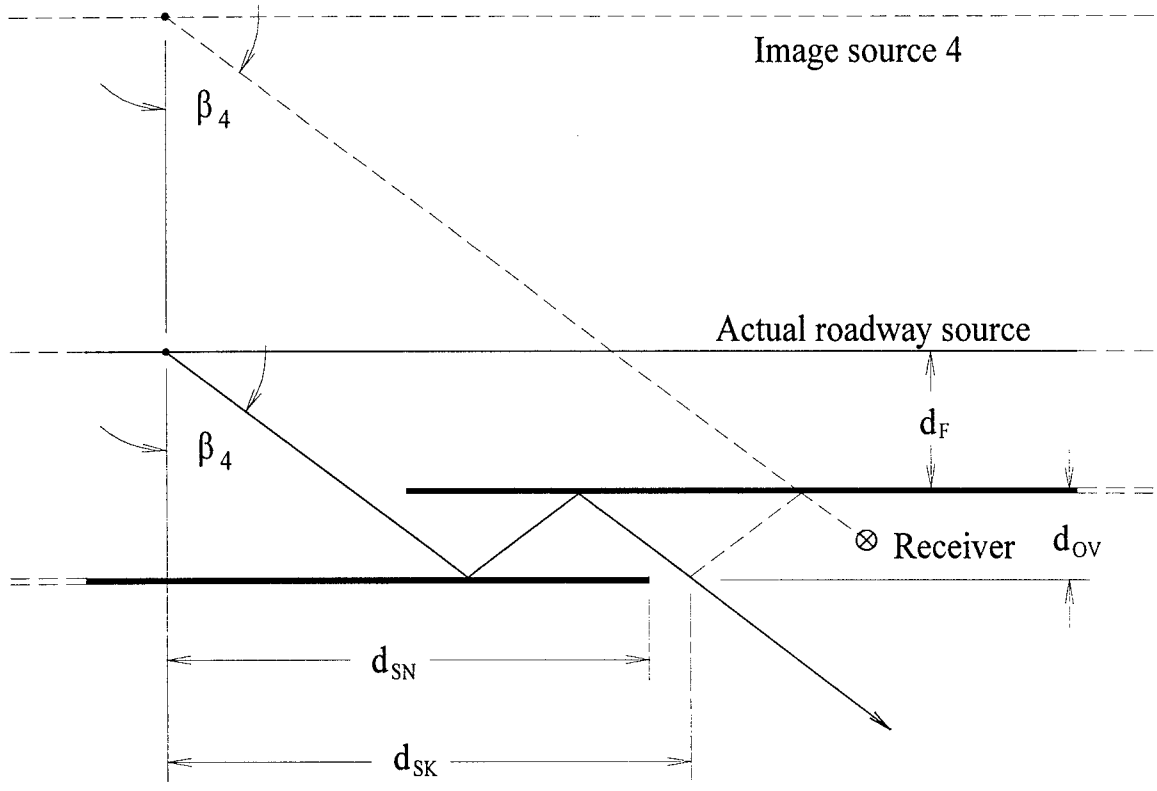


Figure 24. Near barrier next-to-last-reflection check

The results of this check can be attained by application of the following comparison to each prospective image ray.

If $d_{SK} > d_{SN}$ $\Rightarrow$ image ray will not be reflected off the near barrier

If $d_{SK} < d_{SN}$ $\Rightarrow$ image ray will be reflected off the near barrier

$$d_{SK} = \left[d_F + (i-1)d_{OV}\right](\tan\beta_i) \tag{36}$$

$$d_{SN} = X_{\text{OVERLAP END OF NEAR BARRIER}} - X_{\text{IMAGE SOURCE}} \tag{37}$$

where

$d_{SK}$ parallel distance from the $i$th image source to the point where the next-to-last-reflection of the $i$th image ray breaks the plane of the near barrier.

$d_F$ perpendicular distance from the roadway source to the far barrier.

$d_{OV}$ overlap gap width.

$\beta_i$ angle to the $i$th image ray from the perpendicular.

$d_{SN}$ parallel distance from the $i$th image source to the overlap end of the near barrier.

### 4.7.5. Near Barrier Last-Reflection Check

The final check that must be conducted on the horizontal propagation path of reflected image rays is a special case analysis for Case 2 and 3 receivers subjected to odd-numbered image rays. The basic guidelines are the same as for the previous check. However, since odd-

numbered image rays are emitted from image sources located behind the receiver, modifications must be made to account for the geometrical differences. This investigation determines if the near barrier is long enough to reflect the last reflection of the *i*th image ray to the receiver. Figure 25 illustrates an example of this check.

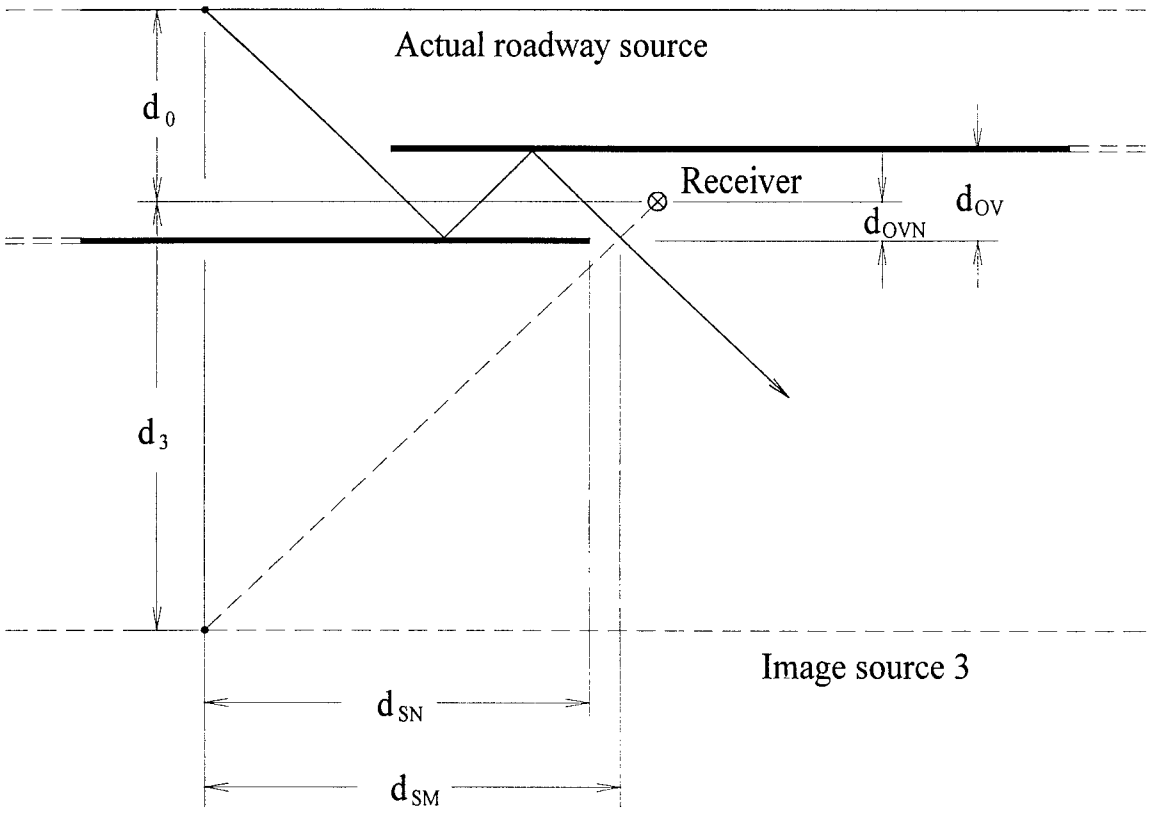


Figure 25. Near barrier last-reflection check

The equality statements used to prove whether or not an image ray is valid based on this analysis follow.

If $d_{SM} > d_{SN}$ $\Rightarrow$ image ray will not be reflected off the near barrier

If $d_{SM} < d_{SN}$ $\Rightarrow$ image ray will be reflected off the near barrier

$$d_{SM} = \left[d_O + d_{OVN} + (i-1)d_{OV}\right](\tan\beta_i) \tag{38}$$

$$d_{SN} = X_{\text{OVERLAP END OF NEAR BARRIER}} - X_{\text{IMAGE SOURCE}} \tag{39}$$

where

$d_{SM}$ parallel distance from the $i$th image source to the point where the last reflection of the $i$th image ray breaks the plane of the near barrier.

$d_O$ perpendicular distance from the roadway source to the receiver.

$d_{OVN}$ perpendicular distance from the receiver to the near barrier.

$d_{OV}$ overlap gap width.

$\beta_i$ angle to the $i$th image ray from the perpendicular.

$d_{SN}$ parallel distance from the $i$th image source to the overlap end of the near barrier.

### 4.7.6. Vertical Propagation Check

Similar to the horizontal path, checks need to be made on the vertical propagation path of the each image ray. The process is much more simple for vertical propagation compared to horizontal. The only check required is to verify that the height of each reflection is lower than the top and higher than the bottom of the barrier on which the reflection is occurring. If this condition is met, the ray will either propagate to the next barrier or to the receiver, if the reflection in question is the last. A derivation is not necessary for this discussion. The top and bottom elevations of each barrier are input by the user during analysis preparation, as discussed in the next chapter. In previous sections dealing with the vertical propagation of various case

receivers equations were derived which enabled the calculation of the elevation of each image ray reflection. These reflection elevations and the barrier elevations are compared. If the ray intersects the vertical plane of the barrier at a point higher than the top of the barrier or lower than the bottom of the barrier, the ray will not be reflected and will not contribute to the receiver's sound level.

# 5. COMPUTER IMPLEMENTATION OF THE MODEL

The theory from Chapter 3 is the main component in the Windows 95 gap analysis computer model that has been developed. Through the process of implementing the theory into Visual Basic program code, there were other issues which required further investigation. The following sections will discuss these issues that were fundamental in formulating the working model.

First, the inputs and outputs of the Gap Analysis Program will be discussed. The assumptions that were made in developing the program will then be discussed. The rest of the chapter will concentrate on technical issues that were addressed during the development of the computer model.

## 5.1. Model Inputs

In order to prepare the program for analysis, there are a number of inputs that must be entered by the user. These inputs involve primarily the geometrical positioning of the barriers, roadways, and receivers, along with the traffic that is present on each roadway. The program was designed to perform checks to ensure the data is valid. Each input category will be discussed briefly to inform the reader of the data required to do an overlap gap analysis. Every category must be completed before moving on to the next. The input categories have been arranged in the following discussion in the same order as found when accessing the GAP interface.

### 5.1.1. Single Barrier Geometry

The data that must be input first for an overlap analysis is the geometry of a single noise barrier that would exist in place of an overlap gap. Figure 26 shows the single barrier geometry input window.

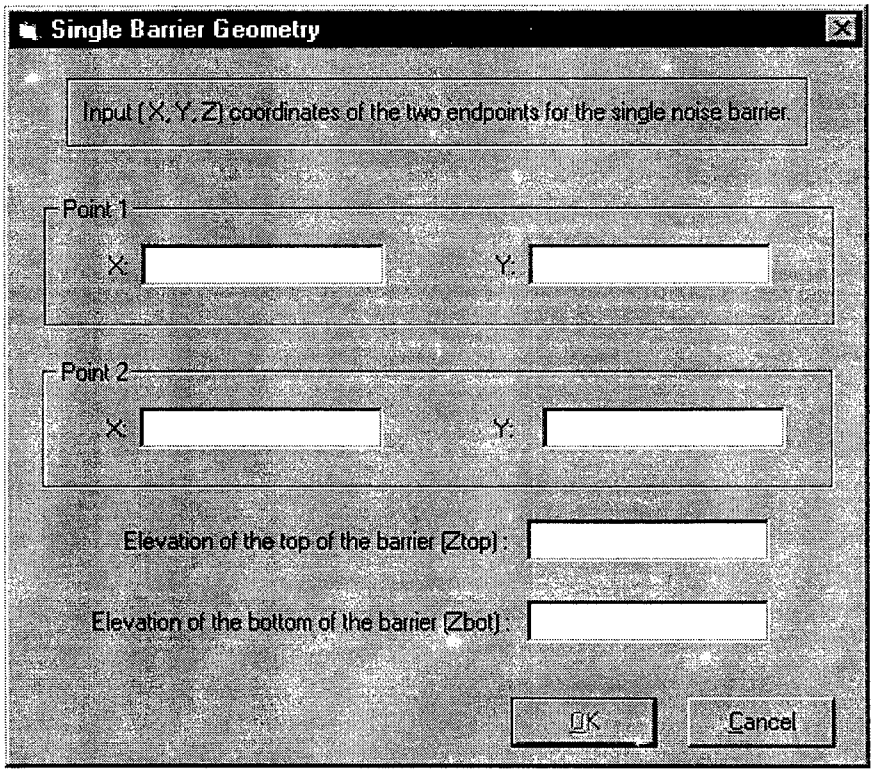


Figure 26. Single barrier geometry input window

The single barrier geometry is needed for two reasons. First, an analysis can be done on the single noise barrier to determine the noise levels at a receiver's position without the overlap gaps. This analysis provides a basis on which to judge the effectiveness of an overlap gap design. The noise levels from an overlap barrier analysis can be compared to those from a single barrier analysis. The difference in noise levels between the two analyses gives an approximation to the insertion loss degradation that will occur due to the overlap gap. Second, the single barrier

geometry is needed in order to specify the location of the far overlap barrier. The next section will cover the relationship between the single and far overlap barriers.

The inputs that are required for the single noise barrier are the X and Y-coordinates of both ends of the barrier. A simplifying restriction of the program is that all barriers and roadways are parallel to each other and to the X-axis. Therefore, the Y-coordinates should be the same for both ends of the single barrier. The program will not prevent the user from inputting coordinates which do not meet these guidelines. However, errors may occur if the data is not input using the aforementioned method. Furthermore, the X-coordinate of the right endpoint must be greater than the X-coordinate of the left endpoint. This is true for all barriers and roadways. Also, the top and bottom elevations of the barrier are needed. It should be noted that the elevation of the single barrier remains constant. A site that is situated on a grade cannot be modeled as such. An average elevation for the barrier must be determined for these inputs.

### 5.1.2. Overlap Barrier Geometry

The specification of the overlap barrier geometry is related directly to the data entered into the single barrier geometry input window. Figure 27 displays the window in which the overlap barrier geometry is assigned.

The first item to be input is the single barrier breakpoint. The breakpoint is defined as the X-coordinate of the far barrier where the overlap gap originates. The breakpoint must be located towards the middle of the single noise barrier defined in the previous step. The program will only accept breakpoint values which are located within 10% of the single barrier length from the midpoint. This is a conservative estimate necessary to guarantee that the overlap is situated near the middle of the specified barrier site. If the overlap were located close to one end, noise

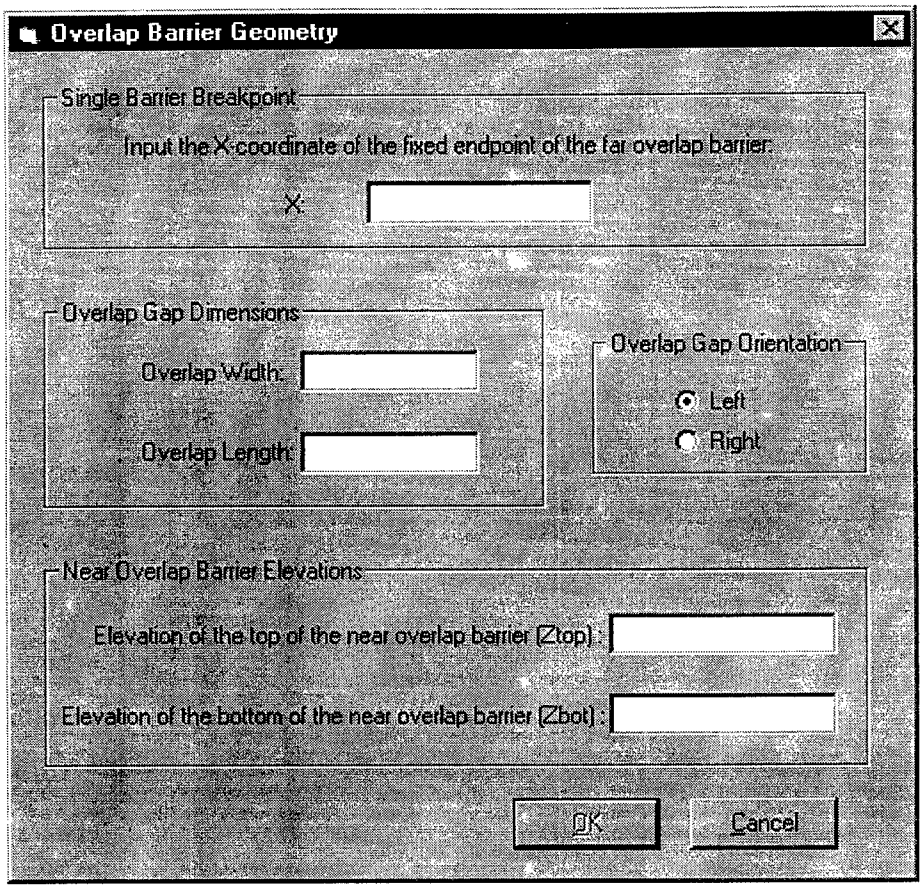


Figure 27. Overlap barrier geometry input window

contributions at a receiver due to side flanking at the end of the barrier could result and would not be accounted for by the program.

The overlap length and width are straightforward. The distance that the near and far barriers extend past one another is known as the overlap length. The overlap width is the perpendicular distance between the two barriers.

The single barrier is related closely to the overlapped barriers through the breakpoint, overlap length, and overlap width. The far barrier is located at the same Y-coordinate as the single barrier. The far barrier is specified as such because all receivers must be positioned on the

residential side of the single barrier. By defining the far wall along this same horizontal alignment, all receivers are assured of being on the residential side of the far barrier as well. One endpoint of the far barrier is situated at the breakpoint. The overlap gap orientation simply defines whether the overlap opens to the left or right relative to a receiver that is positioned behind the barrier and facing the highway. A thorough discussion of the gap orientation can be found later in this chapter. It is important to note that the overlap gap orientation should not be changed after inputting subsequent data as erroneous calculations may result. A new analysis file should be created to test data which involve a different gap orientation.

The near barrier is positioned relative to the placement of the far barrier. The far barrier is always located closest to the highway. The near barrier is offset back from the far barrier a distance equal to the overlap width. The near barrier is always parallel to the highway and far barrier and is also oriented parallel to the X-axis. The near barrier is assigned an endpoint that extends the overlap end of the near barrier a distance equal to the overlap length past the breakpoint of the far barrier. The overlapped barriers combined are the same length as the single barrier when considering the length of the walls from the non-overlap end of the far barrier to the non-overlap end of the near barrier. The near and far walls are each assigned one of the single barrier's endpoints, depending on the gap orientation. The other endpoints are assigned based on the breakpoint and overlap length.

The far wall maintains the same elevations as given to the single barrier. However, the top and bottom elevations of the near barrier can be assigned independently from the far barrier. This is useful since overlapped barriers are on different horizontal alignments and are rarely found at the same elevations.

### 5.1.3. Roadway Geometry

The roadway geometry is input in a manner similar to the single barrier geometry. Figure 28 illustrates the roadway geometry input window.

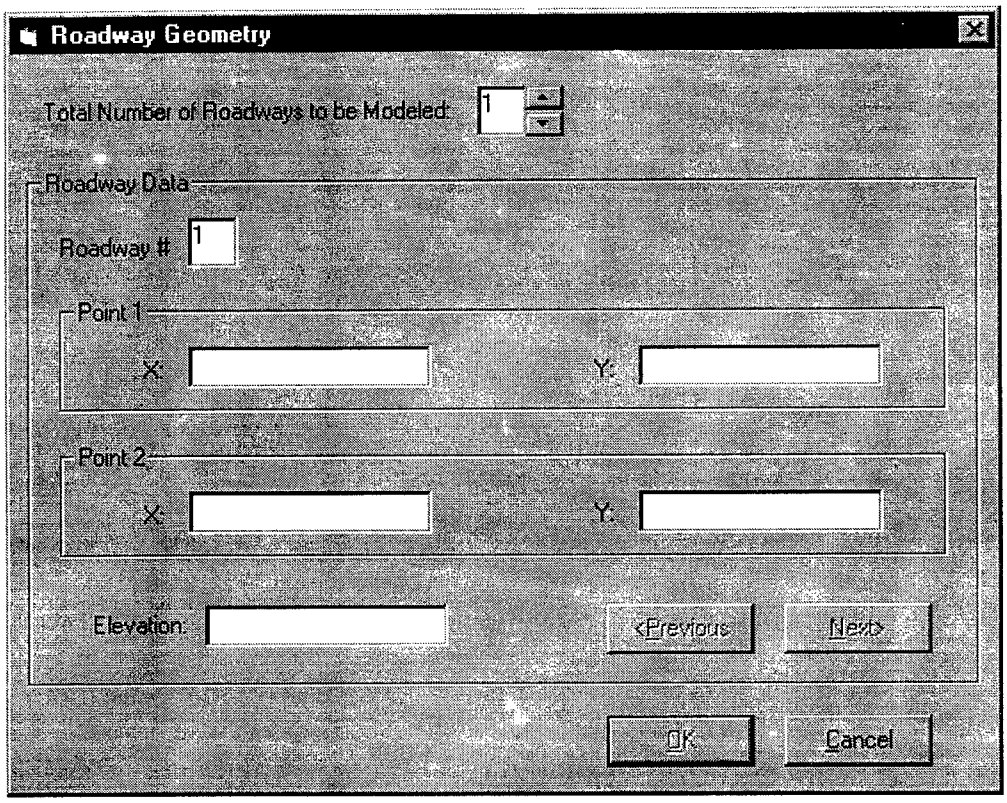


Figure 28. Roadway geometry input window

The X and Y-coordinates of the centerline for each roadway are specified as well as the roadway elevation. Each roadway must be parallel to the noise barriers and the X-axis. Therefore, the Y-coordinates should be the same for each roadway to ensure these conditions are satisfied. Theoretically, the roadway can be of any length. However, it is good practice to assign X-coordinates for each roadway that are close to the endpoints of the single barrier. Each

roadway must extend past all receivers in both directions. As with the barrier elevations, roadway elevations are constant along the length of the road.

A maximum of 10 roadways can be modeled in an overlap gap analysis. The program was designed to model each lane of traffic as separate roadways. This is necessary since precise distances and angular measurements are calculated in the iterative process of analyzing reflections. In other traffic noise prediction models, it is common practice to model several lanes of traffic as one roadway. However, most of these models do not calculate the sound contributions from multiple reflections. It is recommended that each lane of traffic be modeled separately and not as one "equivalent" roadway for best results.

### 5.1.4. Traffic Data

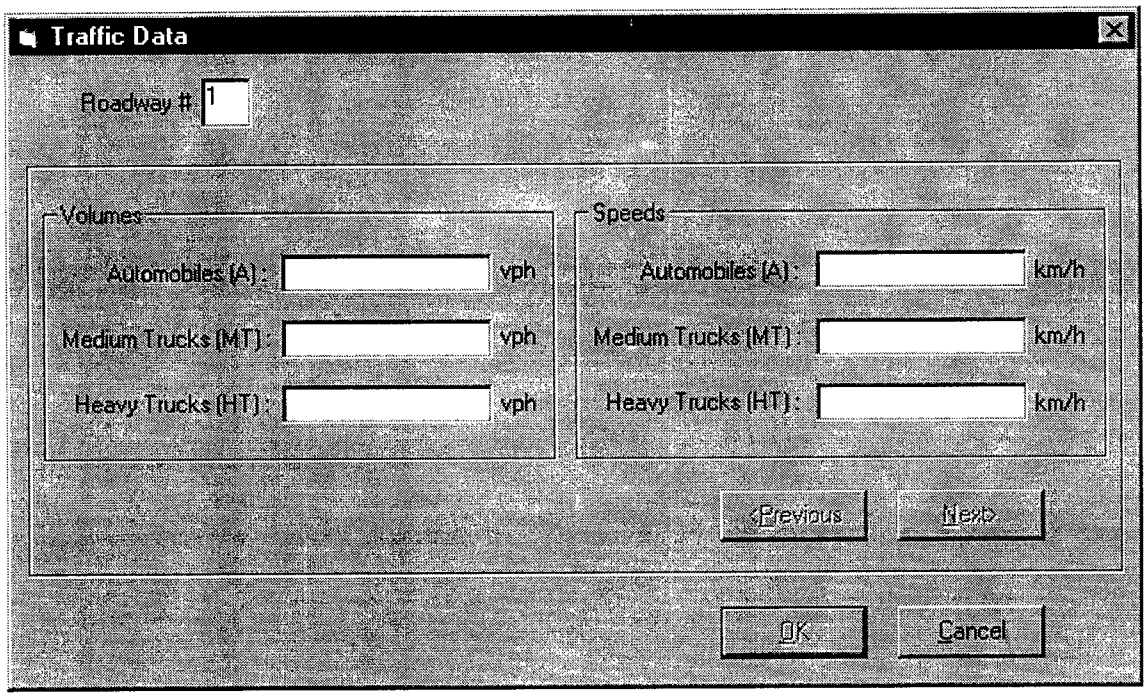


Figure 29. Traffic data input window

For each roadway that is modeled, traffic data is needed to characterize the source. The traffic parameters required, as shown in Figure 29, are the traffic volumes and speeds. These parameters are needed for each roadway for each vehicle classification (automobiles, medium trucks, and heavy trucks).

The traffic volumes input should represent the volumes over a one-hour time period. The speeds must be input in kilometers per hour (km/h). Limitations from the REMEL equations require that speeds be in the range from 45 to 110 km/h [Rudder and Lam 1977]. The program will not accept values outside of this range. Not all volumes for a roadway can be set to zero. Individual classes can have zero volumes but all modeled roadways must have at least one class input.

### 5.1.5. Receiver Geometry

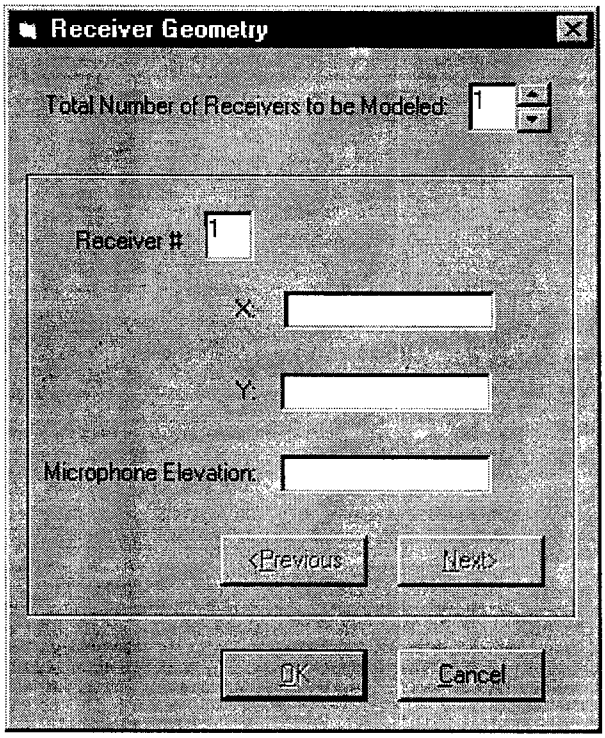


Figure 30. Receiver geometry input window

A maximum of 10 receivers can be modeled in an overlap gap analysis. The required user-inputs are the X and Y-coordinates and the elevation of each receiver. The receiver geometry input window is shown in Figure 30.

A receiver may be located in any of the six regions defined in the section entitled "Overlap Gap Receiver Locations" in Chapter 3. Figure 8 graphically shows the six receiver regions. Receivers not located in these regions can be analyzed by standard noise prediction programs. GAP will not permit the input of receivers outside of these regions.

There are limitations to the placement of receivers in these regions. Although the program will accept any input of receivers within the specified regions, prediction accuracy decreases as the distance between the overlap gap and a receiver increases. A practical limit is to locate all receivers within a 100 meter radius of the overlap gap. The elevation of each receiver must be lower than the top of both noise barriers. This condition ensures that all receivers are in the acoustical shadow zone unless a noise barrier is relatively low or the source elevation is particularly high.

## 5.2. Model Outputs

The results of the noise analysis can be reviewed on screen or output to a printer. The following sections detail the output that the GAP model provides for the user.

### 5.2.1. Single Barrier Analysis

The results from the single barrier analysis can be reviewed in the single barrier analysis output window as shown in Figure 31. This window displays the equivalent continuous sound level for each receiver as if protected by a single noise barrier with no discontinuities.

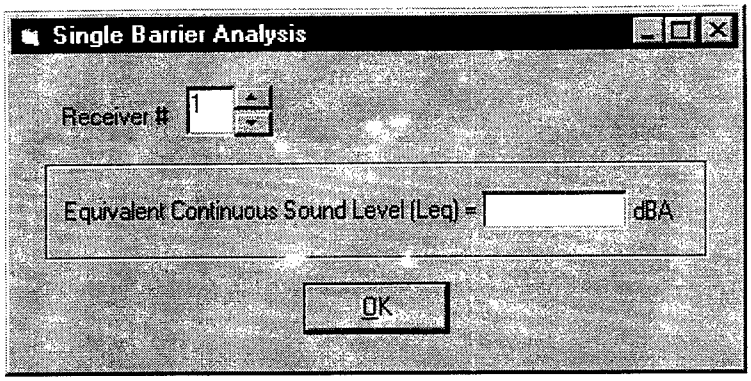


Figure 31. Single barrier analysis output window

### 5.2.2. Overlap Barrier Analysis

The primary objective of this model is to determine the equivalent continuous sound levels at receivers which are influenced by an overlap gap. These sound levels are accessed through the overlap gap analysis output window illustrated in Figure 32. The difference in sound levels between the single barrier and overlap barrier analyses provides the user with an approximation of the insertion loss degradation due to the introduction of the overlap gap in the noise barrier.

In addition to the receiver's sound level, statistics from the overlap gap analysis procedure are also displayed in this window. These statistics provide the user with information regarding a receiver's susceptibility to reflective rays. Included in the statistics is the overlap region in which the receiver is located, denoted by the receiver case. The total number of MRDR analyzed and a count of the MRDR that actually contribute to a receiver's sound level are shown. Equivalent data is displayed for MRR image rays. These statistics are summed to give a total count of reflected rays that are analyzed and a count of the reflected rays which contribute to each receiver's sound level.

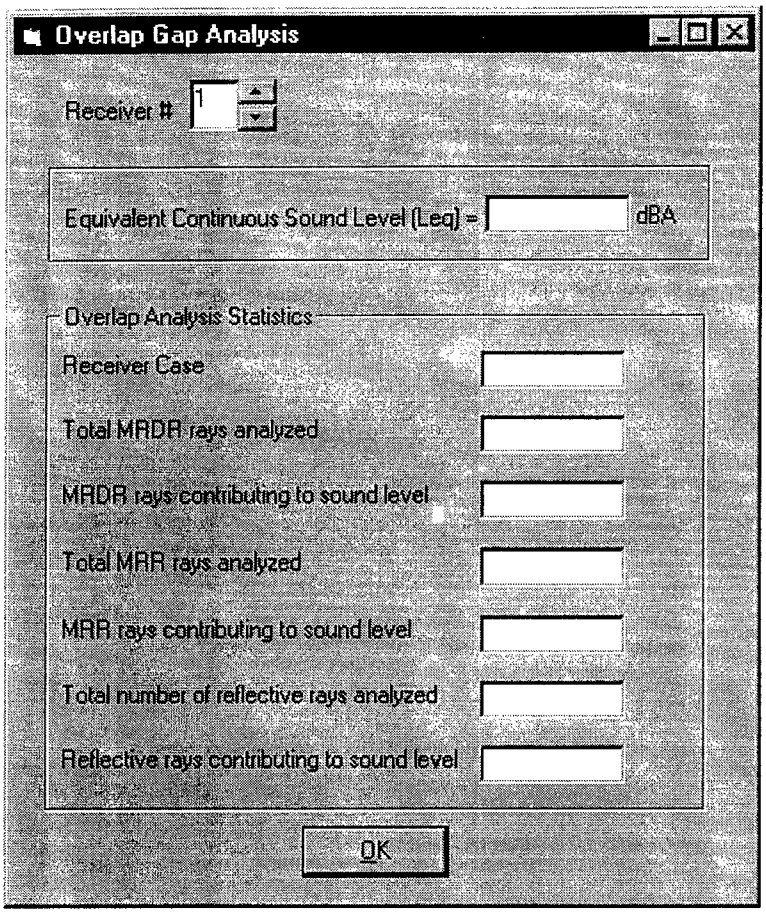


Figure 32. Overlap gap analysis output window

### 5.2.3. Graphical Output of the Overlap Gap Site

In order to verify that the site is modeled correctly, two graphic views can be inspected on the screen. The plan view of the entire site, as shown in Figure 33, and the cross section view at each receiver, displayed in Figure 34, can be accessed through the GAP program after all necessary inputs have been provided. The plan view shows the noise barriers, receivers, centerline location of the roadways, and also indicates the portions of the barriers, if any, which are modeled with absorptive treatment. It should be noted that the plan view is scaled to show only the region including the overlap gap and the receivers. Roadways and barriers may extend beyond what is shown in the plan view.

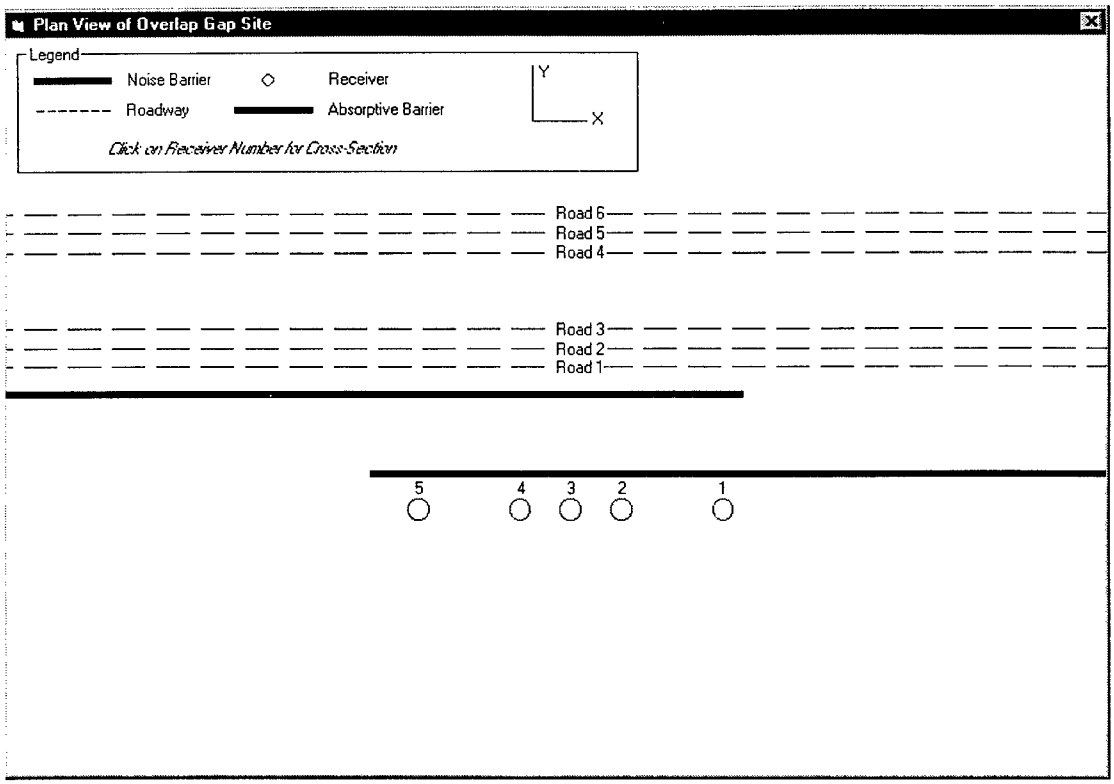


Figure 33. Plan view output window

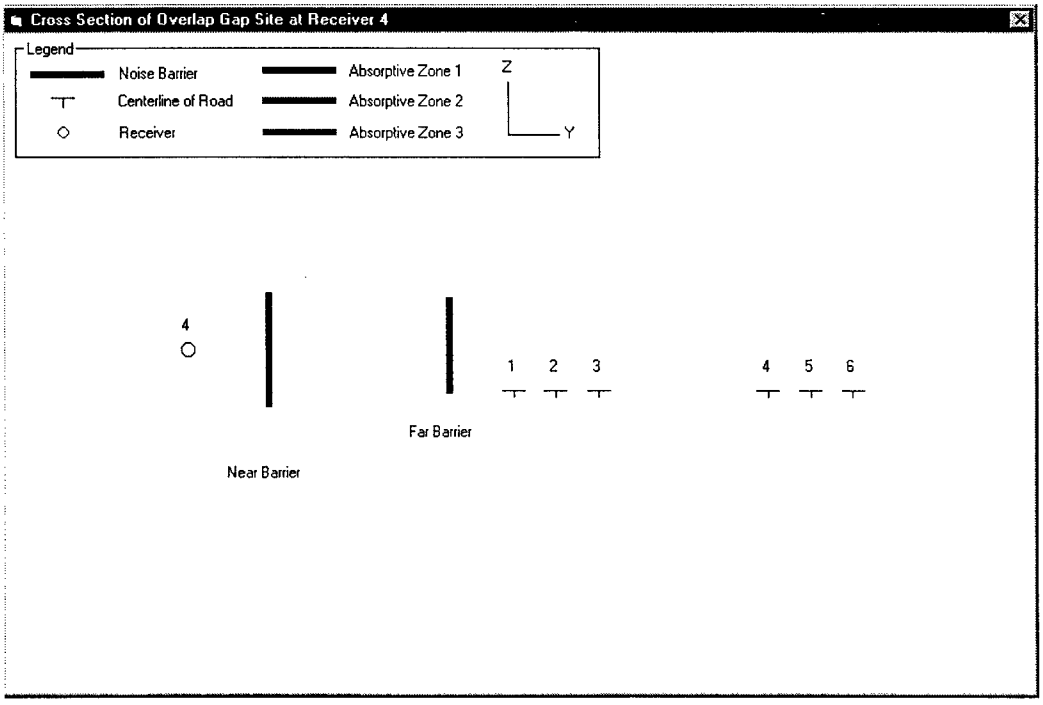


Figure 34. Cross section view output window

The cross section view for each receiver can be accessed by clicking a receiver number on the plan view. This view shows the noise barriers, the centerline of the roadways, and the receiver selected on the plan view. If absorptive treatment has been modeled, the cross section view will delineate between different vertical absorptive zones which have been specified.

### 5.2.4. Output of Geometrical and Analysis Data

The input data and the analysis results can be output to a printer enabling the user to maintain a record of each trial. Figure 35 shows the output analysis results window. This window is accessed to specify the data records to be printed. The user can select different output options from the window, as shown in the figure.

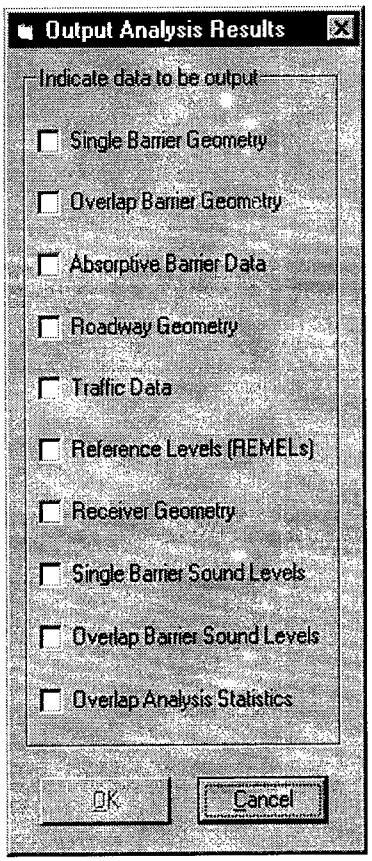


Figure 35. Output analysis results window

## 5.3. Model Limitations

With any program which models real-life phenomena, limitations must be set to manage the complexity of the problem. These limitations prevent an exact analysis of the problem. Assumptions and limitations were required in the formulation of the GAP model. The validation and calibration of the model, as explained in Chapter 6, discusses the effect of these assumptions on the program's performance. The following list explains the simplifications, assumptions, and modifications that were needed to implement the theory into a working analysis and design tool.

1. Reflections are assumed to be specular (sound energy does not scatter upon striking a surface).
2. Noise flanking the ends of a barrier (end diffraction or side flanking) does not significantly affect the sound levels at receivers located at an overlap gap site.
3. Double diffraction does not result in an appreciable attenuation of sound levels.
4. Ground reflections are insignificant and may be ignored.
5. All receivers must be lower than the top edge of both barriers (every receiver is located in the shadow zone).
6. Assume the ground at all sites is acoustically hard ($\alpha$=0).
7. All barriers and roadways must be parallel to the X-axis.
8. Assume all barriers are freestanding walls, not earthen berms.
9. Traffic speeds must be in the range of 45 to 110 km/h.

## 5.4. Conversion of the FHWA Highway Traffic Noise Prediction Equation

Equation 1 is the fundamental equation used to predict noise levels for highway applications. However, the equation was originally formulated for manual methods using a worksheet to compute all applicable reference levels and adjustments. By simplifying the original equation, a form more conducive to computer applications can be attained [Bowlby and Cohn 1986]. The following work does not alter Equation 1 but merely reorganizes the terms for ease of computer implementation.

The FHWA highway traffic noise prediction equation is as follows:

$$L_{eq}(h)_i = (\overline{L_o})_{Ei} + 10\log\left(\frac{N_i \pi D_o}{S_i T}\right) + 10\log\left(\frac{D_o}{D}\right)^{1+\alpha} + 10\log\left(\frac{\psi_\alpha(\phi_1,\phi_2)}{\pi}\right) - \Delta_B \qquad (1)$$

Assuming that the time period is one hour ($T$ = 1 hour) and the site is hard ($\alpha$ = 0), Equation 1 can be reduced to the following:

$$L_{eq} = 10\log(I_{eq})_i - (\Delta_B)_i \qquad (40)$$

where

$$(I_{eq})_i = \left[I_L N_i D_o^{\,2}\left(\phi_{2i} - \phi_{1i}\right)\right]/(1000 S_i D) \qquad (41)$$

$$I_L = 10^{(\overline{L_o})_{Ei}/10} \qquad (42)$$

Recalling that $D_o$ =15 meters,

$$(I_{eq})_i = \left[0.225 I_L N_i\left(\phi_2 - \phi_1\right)\right]/(S_i D) \qquad (43)$$

Combining Equations 40 and 43, the final computational formula with which to calculate the equivalent continuous noise level at a receiver for the $i$th class of vehicles is as follows:

$$L_{eq} = 10\log\left\{\left[0.225 I_L N_i\left(\phi_2 - \phi_1\right)\right]/(S_i D)\right\} - (\Delta_B)_i \qquad (44)$$

## 5.5. Numerical Integration Technique for Barrier Attenuation Computation

The calculation of barrier attenuation for any given noise barrier presents a special problem when implementing the theory into computer code. The integral in the barrier attenuation adjustment, Equation 5 in Chapter 3, cannot be computed using conventional techniques. Numerical methods are required to do the computation of this integral. Several types of numerical techniques are available to do the calculation. Through consultation with faculty experienced in the use of numerical methods [Dhamija 1996], it was determined that Simpson's Rule would be appropriate for use in the barrier attenuation algorithm.

Simpson's Rule is a simple, yet effective procedure for performing numerical integration. The derivation of this technique will not be presented as it is readily available in computer programming texts [Koffman and Friedman 1990].

## 5.6. Determination of Source Region Existence

The various zones in which different mechanisms influencing propagation exist for a specific case receiver were described in Chapter 3 in the section entitled "Determination of Source Regions." This discussion outlines the process that must be performed for each receiver-roadway pair in order to delineate the various source regions. However, it was assumed that a receiver situated in a specific receiver case location would have a predetermined number of source regions. Depending on the orientation of the receiver with respect to both the overlap barriers and the roadway, this may or may not be the case.

Figures 10-11 show the maximum number of source regions which may exist for any given receiver location case. However, some of the source regions may not exist for a given

receiver. This situation would exist if a one region overlapped another region resulting in a duplication of the same source. The model was designed to compare the limiting angles of each source region with adjacent source regions. If any regions overlap, the limiting angles are adjusted accordingly so that each sub-source is only accounted for once.

## 5.7. Calculation of Image Phi Angles

The GAP model divides each roadway into many segments. Each segment is analyzed for contributing reflective image rays. Multiple image sources are examined from each segment to the point where any additional image rays would have no significant impact on the final noise level. After all image sources have been analyzed for a particular segment, the model moves to the next segment and repeats the process of investigating each image source. The angles measured from the perpendicular line between the receiver and the roadway to the ends of each actual source segment are given by this iterative process. However, similar angles must be found for the image segments. This section presents the theory necessary to perform this operation.

The graphical representation of the problem is shown in Figure 36. The goal is to determine the phi angles for each image source segment. In order to accomplish this, the X-coordinates of the endpoints of the actual source segment must be determined from the known phi angles.

$$\tan\phi_{10} = \frac{X_{REC} - LeftX}{d_0}$$

$$LeftX = X_{REC} - d_0\left(\tan\phi_{10}\right) \tag{45}$$

$$\tan\phi_{20} = \frac{X_{REC} - RightX}{d_0}$$

$$RightX = X_{REC} - d_o(\tan \phi_{20}) \tag{46}$$

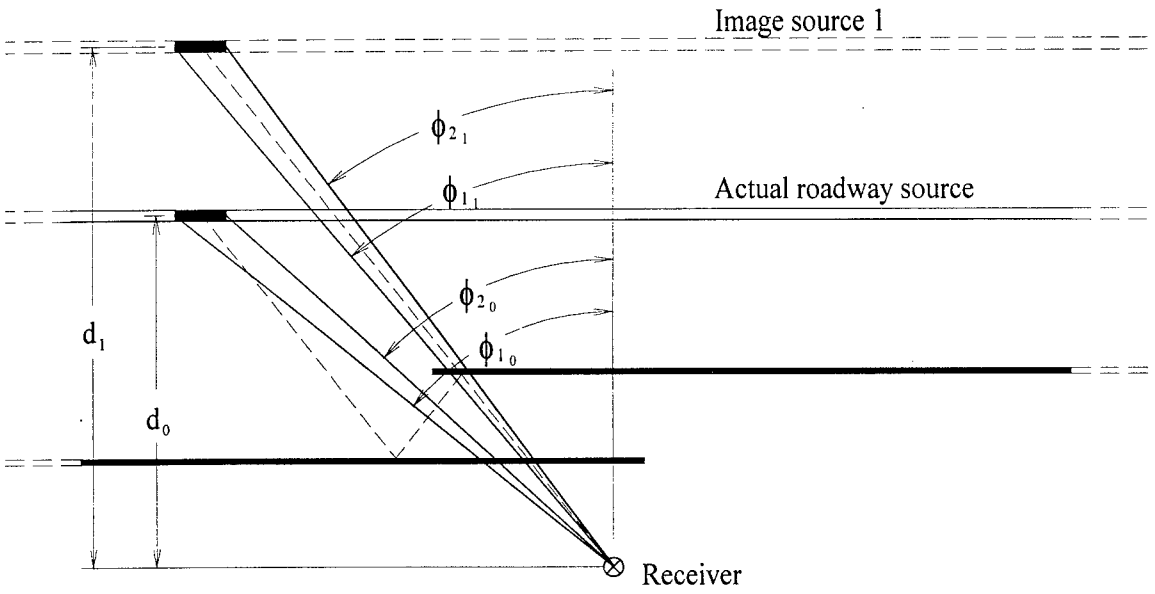


Figure 36. Image source phi angles

where

| | |
|---|---|
| $\phi_{10}$, $\phi_{20}$ | angles from the perpendicular of the receiver to the left and right endpoints of the actual source segment, respectively. |
| $X_{REC}$ | X-coordinate of the receiver. |
| *LeftX*, *RightX* | X-coordinates of the left and right endpoints of the actual source segment, respectively. |
| $d_0$ | perpendicular distance from the actual source to the receiver, as determined in Chapter 3. |

Having determined the X-coordinates of the endpoints of the actual source segment, which are equal to the X-coordinates of the endpoints of the *i*th image source segment, the phi angles to any image segment may be found by using Equations 47 and 48:

$$\phi_{1i} = \arctan\left(\frac{X_{REC} - LeftX}{d_i}\right) \tag{47}$$

$$\phi_{2i} = \arctan\left(\frac{X_{REC} - RightX}{d_i}\right) \tag{48}$$

where

$\phi_{1i}$, $\phi_{2i}$ — angles from the perpendicular of the receiver to the left and right endpoints of the $i$th image source segment, respectively.

$X_{REC}$ — X-coordinate of the receiver.

$LeftX$, $RightX$ — X-coordinates of the left and right endpoints of the ith image source segment, respectively.

$d_i$ — perpendicular distance from the $i$th image source to the receiver, as determined in Chapter 3.

## 5.8. Overlap Gap Orientation Transformation Algorithm

The concept of the overlap gap orientation was introduced earlier in this chapter. An overlap gap can be defined as either left or right orientation. The difference between the two orientations are evident in Figure 37. A distinction must be made between the two orientations due to differences in assigning coordinates to the endpoints of the overlap barriers and in the analysis of an overlap gap.

When inputting data into the overlap barrier geometry window, the user must specify the overlap gap orientation. The default gap orientation is left. Depending on the user's selection, the near and far overlap barriers will be defined accordingly. If the gap orientation is left, the breakpoint is set as the left endpoint of the far barrier. The right endpoint of the far barrier is defined by the right endpoint of the single barrier. The left endpoint of the near barrier is equal

to the left endpoint of the single barrier. The right endpoint of the near barrier is found by adding the overlap length to the X-coordinate of the breakpoint.

If the gap is specified as right orientation, the four endpoints of the overlap barriers are determined differently. The far barrier is defined with the breakpoint as the right endpoint and the left endpoint of the single barrier as the left endpoint. The left endpoint of the near barrier is

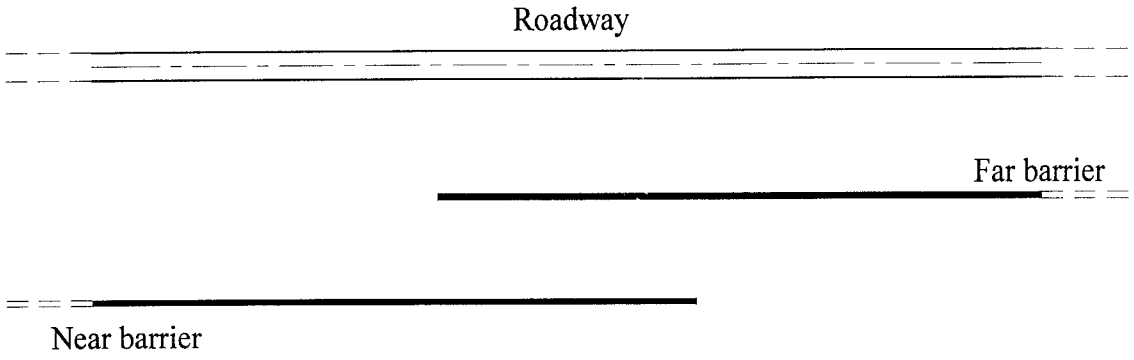


a) Left overlap gap orientation

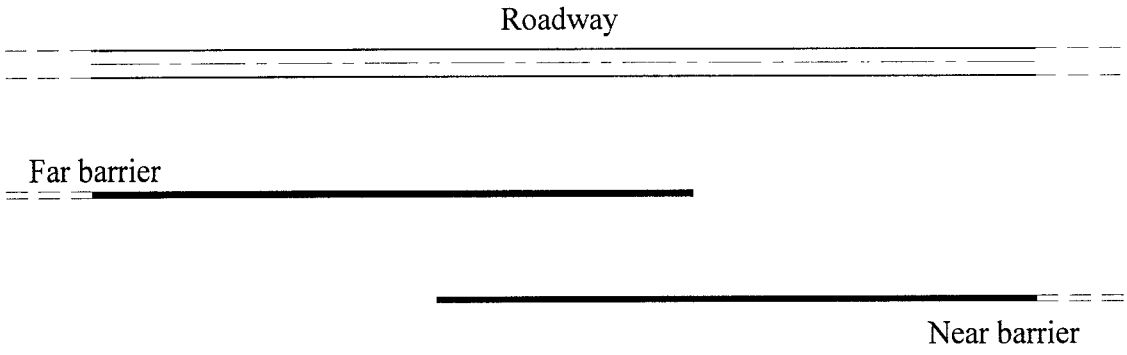


b) Right overlap gap orientation

Figure 37. Overlap gap orientation

located at the X-coordinate of the breakpoint minus the overlap length. Finally, the right endpoint of the near barrier is defined by the right endpoint of the single barrier.

The geometry of each orientation is different. It is apparent that the program must be able to analyze an overlap gap for either orientation. There are two approaches that can be used to accomplish this task. First, separate algorithms can be developed to analyze each gap orientation. However, the code to perform the required analyses is somewhat lengthy. The duplication of code would greatly increase the size of the program. Also, every algorithm would need to be developed and tested separately for both orientations. The second approach, the chosen method, is to formulate a single algorithm which would modify one orientation into the other gap orientation. Through this adjustment, every orientation could be analyzed using the same set of analysis algorithms, greatly decreasing the length of code and the time required to produce the code.

The code was developed for the analysis of overlap barriers with left gap orientations. Therefore, the transformation algorithm is needed to modify right gap orientation data to that of left gap orientation data before an analysis is performed. The critical factor of an overlap gap examination is the location of the receiver. In order to perform a transformation of gap orientation, each receiver's location relative to the near and far barriers and the roadways must be maintained. This can be accomplished by establishing a mirror line through each receiver perpendicular to the barriers and roadways. The coordinates of the receivers do not change in the transformation process. However, the X-coordinates of the endpoints of all barriers and roadways are transformed relative to the established mirror line. The Y-coordinates remain constant for all entities throughout this operation. Since the barriers and roadways are

transformed relative to each receiver, this transformation process must be performed prior to the computation of sound levels at each receiver.

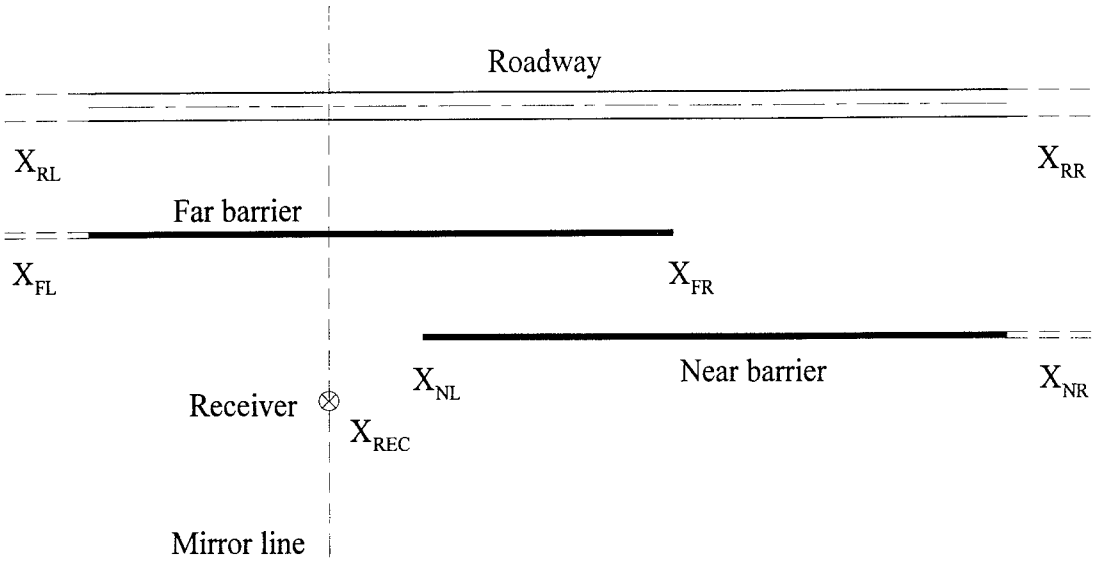


a) Right overlap gap orientation

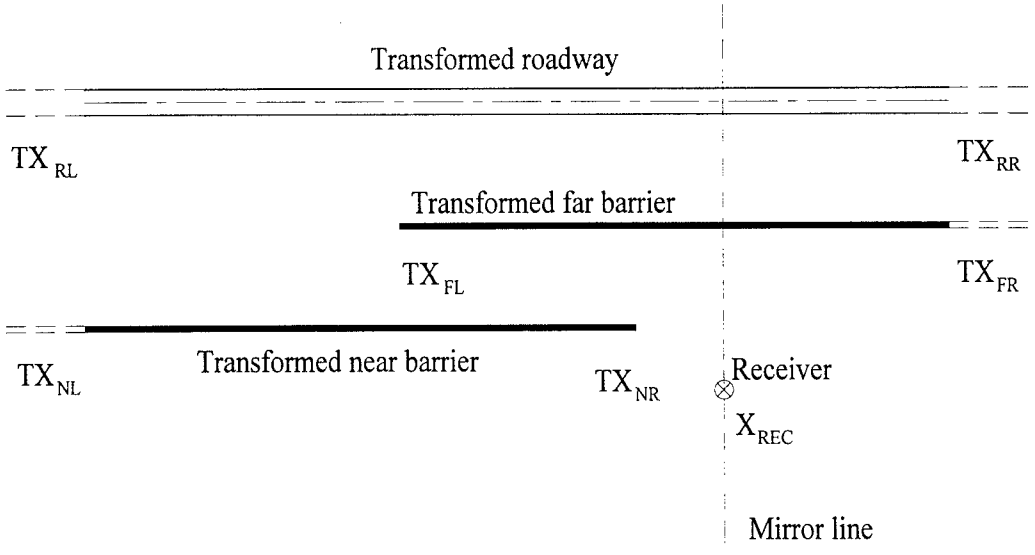


b) Transformed right overlap gap orientation

Figure 38. Transformation of a right orientation overlap gap

An example of the process used to transform a right overlap gap is shown in Figure 38. Following are the equations used to perform the operation.

$$\text{Far barrier} \begin{cases} TX_{FL} = (2 \times X_{REC}) - X_{FR} \\ TX_{FR} = (2 \times X_{REC}) - X_{FL} \end{cases}$$

$$\text{Near barrier} \begin{cases} TX_{NL} = (2 \times X_{REC}) - X_{NR} \\ TX_{NR} = (2 \times X_{REC}) - X_{NL} \end{cases}$$

Each roadway is transformed in a similar manner:

$$\text{Roadway} \begin{cases} TX_{RL} = (2 \times X_{REC}) - X_{RR} \\ TX_{RR} = (2 \times X_{REC}) - X_{RL} \end{cases}$$

## 5.9. Atmospheric Attenuation

As a sound wave travels through the air, a small portion of the wave's energy is lost. The losses occur because of heat conduction and viscosity of the air as well as rotational and vibration relaxation of oxygen molecules in the air [Beranek 1971]. These losses are insignificant for waves that travel only short distances. For the analysis of image rays propagating through the overlap gap, the distance that a ray travels is long enough to generate a measurable amount of atmospheric attenuation. This attenuation is quantified by the following equation [Bowlby, Higgins, and Reagan 1982]:

$$\Delta_A = \left(1.772 \times 10^{-3}\right) d \tag{49}$$

where

$\Delta_A$ atmospheric attenuation in decibels.

$d$ distance from source to receiver in meters.

The attenuation produced by the atmosphere is generally less than one decibel for most source-receiver distances in an overlap gap analysis. The addition of this correction to the model is needed to refine deficiencies of the FHWA traffic noise equation.

## 5.10. Design Alternatives to Improve Overlap Gap Design

The discussions up to this point have focused on the analysis of noise barrier overlap gaps. From the theory developed, noise levels at receivers located at an overlap gap site can be computed. However, the purpose of this model is not only to enable the user to analyze an existing overlap gap, but also to design new overlap gaps or to aid in the retrofitting of an existing gap.

The technique that should be followed is an iterative process. Successive trials must be performed to approach the optimal design for a particular overlap gap. Each trial should be conducted to minimize the insertion loss degradation caused by the introduction of the overlap gap into the noise barrier. The design of an overlap gap is based on two criteria: the overlap gap ratio and the application of absorptive treatment. The ensuing sections will focus on these design parameters.

### 5.10.1. Overlap Gap Ratio

The overlap gap ratio is the ratio of the overlap length to the overlap width. A ratio that has been used frequently in overlap gap design is a 2 to 1 ratio [Simpson 1976]. Different overlap gap ratios can be investigated quickly with the GAP program. The two parameters dictating the

overlap gap ratio are the length of the overlap and the width of the gap which are entered in the overlap barrier geometry input window shown in Figure 27.

The selection of these parameters is governed by the physical propagation of sound waves in an overlap gap. As the overlap length is increased, some image rays may not be able to influence a receiver, while others may be forced to travel longer distances through an increased number of reflections to reach a receiver. As the propagation distance increases, the energy of the image ray decreases due to geometric spreading and atmospheric attenuation, as explained in previous sections. Also, by increasing the overlap length, fewer direct rays from the source can propagate to receivers. As the gap width increases, a similar situation occurs. Each image ray must travel greater distances to reach a receiver, thus reducing the effect that the ray will have on the receiver.

These are the only methods, excluding increasing the barrier height, to reduce the insertion loss degradation at an overlap gap constructed with reflective noise barriers. Barrier height increase is usually not a practical alternative as the acoustical design of the single barrier dictates the barrier height. Increasing the barrier height to reduce the sound levels due to the localized effect of an overlap gap will most likely not be an economically feasible alternative. Further, it would have little effect on the sound levels, since barrier height increases would do nothing to attenuate the more influential MRR. The most practical alternative besides changing the geometrical dimensions of an overlap gap is the application of absorptive material to the noise barriers.

### 5.10.2. Modeling of Absorptive Treatment

The primary problem with overlap gaps is the propagation of sound waves through the gap by reflective mechanisms. Absorptive panels are an effective method of attenuating these reflective sound waves. Every ray that strikes an absorptive surface will lose a portion of its energy. The amount of energy that is lost is dependent on the acoustical properties of the absorptive treatment and the frequency of the sound wave. The acoustical properties of absorptive panels are specified by the panels' noise reduction coefficient (NRC). The NRC is the arithmetic mean of sound absorption coefficients at 250, 500, 1000, and 2000 Hz. NRC values range from 0.00 for totally reflective to 1.00 for totally absorptive. Sound absorption coefficients are determined in laboratory experiments and are based on the sound absorption characteristics of a material.

The placement of absorptive panels can vary greatly. Little research has been conducted to determine the optimal position of absorptive treatment at an overlap gap. The GAP model allows the user to specify the location of absorptive panels both vertically and horizontally on each noise barrier. Figure 39 shows the window for the input of the location and acoustical characteristics of the absorptive panels.

A maximum of three absorptive zones can be specified on a respective noise barrier. This gives the user flexibility to refine a design for cost-effectiveness. By specifying three zones, the barrier can be modeled with absorptive panels located in the middle of the barrier without treating the top or bottom sections. This is more economical as less material is needed and the barrier performance is not jeopardized since most reflections occurring at the top or bottom of a barrier do not influence a receiver. Each zone is specified by its top and bottom elevations and

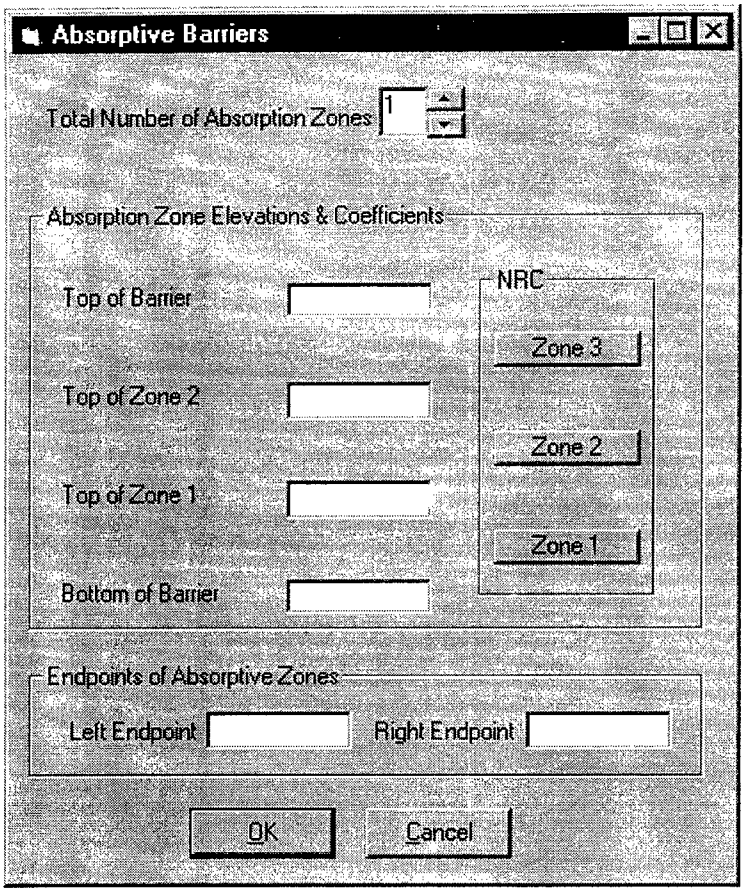


Figure 39. Absorptive barriers input window

its NRC value. The orientation of the absorptive zones for a three-zone barrier is shown in Figure 40. The model is designed so that separate zones and absorptive coefficients can be specified for the near and far barriers. The program defaults to a one-zone barrier with no absorptive treatment (NRC=0.05) if no zones are specified. An NRC of 0.05 is representative of a typical reflective barrier.

In addition to specifying the vertical location of the individual absorptive zones, horizontal limits for the treatment can also be set for each barrier. The default settings are the coordinates defining the endpoints of the overlap for both barriers. However, the limits can be

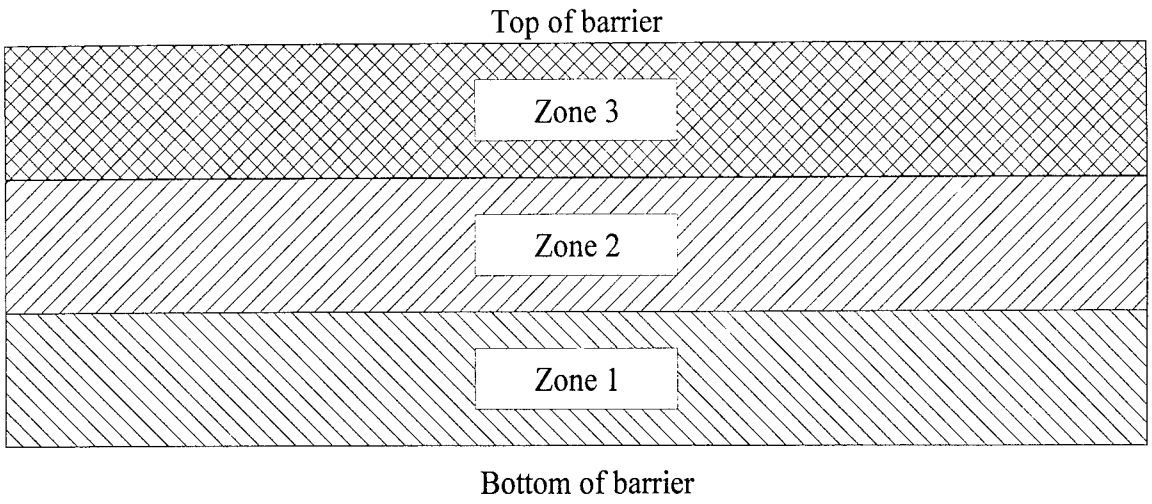


Figure 40. Orientation of absorptive zones

modified for each barrier independently to include less of the overlap length by changing the endpoints of the absorptive zones. Conversely, the zones may also be expanded to include barrier surfaces outside of the overlap gap as well.

The method used to compute the effect of the absorptive treatment on a receiver deals with the modification of the FHWA traffic noise equation. The model first analyzes each image ray to find the height of each reflection, the respective barrier on which the reflection occurs, and the horizontal location of the reflection on that barrier. An evaluation is then made to determine in which absorptive zone the reflection occurs. Based on these findings, the noise level at each reflection is multiplied by a factor based on the NRC for that zone. The factor which is utilized is one minus the NRC value (1 - NRC). For a totally reflective surface (NRC = 0.00), the sound level is not attenuated at all. The sound level is completely absorbed for a totally absorptive surface (NRC = 1.00). This analysis is performed for every reflection that occurs for each image ray.

If a material with a sufficient NRC rating is used, the effect that reflective mechanisms influencing propagation have on a receiver can be reduced. By applying both techniques of modifying the overlap gap dimensions and modeling absorptive treatment, a design may be attained that is effective at minimizing the insertion loss degradation at an overlap gap site.

## 5.11. GAP Version 2.0

Sound absorptive materials are more effective in reducing noise levels at some frequencies than others. Therefore, the frequency of the sound waves must be taken into account to determine the influence of absorptive barriers. The previous section discusses the method of using the noise reduction coefficient (NRC) for sound absorption calculation. However, the NRC is a composite of the absorption coefficient for four frequency bands: 250, 500, 1000, and 2000 Hz. While the frequency range that is audible to the human ear is approximately 20 - 20,000 Hz, most highway traffic noise consists of sound wave frequencies between 50 - 10,000 Hz.

In the 50 - 10,000 Hz range, there are eight octave bands with center-band frequencies of 63, 125, 250, 500, 1000, 2000, 4000, and 8000 Hz. Most of the equivalent continuous sound level experienced by a receiver consists of noise from frequencies in this range. To evaluate the performance of absorptive treatment more effectively, GAP Version 2.0 was created. Version 2.0 allows the user to specify an absorption coefficient for each of the eight octave band center frequencies. This allows greater flexibility in analyzing different absorptive materials.

Version 2.0 uses different REMEL equations than Version 1.0 to calculate the reference noise levels produced by the source. These equations allow the computation of noise levels at each individual octave center-band frequency [Rudder and Lam 1977]. All supporting

algorithms were upgraded to assure compatibility with these REMEL equations. Version 2.0 also accounts for the individual octave center-band frequencies in the barrier attenuation algorithm. Since the calculations are more involved in Version 2.0, greater computational time is required to complete noise analyses.

Input and output dialog boxes have been added or modified in Version 2.0 to accommodate these new features. Figure 41 shows the input window for specifying the absorption coefficients of absorptive treatment for the eight octave band center frequencies. These absorption coefficients can range from 0.0 for a totally reflective barrier to 1.0 for a totally absorptive barrier.

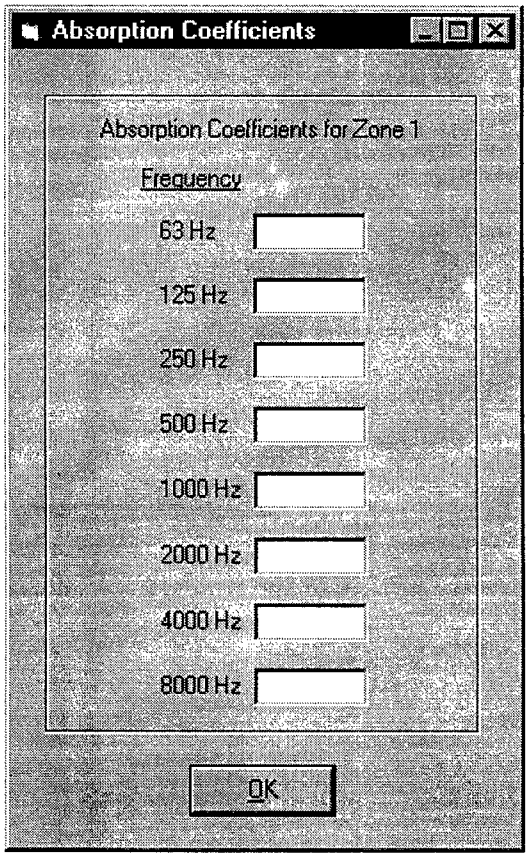


Figure 41. Absorption coefficient input window (Version 2.0)

The results from a GAP Version 2.0 overlap gap analysis are more thorough in that the sound level for each octave band center frequency is determined. After performing an overlap gap analysis, the user may view the individual noise levels for each of the eight octave band center frequencies through the overlap gap analysis output window. These noise levels are displayed in the octave levels output window, as shown in Figure 42. This data can also be output to a printer by selecting the appropriate options in the output analysis results dialog window.

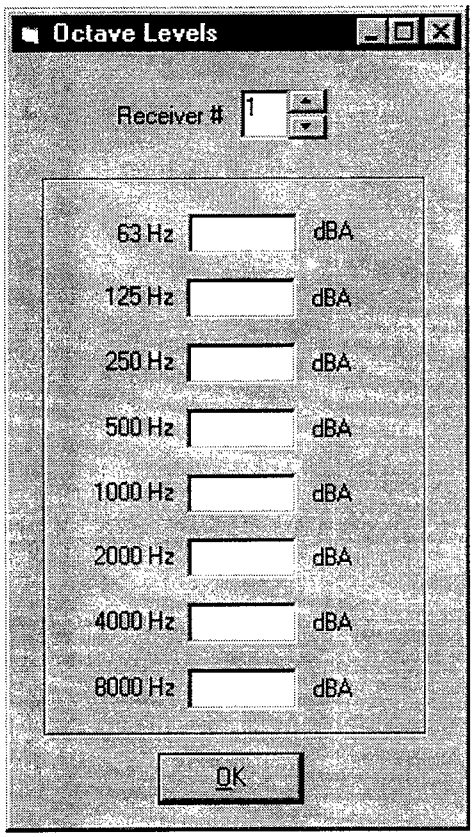


Figure 42. Octave levels output window

# 6. FIELD DATA COLLECTION

A vital step in any modeling process is the collection of field data to test the model for accuracy. The evaluation of the theory derived in the previous chapters is only as good as the data available. Therefore, many precautions were taken in the field to ensure that data was collected with the utmost care. This chapter will detail the steps taken to gather the necessary data at the noise barrier overlap gaps. The sites chosen for study will also be reviewed.

## 6.1. Field Procedure

The preliminary site selection and traffic noise data collection procedures will be discussed in this section. The American National Standard, "Methods for Determination of Insertion Loss of Outdoor Noise Barriers," was followed where appropriate for all measurements performed during the project [Acoustical Society of America 1987].

### 6.1.1. Site Selection

Through previous studies and consultation with Ohio Department of Transportation officials, all noise barrier overlap gaps were identified within the central and southern Ohio region. The construction plans from these gaps were reviewed to exclude sites which were situated in terrain that was not fairly level.

The ideal overlap gap site for noise measurement purposes would be situated on level terrain, have far and near barriers of approximately the same top and bottom elevations, and have barriers that were parallel to the roadways. This is considered ideal because it limits the number

of terrain variations to be accounted for in the validation process. Actual overlap gaps will have many terrain variations. However, the model can best be calibrated by data that is collected from sites which most closely matches the model's limitations. It is also desirable to study sites which have noise barriers constructed from different materials and different overlap gap orientations. After identifying the potential overlap gap sites, a field inspection was performed. Many sites were eliminated due to terrain inconsistencies, poor barrier alignment with the roadway, and surrounding noise disturbances which might have influenced the measurements.

The next step in the process was to acquire permission from property owners near the overlap gaps to perform noise measurements at their residences. Although most microphones could be placed in the right-of-way of the highway, all sites required some measurements to be taken at distant receivers located on private property.

In gaining permissions, the property owner was contacted in person by the field supervisor. A summary of the project was conveyed to the resident. Following this brief introduction to the project, a description of the work to be performed at the resident's property was presented. The property owner was given an estimation of time required to complete the work.

After permission was gained from the property owner, the microphone locations were inspected to ensure that they would be suitable for noise measurements. The main concerns were ambient noise disturbances and any natural or structural elements that could result in interference. Ambient noise disturbances consist of barking dogs, air conditioners, children, wind chimes, birds, or any other item that produce noise levels high enough to contaminate a pure sampling of the highway noise levels.

### 6.1.2. Weather Conditions / Measurements

If a site was suitable for measurement and passed all the aforementioned requirements, an acoustical measurement was performed. Before any measurements were conducted, weather conditions were determined and monitored to ensure conformity with ANSI S12.8 [Acoustical Society of America 1987]. All measurements were performed with dry pavement and no precipitation. The ambient air temperature, relative humidity, and cloud cover were recorded on a measurement data sheet at the beginning of each noise measurement.

No measurements were performed when the wind speed was greater than 4.5 m/s. Most measurements were conducted when the wind speed was calm or less than 1.0 m/s. Any wind that was present during the measurements probably had little effect on the microphones since all receivers were located at relatively short distances from the source. The wind speed was monitored throughout the measurement period to ensure that the maximum speed was not surpassed. Also, a hand-held weather radio was consulted throughout the measurement period to receive general weather conditions from nearby monitoring stations. The average wind speed and wind direction for the measurement period were recorded on the measurement data sheet.

### 6.1.3. Acoustical Equipment / Setup Procedures

All measurements were performed using fast response, A-frequency weighted sound levels. Intervals of one-minute lengths were recorded so that intervals contaminated with background noise could be eliminated before the data was reduced. A complete listing of the equipment used can be found in Appendix A.

The sound level meters were checked before and after each measurement to detect any drift in calibration. The before and after calibration levels were recorded on the measurement data sheet.

After calibration, each microphone was fitted with a windscreen and positioned at a 70° angle to the horizontal to meet the specifications for random incidence response microphones. Depending on their use, the meters were then placed on either a tripod positioned at various heights or on a reference pole 1.5 meters above the top of the noise barrier.

### 6.1.4. Measurement Procedures

During each measurement, a noise monitoring sheet was completed to document the measurement conditions. Included on this sheet were the name of the site, measurement type, date, and name of the field operator. A sketch was drawn while at the site showing the location of the microphones. The serial number of each sound level meter was recorded so that the data could be downloaded to the proper directory on a laptop computer for data analysis.

Each one-minute interval was monitored during the measurement by a field operator stationed near the grid of sound level meters. If there were any disturbances such as a vehicle pass-by on a local street or a dog barking during an interval, the interval was noted as contaminated and later discarded during data reduction. The measurement continued at each microphone position until either the predetermined stop time was reached or an adequate number of uncontaminated intervals were collected.

After the measurement was complete, the post-measurement calibration was performed and the data was downloaded from the sound level meters to a laptop computer. Each meter had a separate directory created on the laptop in which to place the acquired noise data. A software

utility program provided with the sound level meters was used to perform the download. The software created a binary file which had a filename consisting of the date, month, and hour that the measurement started. All related data could then be extracted from this binary file through the data reduction process in the laboratory.

### 6.1.5. Traffic Data

A major part of the measurement process was the collection of traffic data on the mainline of the highway. Many alternatives were considered to accomplish this task such as manual counts, radar detectors, and loop detectors. However, these methods were all dismissed due to either shortages of personnel, cost, or lack of portability. The technique chosen was the recording of traffic using a video camera.

This method enabled all traffic parameters (volumes, speeds, and classifications) to be collected. A video camera was setup on an overpass near the overlap gap site prior to the beginning of the noise measurements. The camera was oriented so that it was parallel with the centerline of the median. Traffic cones were then placed along the highway at a predetermined reference distance. The camera was positioned so that all lanes of traffic could be viewed at the points where the cones were located. This enabled the approximate measurement of traffic speeds (neglecting vehicle acceleration) based on the time it takes an individual vehicle to travel the predetermined distance.

An advantage of the video method for traffic data collection was the positive identification of vehicle classifications. Most systems classify vehicles based on length. However, noise modeling uses the number of axles on a certain vehicle for classification purposes. The review of the traffic data on video enabled the positive identification of all vehicle

classes. Another advantage of this method is the permanence of the data. Any recording can be reviewed at a later time to clarify any issues that may arise. The primary disadvantage of the video technique was the large amount of time that was required to analyze the data.

The clock on the video camera was synchronized with the clocks of the sound level meters. This enabled modeling an overlap gap with the same traffic that existed when the noise measurements were conducted. The traffic data collected at the field measurement sites is found in Appendix B.

## 6.2. Measurement Sites

The field investigations were used to determine the sites best situated for noise measurements. This inspection resulted in the selection of two sites near Cincinnati, one site south of Dayton, and one site north of Columbus which were considered to be suitable for analysis. The research objectives in Chapter 2 only specify overlap gaps in Cincinnati for investigation. However, due to unsatisfactory terrain at many of the Cincinnati sites, additional overlap gaps were identified for measurement in Columbus and Dayton.

The coordinates of the barriers, roadways, and receivers input into the program to model these sites have been included in Appendix C. The breakpoint of the overlapped barriers was assigned the arbitrary X and Y-coordinates of (2000, 2000). All other coordinates were then measured from this reference point to arrive at the values shown in the appendix.

The microphones were located in a grid at each measurement site. They were placed so that data from each of the receiver regions could be attained from each site. Also, the microphones were positioned so that there were many variable receiver distances to fully test the capabilities of the GAP model.

### 6.2.1. Cincinnati Overlap Gap #1

The site considered the most ideal for modeling purposes is located north of Cincinnati on I-71 in the community of Montgomery. There is little terrain variation at this site. Therefore, both the near and far barriers are similar in top and bottom elevations. The barriers are considerably high at this site, ranging from 5.0 to 6.1 meters.

The noise barriers are typical post-and-panel construction fabricated from reflective concrete panels. The overlap is a right orientation gap. Figure 43 illustrates the Cincinnati overlap gap #1 site with the measurement receiver locations indicated.

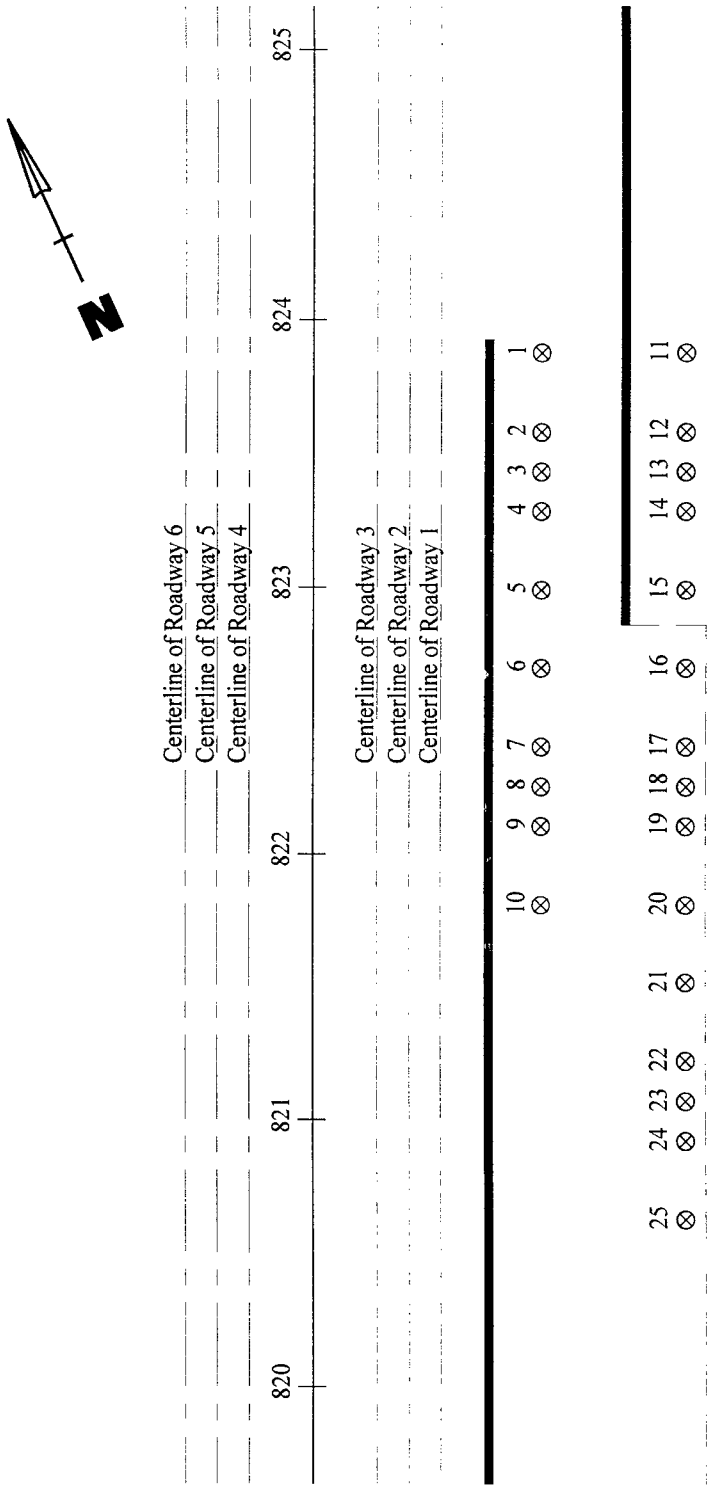


Figure 43. Cincinnati overlap gap #1

### 6.2.2. Cincinnati Overlap Gap #2

This site is located within the same noise barrier project as the previous overlap gap. However, fluctuations in the terrain make this site less valuable for noise measurements. Also, the overlap gap is situated on a slight grade which may have influenced the reference levels produced by the traffic stream. The barriers are 5.1 to 5.8 meters in height at the site. These barriers are also situated to form a right overlap gap orientation. A graphical representation of the site is provided in Figure 44. It should be noted that unlike the other three sites which consisted of 30 receiver locations, only 24 measurements were conducted at this overlap gap. Excessive change in ground elevation at distant receivers prompted the reduction in the number of measurement positions.

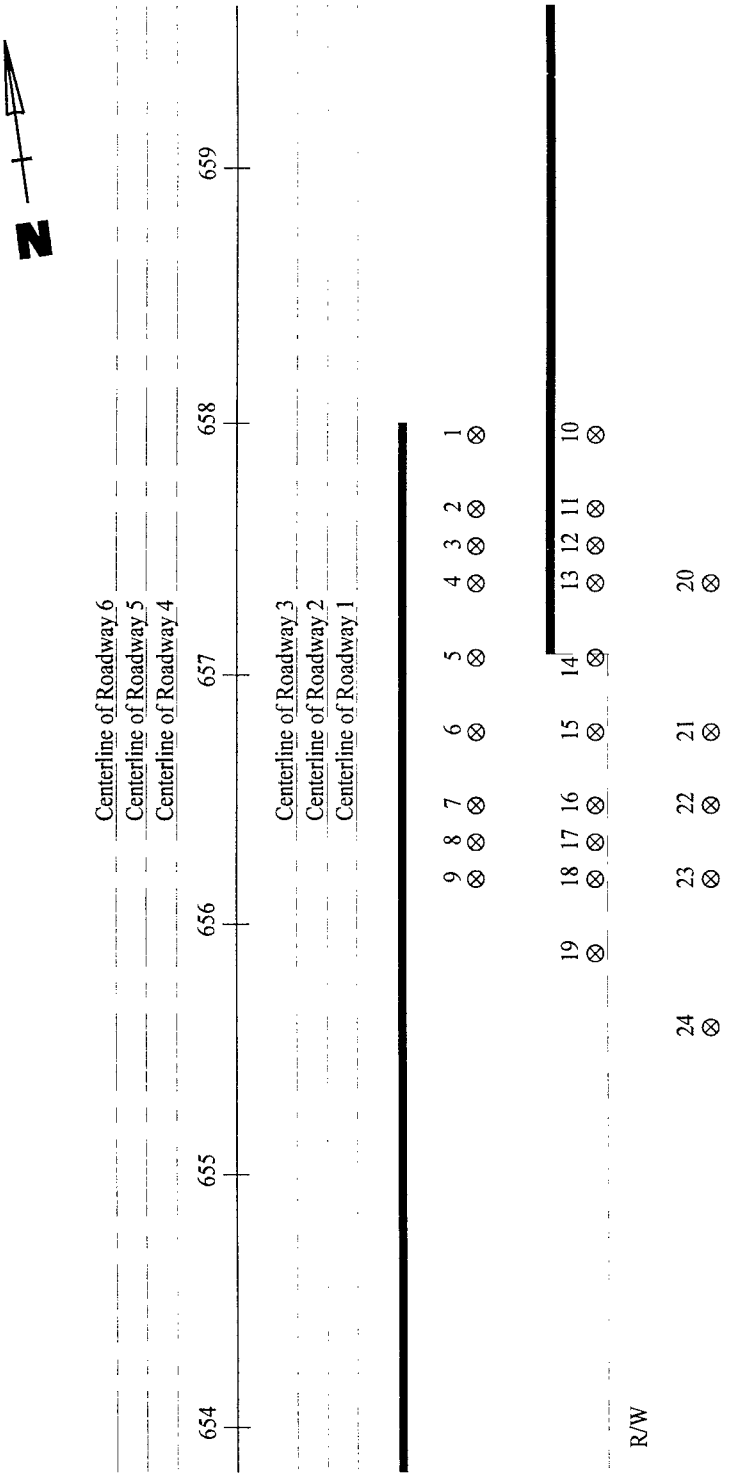


Figure 44. Cincinnati overlap gap #2

### 6.2.3. Columbus Overlap Gap

The measurements performed at the Columbus overlap gap site can be seen in Figure 45. This site is located on I-71 in the cities of Columbus and Westerville. The highway is located on fill resulting in the bottom of the far barrier having a higher elevation than the base of the near barrier. However, the rest of the measurement site is primarily level. The barriers are constructed of steel posts and steel reflective panels. This site was the only left orientation overlap gap investigated in the study. Barrier heights range from 6.0 to 6.4 meters. The roadway alignment at the Columbus overlap gap site is parallel with the noise barriers.

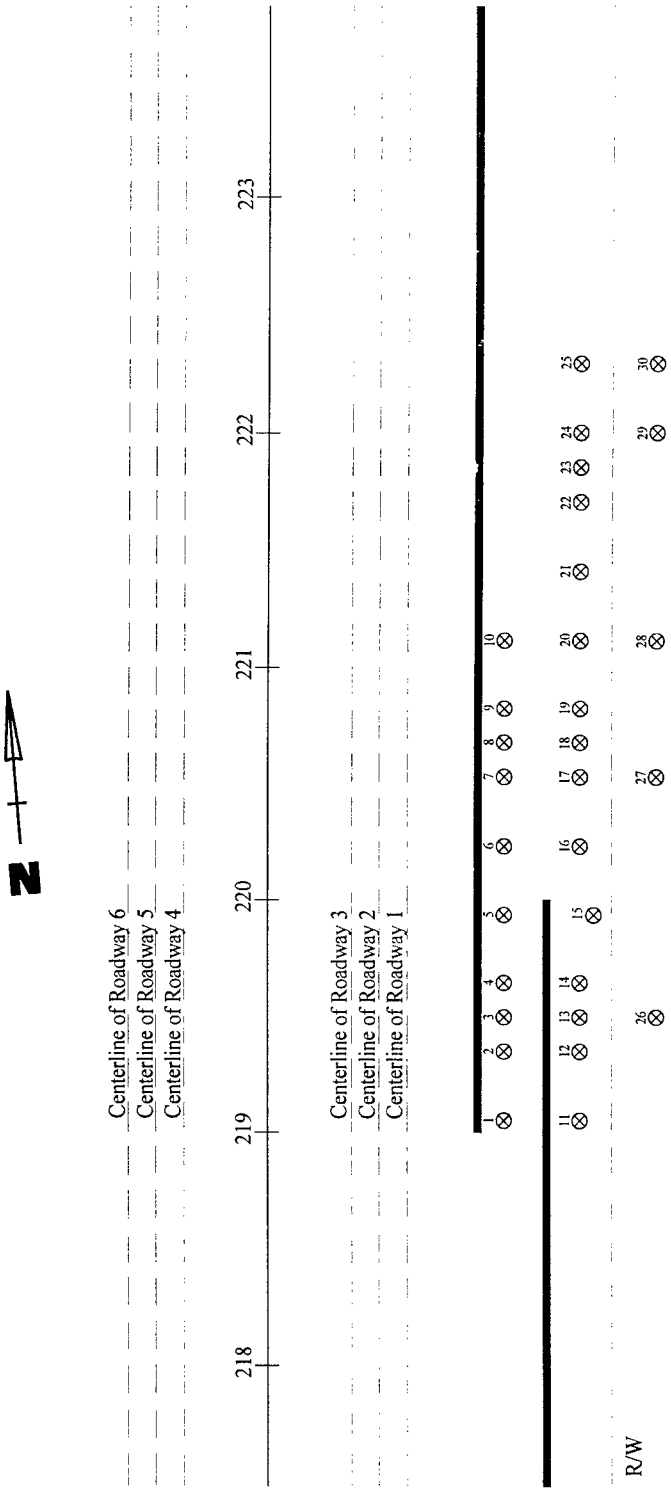


Figure 45. Columbus overlap gap

### 6.2.4. Dayton Overlap Gap

The final overlap gap site investigated is located south of Dayton on I-675 in the community of Centerville. Figure 46 shows the receiver positions for the Dayton site. A portion of the highway at this site is on a horizontal curve. This creates a limitation in modeling the overlap gap with the GAP program as the roadways must be input parallel to the noise barriers. The terrain is rolling at the site which added complexity to the noise measurements. Similar to the Cincinnati sites, the noise barriers are made of a reflective concrete post-and-panel type construction. The barrier heights are relatively low, ranging from 2.1 to 4.0 meters. The overlap is a right gap orientation.

Figure 46. Dayton overlap gap

# 7. MODEL VALIDATION

The GAP model was developed, based on image theory methods discussed in previous chapters, to calculate the effect of barrier overlap gaps on the noise environment at an overlap gap site compared to a continuous noise barrier. Using contrived data, the model was tested and the resulting trends seemed reasonable. However, there is a need to validate the model by comparing its results with data measured at actual overlap gap sites.

Ideally, in order to directly evaluate the accuracy of the model using full scale barriers and field measurements, a continuous single barrier would be required. Measurements would be made, followed by reconstruction of the barrier to form an overlap gap. Finally, measurements would be performed after construction was completed. The predicted difference in levels could then be compared to the measured difference in levels to determine the accuracy of the model for its intended function. Since such an evaluation was not feasible, an alternative method of validation was chosen.

The model was used to predict the actual (i.e. absolute) noise levels for an existing overlap gap site rather than the difference in levels (i.e. relative) between a continuous barrier and a barrier with an overlap gap. This method of validation was not only feasible but also offered a more rigorous evaluation. That is, predicting the difference in levels is less difficult than predicting the actual levels.

Two sources of data were used to perform this validation. First, field measurements were conducted at four overlap gap sites in Ohio. Next, existing data from measurements performed

on an overlap gap retrofitted with absorptive treatment in California was acquired [Hatano 1980]. These measurements were used to test the accuracy of the GAP model.

Due to the complexity of the physical phenomenon, a number of assumptions were used to develop the model. These assumptions created limitations in the applicability of the program. Ideally, an overlap gap site used for model validation would be situated on level terrain, have far and near barriers of approximately the same top and bottom elevations, and have barriers that are parallel to the roadways. This is considered ideal because it would match the assumptions in the model. Consequently, when evaluating field sites for measurement purposes, these conditions were favored. However, no sites were found that matched all required conditions. Some sites were found to be more appropriate than others. These sites were rated more highly in testing the model's algorithms against actual field conditions.

This chapter will focus on the comparison of the predicted results with the field data. The results from both the field measurements and the GAP analyses will be presented. Then, a discussion of possible sources of error will be presented. Finally, the calibration of the model will be conducted along with preliminary testing of the program's absorptive barrier modeling capabilities.

## 7.1. Comparison of Field and Model Results

The results of the field measurements, which are average values of all acceptable one-minute measurements at each microphone position, are presented in Appendix D for each study site. The single and overlap noise levels computed by the GAP model are also presented in this appendix. The results from each site will be compared. Following this discussion will be a comparison of the various sound levels at receivers grouped in the same case regions at different

sites. It should be noted that the reported noise levels have been shown to one-tenth of a decibel. Generally, noise measurements are only displayed to the whole decibel since the sound level meters and measurement methods are only accurate to ±1 dB for this type of field work. However, the data has been displayed to this degree of precision for statistical analysis purposes.

The results found in Appendix D were analyzed by comparing the predicted noise levels with the measured noise levels at each site. This was conducted by calculating the difference between the overlap barrier levels predicted by the GAP model and the actual field measured noise levels. These differences (*Overlap - Field* in Appendix D) were then compared. The average difference for each site ranged from 1.1 dB for the Columbus site to 2.6 dB for the Dayton site. The overall average difference for all four sites was 1.8 dB. Figures 47 - 48 illustrate the average difference between the predicted and measured overlap gap noise levels. From these figures, the residuals appear to be randomly distributed. The majority of the predicted levels produced by the GAP model were higher than the levels measured in the field.

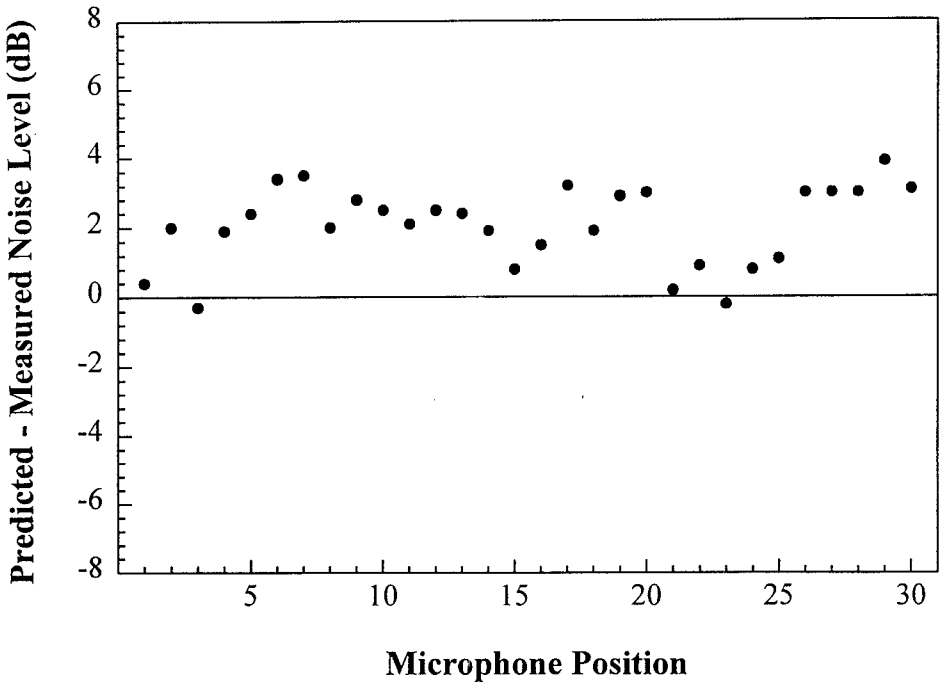


Figure 47. Noise level difference vs. microphone position (Cincinnati #1)

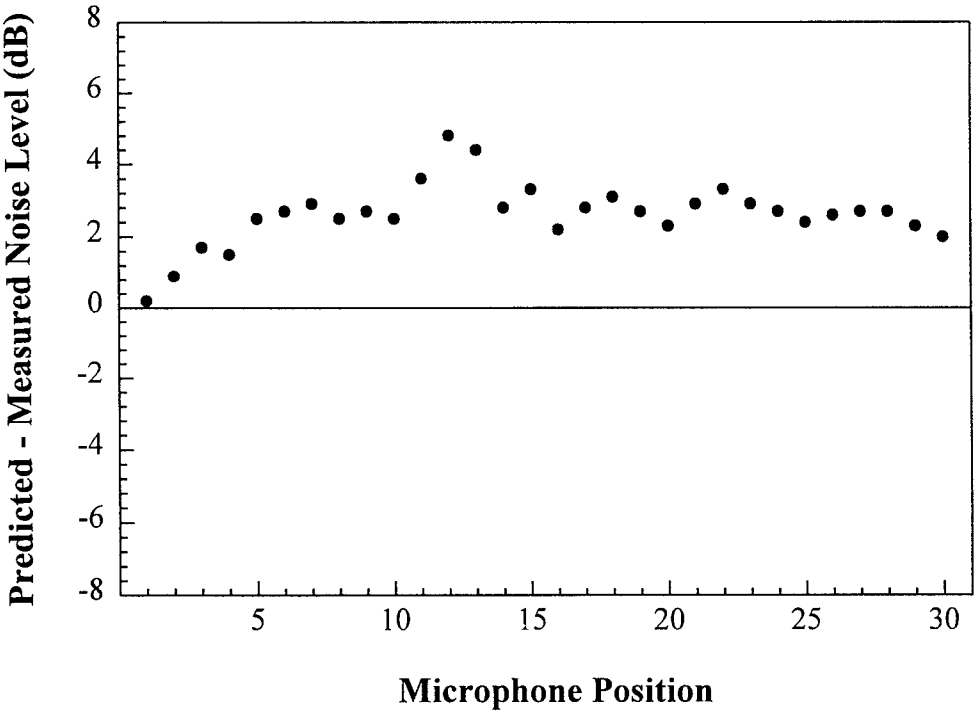


Figure 48. Noise level difference vs. microphone position (Dayton)

The results show that the Cincinnati #1, Columbus, and Dayton sites all had a fairly similar distribution of differences between predicted and measured noise levels. Of these three, Columbus has the greatest variation with several microphone positions actually having negative predicted vs. measured noise level differences. The other site studied, Cincinnati #2, had results that were different from the other three sites. The microphones in positions 18 - 24 showed an upward trend in error. The Cincinnati #2 site had a relatively high degree of terrain variation. The microphones in positions 18 - 24 were located in the areas with the most terrain variation.

In order to investigate the results more closely, an analysis was performed to compare the results of each case receiver group for all four sites. The results of this analysis are shown in Figures 49 - 50. It was hypothesized that receivers from the same case would have similar results for data distribution and average differences between predicted and measured noise levels. This hypothesis is generally supported as indicated in the figures. The Cincinnati #2 overlap gap data showed the most scatter when compared to similar receiver cases at the other sites. The Columbus overlap gap also showed a larger range of data values for Case 2 and 3 receivers.

To evaluate the accuracy of the GAP program at predicting the noise levels for each receiver case, the average predicted vs. measured differences were investigated for each receiver case. For case 2, 3, and 5 receivers, average differences of predicted vs. measured noise levels were relatively small, ranging from 1.0 dB for Case 5 to 1.7 dB for Case 3. Case 4 had an average difference of 2.9 dB. Case 1 receivers showed the largest variation, with an average difference of 4.8 dB. Based on the propagation theory used to develop the model, few reflected

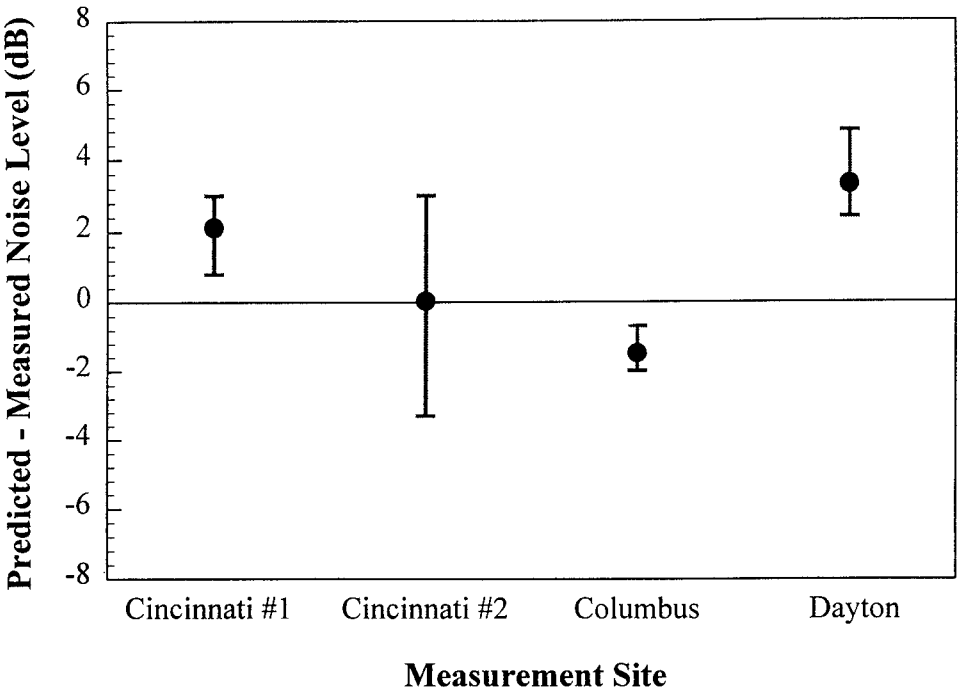


Figure 49. Noise level difference for case 1 receivers

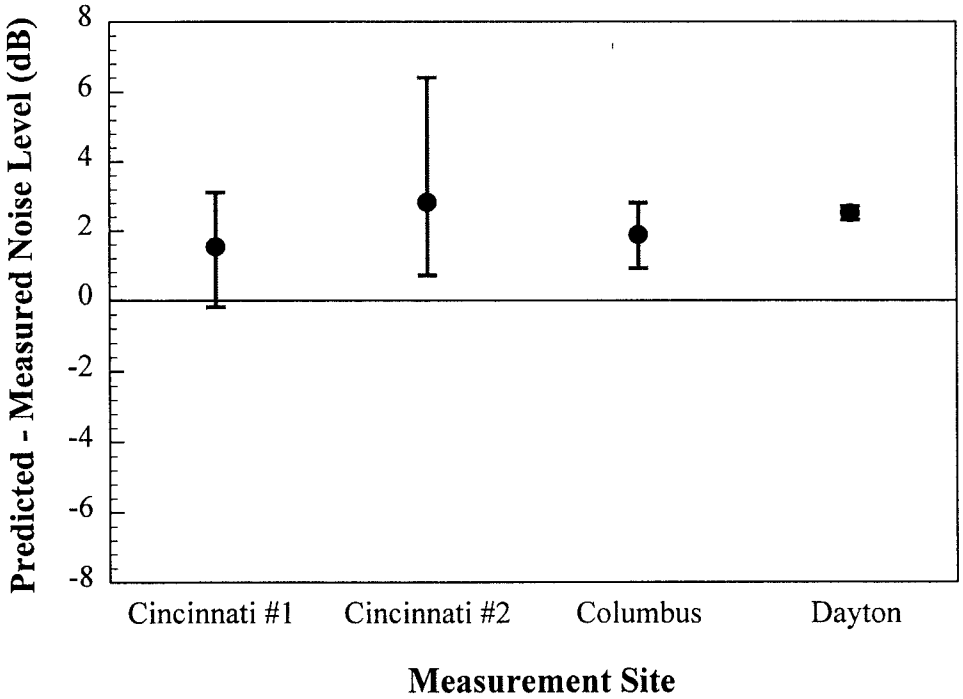


Figure 50. Noise level difference for case 5 receivers

rays can propagate through an overlap gap to contribute to the sound level at Case 1 receivers. No sound levels at receivers from Case 6 were measured in the field due to the limited size of the Case 6 zone.

Overall, the average difference between predicted and measured noise levels for all receiver cases was between 2 and 3 dB. This result is consistent with the existing STAMINA 2.0 noise model, which has been found to over-predict noise levels by an average of 2 to 3 dB at first row receiver sites with barriers [Herman and Bowlby 1997]. As a reference, when considering this discrepancy, it is crucial to recognize that a 3 dB change in noise levels is considered by many acousticians to be the smallest change in noise levels over a period of time that can normally be detected by the human ear. These discrepancies must further be qualified by the fact that the equipment and measurement methods used to obtain the field data, Type 1 precision integrating sound level meters, will limit the accuracy of the data to ± 1 dB. In light of these considerations, the differences that resulted from the comparison of predicted levels with measured or actual levels are quite acceptable providing confidence in the results of its intended use to give a relative comparison between noise levels with and without the overlap gap.

Beyond the validation process, there is value in studying the performance of GAP for sites that deviated substantially from ideal conditions. This is important to determine how the model's accuracy is affected at sites that do not conform to the limitations. There were discrepancies at sites which had highly varied terrain. However, since these discrepancies were only present at a portion of the site's microphone positions, the majority of the field data could still be applied in the calibration process. The following discussion identifies the microphones

that were excluded from this process due to relatively large violations of the program's limitations.

Microphone #12 from the Cincinnati #2 site was removed due to its height in comparison to the noise barriers. The microphone was actually slightly higher than the far barrier. In order to obtain a predicted noise level from the analysis, microphone #12 was initially input at a slightly lower elevation so that it would be accepted by GAP. However, the field measurements were obviously influenced by the lack of shielding due to the actual microphone elevation above the far barrier. Consequently, the result was not considered for calibration purposes.

Microphone #14, also from the Cincinnati #2 site, was discarded. The microphone was located 0.5 meters past the end of the near barrier. At this position, the receiver is susceptible to contributions due to the diffraction of sound waves at the end of the barrier. The model does not account for this mechanism which influences the sound level. Two other positions at the Cincinnati #2 site, microphones #23 and #24, are also suspect. The terrain at this site slopes away from the overlap gap area. The ground elevations at these receivers were considerably lower than the base elevations of the noise barriers. Due to this difference in elevations, ground attenuation can have considerable effect on the measured noise levels. Since the model does not consider ground attenuation in its prediction algorithms, the predicted noise levels may be in error. Therefore, these microphones should not be considered for calibration.

Even though noise levels at several other microphone positions might not be included due to large predicted versus measured differences in noise levels, no additional receivers were removed to preserve the random nature of the testing process. The receivers that were not included were all from the Cincinnati #2 site, which exceeded the model limitations due to terrain variations more than the other sites.

A similar process was conducted for results predicted by the Version 2.0 program, which can be found in Appendix E. The average difference between the Version 2.0 predicted sound levels and the measured sound levels ranged from 0.1 dB for the Cincinnati #2 site to 1.1 dB for the Dayton site. The overall average difference for all four sites was 0.5 dB. Each site's average difference between predicted and measured noise levels at each microphone position is shown graphically in Figures 51 - 52.

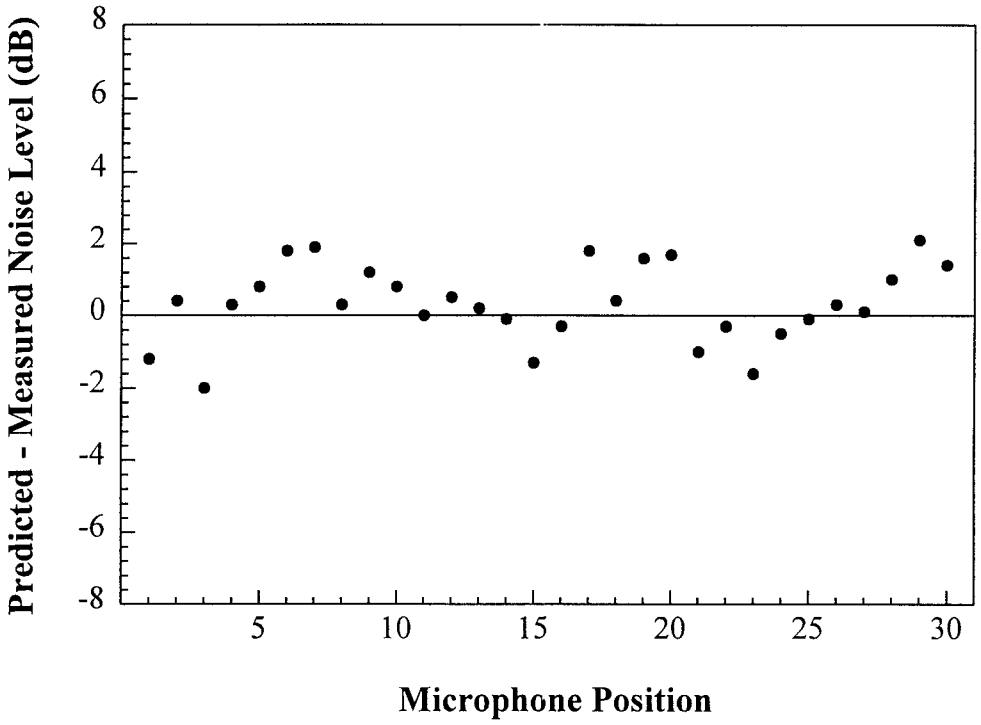


Figure 51. Noise level difference vs. microphone position (Cincinnati #1-Version 2.0)

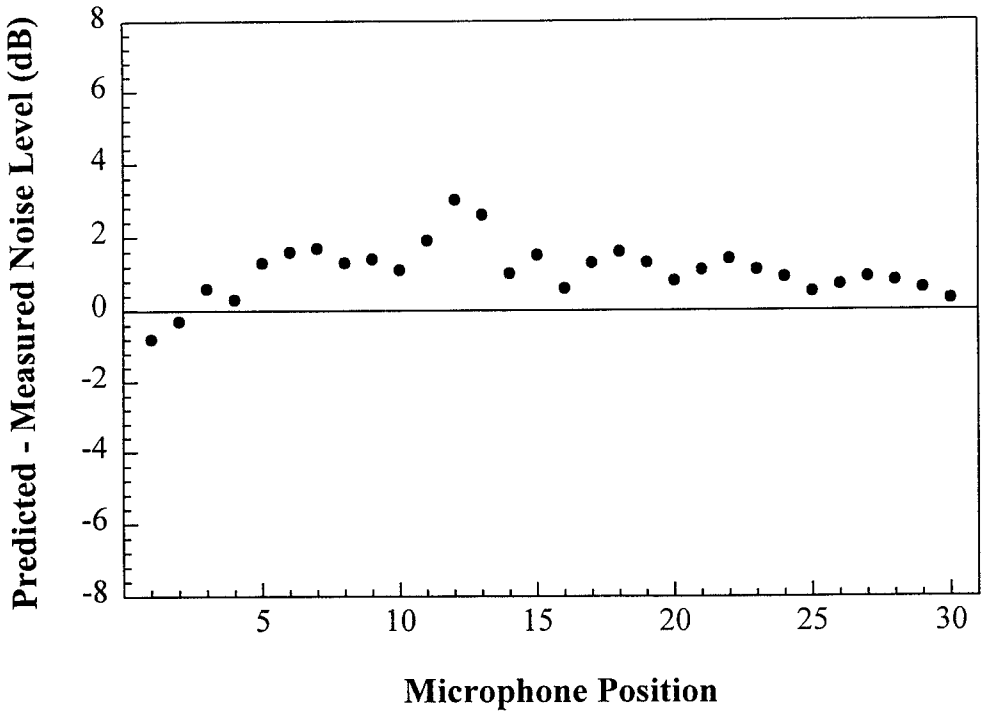


Figure 52. Noise level difference vs. microphone position (Dayton-Version 2.0)

These figures show that the Version 2.0 model slightly over-predicts the absolute sound levels at some receptors while under-predicting the levels at others. The trends in the data generally follow the Version 1.0 results.

The results of each receiver case for the Version 2.0 results were grouped for analysis. The results from this analysis are shown in Figures 53 - 54. The dispersion of these results are similar to the results from the Version 1.0 analysis. When comparing the two versions of the GAP model, Version 2.0 predicts the absolute noise levels slightly better than Version 1.0. Most receiver cases resulted in a slight over-prediction compared to measured levels. However, this over-prediction was less than that experienced with Version 1.0.

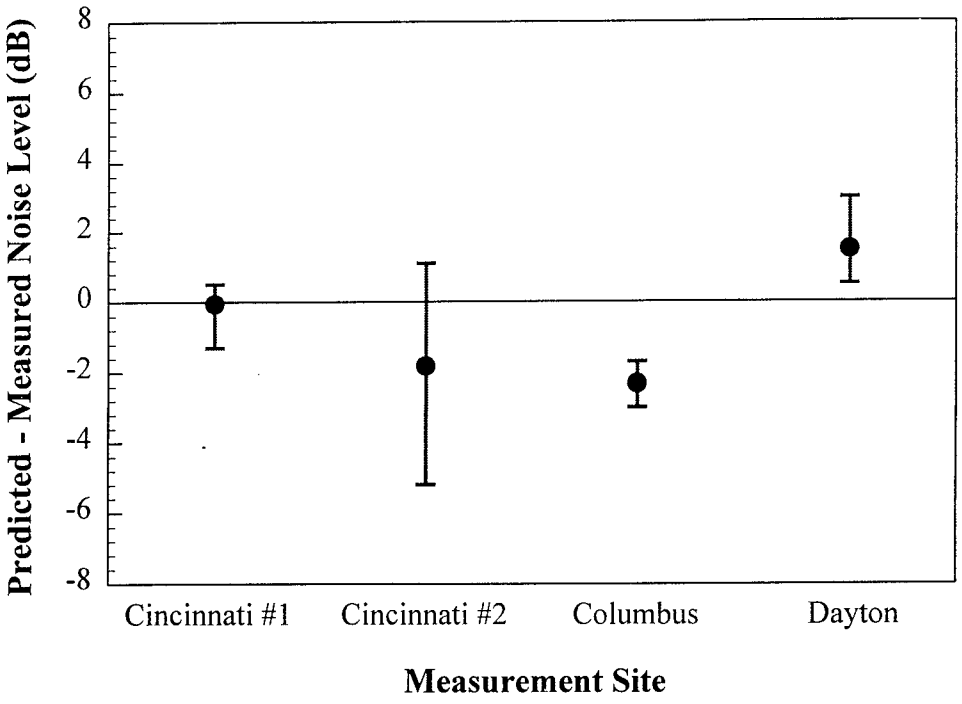


Figure 53. Noise level difference for case 1 receivers - Version 2.0

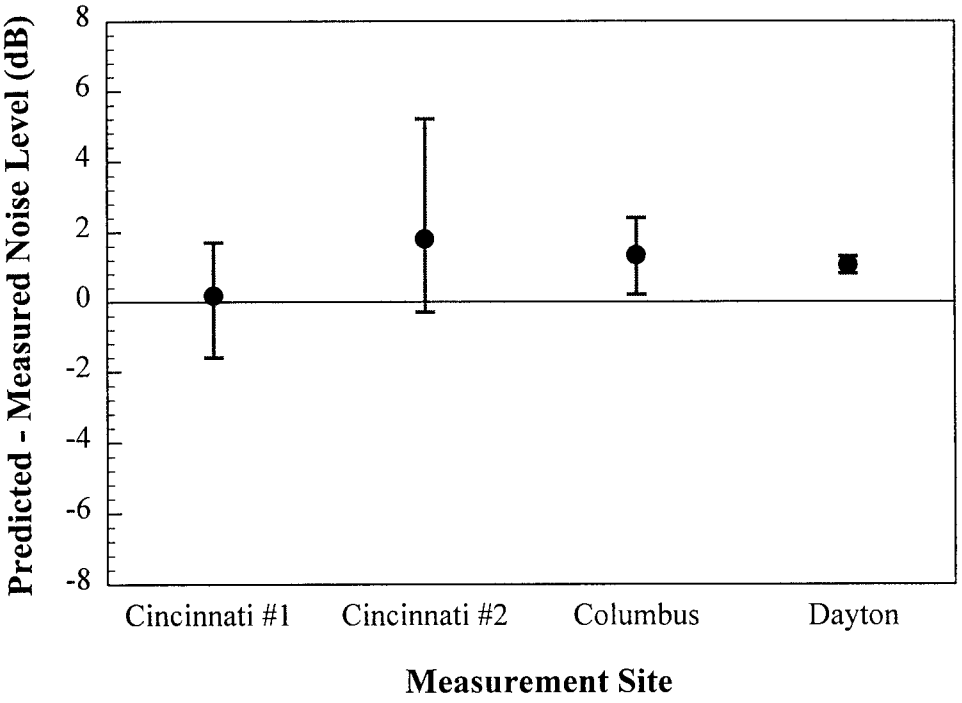


Figure 54. Noise level difference for case 5 receivers - Version 2.0

Due to these favorable results, Version 2.0 does not require calibration to improve its noise level prediction capabilities. The majority of the results were in the ± 1 - 2 dB range. This is very acceptable for this type of work Consequently, the uncalibrated model's performance is satisfactory for noise barrier overlap gap modeling.

## 7.2. Potential Sources of Error

As discussed in the previous section, there were some discrepancies between the actual field measured noise levels and the noise levels produced by the GAP model. These differences arise primarily due to assumptions that were made in the development of the model. This section will focus on other possible sources of error that may be responsible for the inconsistencies. It should be noted that this discussion is not exhaustive. Rather, the most apparent factors that may have had an influence on the results have been addressed.

The overlap gap sites were modeled as hard sites. In reality, a significant portion of each site could be modeled as soft site. When modeled as a soft site, greater attenuation is provided to the receivers which would tend to reduce the noise levels. On the other hand, any rays reflected from the pavement or other reflective surfaces other than the noise barriers were not considered. Those rays could increase levels at a given receiver.

The measurement data was collected at overlap gap sites which were designed with stepped-down barrier end treatment for aesthetic purposes. Stepped barrier overlap gaps cannot be precisely analyzed since GAP models the barriers as being full height without stepped barriers. Compared to the full height model, an actual noise barrier with stepped end treatment would allow more direct rays to enter the overlap gap region causing an increase in noise levels. On the other hand, many rays would not be reflected to potential receivers due to the less than

full height barrier end sections. These rays would simply travel over the top of one of the stepped sections before reaching a receiver. While it is possible for these two scenarios to cancel the effect of each other, the potential for error exists.

End diffraction, or side flanking of noise at the ends of the barriers, and double diffraction at the top edges of the two barriers in the overlap region are not accounted for in the model. Based on the field measurements, the actual noise level is usually greater than the predicted level for receivers located close to the end of the near barrier. On the other hand, actual noise levels would be reduced where double diffraction was present compared to predicted levels which include the effect of diffraction at one wall only.

Possible errors in the modeling of the traffic data existed. The FHWA equation assumes that each vehicle within a classification has the same source height. Further, the source heights are intended to be composite source heights representing the various components from each vehicle. This is an approximation at best and could result in significant changes in the predicted noise levels when considering the number of rays examined for a typical analysis.

The REMEL equations are limited to a maximum speed of 110 km/h. There were some traffic speeds which were measured at higher speeds. Therefore, the actual speeds were reduced to satisfy this maximum speed restriction. Also, due to the large amounts of time required to analyze the video tapes, speeds were only calculated during one measurement interval at each site. The remaining intervals were modeled using the same speed data. Therefore, the speeds used for each roadway may have contained inaccuracies.

Due to the geometrical complexities of the problem, the limitation of modeling all barriers and roadways parallel to one another was imposed. For the same reason, all roadways

and barriers had to be modeled as straight, not curved. No actual noise barrier site has this exacting geometry.

Finally, GAP cannot model roadways with a median barrier. Two sites, Cincinnati #1 and #2, had median barriers approximately one meter in height. This median barrier acts as another barrier which would shield most automobile noise and a significant portion of medium and heavy truck emissions in the far lanes. Therefore, the predicted levels would appear to be over-predicting the sound levels when compared to the actual measured sound levels.

### 7.3. Calibration of the GAP Model - Version 1.0

The GAP model was designed to predict the noise levels for receivers located near a noise barrier overlap gap. Many limitations exist and assumptions were necessary to simplify the development of the model due to the highly complex nature of the problem. Whenever assumptions are made, discrepancies usually result between the actual physical phenomenon and the model predictions. This is the case with the GAP model. However, these differences are minimal.

In order to reduce the difference of the predicted noise levels with that of the actual noise levels, the model was calibrated using actual field data. Comparisons show that, on the average, the model tends to over-predict the noise levels at all receivers locations. The amount that the model over-predicts has been classified in Appendix F. This appendix shows the receiver locations grouped by receiver case for all sites studied, excluding the microphone locations discarded from the Cincinnati #2 overlap gap.

The data presented in Appendix F shows the calibration factors that were developed to refine the predictions produced by the GAP model. Each receiver case was inspected

individually. Within a particular receiver case, the average difference between the predicted and measured noise levels was calculated at each site. These differences for all four sites were then averaged. This average is the calibration factor that is applied within the overlap barrier analysis portion of the model. Table 3 is a summary of the factors used to calibrate the model. It should be noted that no noise levels from Case 6 receivers were measured in the field, as explained earlier in this chapter. Therefore, the calibration factor for Case 6 receivers was found by averaging the factors for Case 4 and 5. This is valid because Case 6 receivers are actually specialized Case 4 and 5 receivers. These cases are very similar, as evidenced by their calibration factors, 2.4 and 2.0 dB, respectively. These calibration factors are subtracted from the levels calculated by the model to reduce the over-prediction of the noise levels.

Table 3. GAP calibration factors

| Receiver case | Calibration factor (dB) |
|---|---|
| 1 | 1.2 |
| 2 | 1.0 |
| 3 | 2.3 |
| 4 | 2.4 |
| 5 | 2.0 |
| 6 | 2.2 |

The four noise barrier overlap gap sites were modeled after the calibration factors were applied to the GAP theory. The calibrated results can be found in Appendix G. From an inspection of the results, it is clear that the calibration process reduced the amount of over-

prediction. In fact, a large number of sites actually show results that are under-predicted. The final range of the average differences for the four sites are -0.7 dB at the Columbus site to 0.9 dB at the Dayton site. The Cincinnati sites have average differences of 0.3 and -0.4 dB for the first and second site, respectively. Based on the 3 dB criteria of the lowest discernible change in noise levels, the calibrated GAP model correctly models the majority of receivers tested.

It should be noted that data from only four sites were used to calibrate the GAP model. This data is limited in range and does not represent all noise barrier overlap gap sites in general. The calibrated model should only be used to test sites which have characteristics similar to those measured in this research. All other sites not closely resembling these sites should be analyzed using the uncalibrated model.

### 7.4. Absorptive Barrier Testing

No noise barrier overlap gaps have been retrofitted with absorptive treatment in the state of Ohio at the time of this research. Therefore, it was not possible to perform field measurements to acquire data for the testing of the absorptive treatment algorithms of the model. However, previous work has been completed in California on an absorptive overlap gap [Hatano 1980]. This research involved the acoustical measurement of overlap gaps before and after absorptive treatment was applied to the inner surfaces of the noise barrier overlap gap. One of the California sites has been investigated using the Version 1.0 calibrated GAP model to test the absorptive capabilities of the program. The site geometry, traffic data, and measured noise levels from this investigation can be found in Appendix H. The CalTrans report should be consulted for measurement procedure, site description, and related data.

The analysis results show that the Version 1.0 calibrated model under-predicts the measured noise levels when the site is modeled as both non-absorptive and absorptive. The non-absorptive analysis resulted in an average difference of -3.0 dB between the predicted and measured noise levels. The absorptive analysis produced an average difference of -3.3 dB between the predicted and measured noise levels. This result is encouraging as the relative decrease in noise levels between non-absorptive and absorptive barriers is similar for both predicted and measured noise levels.

The acoustical specifications of the absorptive panels attached to the noise barriers were not provided in the report's documentation. Therefore, the noise reduction coefficient (NRC) of the absorptive treatment was approximated to be 0.85. If this coefficient was too high, it would lead to the overlap barrier noise levels predicted by the GAP model to be too low. Closer inspection of the data shows that Microphone #3 is located close to the end of the near barrier. This microphone is in a position that is likely to be influenced by end diffraction or side flanking. Since the model does not account for this mechanism, the measured noise levels would be higher than the predicted levels, which is the case with this analysis.

Another source of error that may be present in this analysis is the calibration process. The GAP model was calibrated with data from 1996-1997 traffic sources. The work in California was performed in 1979-1980. The source emissions have changed over that time period due to developments in the automobile and tire industries. The calibration performed in the previous section corrected errors that may have existed with the source emissions. Since the calibration factors reduced the final overlap noise levels, this may have had an effect on the predicted overlap levels being low.

Due to these error sources, the absolute noise levels should not be the primary finding upon which to evaluate the outcome of the analysis. Rather, the trends between the predicted and measured noise levels should be investigated. Inspection of these trends show that the predicted levels changed in the proper direction and by a similar magnitude. These preliminary results are promising and warrant additional research for the optimization of noise barrier overlap gap design.

# 8. CONCLUSIONS AND RECOMMENDATIONS

## 8.1. Conclusions

A computer program, the Gap Analysis Program (GAP), was developed to assist in the analysis and design of overlap gaps in existing and proposed highway noise barriers.

The development was initiated due to findings in previous research which indicated the noise environment is degraded at overlap gap locations. It was hypothesized that multiple reflections were the primary reason that the insertion loss degradation was occurring. Due to the presence of many overlap gaps at several noise barrier sites, the importance of determining the effect of these gaps was apparent.

Algorithms necessary to analyze the physical phenomena of noise propagation at a barrier overlap gap were formulated. This involved the generation of theory to evaluate the multiple paths that sound waves can travel to reach a receiver. The process was further complicated by the fact that the source is dynamic. A method to deal with moving sources to compute the effect of their sound emissions on distant receivers was devised, as explained in Chapter 3 in the section, "Image Ray Analysis." The modeling of the overlap gaps was enhanced by enabling the effect of absorptive treatment to be studied.

In order to simplify the computation of noise levels from all the involved mechanisms, the theory was programmed to allow computer modeling. The algorithms were coded using the Visual Basic language to develop a Windows 95 application. This program can analyze a noise barrier overlap gap with a maximum of 10 receivers and roadways. Graphic output may be

investigated after entering all the necessary parameters to assure the user that the data was input correctly. The program includes features which allow the management of files and the printing of input data and analysis results.

Field work was completed at four noise barrier overlap gap sites in central and southwestern Ohio. Noise measurements were performed at multiple receiver locations at each site. The geometry of the barriers, roadways, and receivers were carefully recorded to enable proper modeling of the test sites. Traffic data was collected during the noise measurement intervals for inputs into the program.

The collected data from the field measurements was processed for input into the GAP model. Many tests were conducted using the trial data. The results were analyzed to determine the model's accuracy with actual measurements. Calibration factors were developed to correct discrepancies which existed between the predicted results and actual field measurements.

The following list details the findings of the research on the traffic noise barrier overlap gaps:

1. Many mechanisms exist which influence the propagation of sound waves at overlap gap sites. These mechanisms include direct propagation, diffracted sound waves, reflected sound waves without diffraction, and reflected sound waves with diffraction.
2. Multiple reflections are the primary reason for noise level increases at noise barrier overlap gap sites, as currently designed.
3. Receivers are subject to different mechanisms which influence propagation depending on where the receiver is located in the overlap gap region. This research has identified six receiver regions corresponding to the influencing mechanisms which can affect the noise levels at the receiver.

4. The traffic noise source may be analyzed to determine the existence of reflected rays by dividing the surface into many short segments. Each segment's contribution to the overall noise level may be found by assuming that the mid-angle location of the segment is the energy centroid of the segment.
5. Reflective propagation paths can effectively be modeled by utilizing image ray theory to determine necessary ray angles and path lengths.
6. Absorptive treatment is a potential method to attenuate the reflections that occur at a noise barrier overlap gap site.

## 8.2. Recommendations

This report provides a comprehensive tool for transportation officials to aid in the analysis and design of noise barrier overlap gaps. Many advancements have been made on past work in this area. However, the following issues still exist for further development.

1. An overlap gap at the Cincinnati project needs to be retrofitted with absorptive treatment to investigate the benefits of using absorptive panels to attenuate the reflected sound waves. The results would be evaluated with both before and after field measurements and GAP model predictions.
2. There is a need to incorporate a ground attenuation algorithm into the model to evaluate the effects of the terrain on the propagation of sound at overlap gap sites.
3. The effect that stepped end treatments have on the propagation of sound waves at an overlap gap site should be investigated.
4. The refinements of end diffraction and double diffraction should be considered in the model to give the user a wider range of receiver placement.

5. A non-intrusive traffic data collection method needs to be developed to minimize the time and reduce the work required for traffic data collection for validation and calibration of future model enhancements.
6. Reference energy mean emission levels (REMELs) needed to be formulated which allow a greater range of use than the existing 110 km/h limitation.
7. The analysis modules of the model need to be revised to accommodate complex geometric designs. These include the following: curved roadways and barriers, roadways and barriers on grades, and non-parallel barriers and roadways.
8. The effect of median barriers needs to be investigated to evaluate their influence on the measurement results.

## REFERENCES


Acoustical Society of America. 1987. American national standard: methods for determination of insertion loss of outdoor barriers. New York: Acoustical Society of America. ANSI S12.8-1987.

Anderson, G.S. 1996. Private communication with author. 10 December.

Anderson, G.S. and C.W. Menge. 1996. FHWA traffic noise model (FHWA TNM®), version 1.0: user's guide. Cambridge, MA: John A. Volpe National Transportation Systems Center, Acoustics Facility. FHWA-PD-96-009.

Barry, T.M., and J.A. Reagan. 1978. FHWA highway traffic noise prediction model. Washington D.C.: Federal Highway Administration, U.S. Department of Transportation. FHWA-RD-77-108.

Beranek, L.L., ed. 1971. Noise and vibration control. New York: McGraw-Hill.

Bowlby, W. 1992. In-service experience with traffic noise barriers. Washington D.C.: Transportation Research Board. NCHRP Report 181.

Bowlby, W. and L.F. Cohn. 1983. IMAGE-3: Computer-aided design for parallel highway noise barriers. Transportation Research Record 937. Washington D.C.: Transportation Research Board. National Research Council.

_____. 1986. A model for insertion loss degradation for parallel highway noise barriers. Journal of the Acoustical Society of America. 80, no. 3: 855-866.

Bowlby, W., J. Higgins, and J.A. Reagan (eds.). 1982. Noise barrier cost reduction procedure, STAMINA 2.0/OPTIMA: user's manual. Washington D.C.: Federal Highway Administration. U.S. Department of Transportation. FHWA-DP-58-1.

Cohn, L.F. 1981. Highway noise barriers. Washington D.C.: Transportation Research Board. NCHRP Report 87.

Dhamija, D. 1996. Private communication with author. 3 September.

Federal Highway Administration. 1982. Procedures for Abatement of Highway Traffic Noise and Construction Noise. Washington D.C.: U.S. Department of Transportation. 23 CFR Part 772.

Hatano, M.M. 1980. Maintenance access for noise barriers. Sacramento: California Department of Transportation. CA/TL-80/19.

Herman, L.A. and W. Bowlby. 1997. Case history: an evaluation of STAMINA 2.0 based on I-440 field measurements. Noise Control Engineering. 45 (January - February): 52 - 59.

Herman, L.A., C.M. Clum, and M.A. Finney. 1997. Preliminary assessment of traffic noise barrier effectiveness for project HAM-71-11.44. Columbus, OH: Ohio Department of Transportation. FHWA/OH-96/009.

Koffman, E.B. and F.L. Friedman. 1990. Problem solving and structured programming in FORTRAN 77. Reading, MA: Addison-Wesley Publishing Company, Inc.

Kurze, U.J. and G.S. Anderson. 1971. Sound attenuation by barriers. Applied Acoustics. 4: 35-53.

Lee, V., S. Slutsky, E. Ken, R. Michalove, and W. McColl. 1990. "Barrier overlap analysis procedure." Transportation Research Record 1255. Washington D.C.: Transportation Research Board. National Research Council.

Organization for Economic Cooperation and Development. 1995. Roadside noise abatement. Paris: Road Transport Research. IRRD No. 870922.

Reagan, J.A. 1978. Determination of reference energy mean emission levels. Washington D.C.: Federal Highway Administration, U.S. Department of Transportation. FHWA-OEP/HEV-78-1.

Rudder, F.F. Jr. and P. Lam. 1977. Users manual: TSC highway noise prediction code: MOD-04. Washington D.C.: Federal Highway Administration, U.S. Department of Transportation. FHWA-RD-77-18.

Simpson, M.A. 1976. Noise barrier design handbook. Washington D.C.: Federal Highway Administration, U.S. Department of Transportation. FHWA-RD-76-58.

# APPENDIX A

# LISTING OF EQUIPMENT

| Equipment | Model | Serial Number |
|---|---|---|
| Larson-Davis acoustic calibrator | CA 200 | 0423 |
| Larson-Davis sound level meter | 812 | 0336 |
| Larson-Davis sound level meter | 812 | 0337 |
| Larson-Davis sound level meter | 812 | 0338 |
| Larson-Davis sound level meter | 812 | 0339 |
| Larson-Davis sound level meter | 812 | 0340 |
| Larson-Davis sound level meter | 812 | 0341 |

# APPENDIX B

# TRAFFIC DATA FOR OVERLAP GAP FIELD MEASURMENTS

## TRAFFIC DATA FOR CINCINNATI OVERLAP GAP #1

| Mic. # | Lane # | Volumes (veh/h) | | | Speeds (km/h) | | |
|---|---|---|---|---|---|---|---|
| | | A | MT | HT | A | MT | HT |
| 1 - 5 | 1 | 1877 | 34 | 69 | 126.1 | 115.5 | 120.8 |
| | 2 | 1089 | 26 | 103 | 145.8 | 141.6 | 137.6 |
| | 3 | 926 | 9 | 9 | 121.2 | 118.6 | 125.4 |
| | 4 | 1080 | 0 | 26 | 117.6 | 0.0 | 110.7 |
| | 5 | 1003 | 26 | 137 | 111.7 | 107.1 | 109.7 |
| | 6 | 891 | 60 | 43 | 119.3 | 107.6 | 113.1 |
| 6 - 10 | 1 | 1937 | 69 | 51 | 107.4 | 109.3 | 109.7 |
| | 2 | 891 | 51 | 103 | 112.7 | 109.7 | 104.7 |
| | 3 | 1029 | 26 | 34 | 113.5 | 111.6 | 109.7 |
| | 4 | 1140 | 26 | 0 | 109.7 | 107.9 | 0.0 |
| | 5 | 1080 | 43 | 77 | 107.6 | 105.0 | 99.5 |
| | 6 | 857 | 77 | 103 | 109.7 | 109.7 | 104.5 |
| 11 - 15 | 1 | 2422 | 65 | 49 | 81.3 | 84.4 | 82.8 |
| | 2 | 1025 | 11 | 82 | 93.4 | 93.4 | 95.4 |
| | 3 | 1549 | 5 | 9 | | | |

## TRAFFIC DATA FOR CINCINNATI OVERLAP GAP #2

| Mic. # | Lane # | Volumes (veh/h) | | | Speeds (km/h) | | |
|---|---|---|---|---|---|---|---|
| | | A | MT | HT | A | MT | HT |
| 1 - 5 | 1 | 797 | 103 | 51 | 98.5 | 96.0 | 93.7 |
| | 2 | 1123 | 26 | 129 | 101.1 | 101.1 | 96.0 |
| | 3 | 917 | 0 | 0 | 106.7 | 0.0 | 0.0 |
| | 4 | 1020 | 34 | 86 | 103.8 | 97.3 | 101.1 |
| | 5 | 1029 | 26 | 94 | 96.0 | 96.0 | 93.7 |
| | 6 | 1071 | 86 | 129 | 106.7 | 98.5 | 93.7 |
| 6 - 9 | 1 | 857 | 34 | 94 | 98.5 | 96.0 | 93.7 |
| | 2 | 934 | 26 | 60 | 101.1 | 101.1 | 96.0 |
| | 3 | 489 | 26 | 9 | 106.7 | 106.7 | 120.0 |
| | 4 | 617 | 0 | 17 | 103.8 | 0.0 | 101.1 |
| | 5 | 891 | 0 | 111 | 96.0 | 0.0 | 93.7 |
| | 6 | 994 | 69 | 77 | 106.7 | 98.5 | 93.7 |
| 10 - 14 | 1 | 923 | 75 | 53 | 98.5 | 96.0 | 93.7 |
| | 2 | 983 | 23 | 90 | 101.1 | 101.1 | 96.0 |
| | 3 | 608 | 0 | 0 | 106.7 | 0.0 | 0.0 |
| | 4 | 975 | 0 | 8 | 103.8 | 0.0 | 101.1 |
| | 5 | 1005 | 38 | 120 | 96.0 | 96.0 | 93.7 |
| | 6 | 1073 | 68 | 98 | 106.7 | 98.5 | 93.7 |
| 15 - 19 | 1 | 986 | 60 | 69 | 98.5 | 96.0 | 93.7 |
| | 2 | 1003 | 17 | 146 | 101.1 | 101.1 | 96.0 |
| | 3 | 720 | 9 | 0 | 106.7 | 106.7 | 0.0 |
| | 4 | 617 | 9 | 0 | 103.8 | 97.3 | 0.0 |
| | 5 | 831 | 26 | 137 | 96.0 | 96.0 | 93.7 |
| | 6 | 1063 | 43 | 86 | 106.7 | 98.5 | 93.7 |
| 20 - 24 | 1 | 878 | 45 | 120 | 98.5 | 96.0 | 93.7 |
| | 2 | 1065 | 45 | 158 | 101.1 | 101.1 | 96.0 |
| | 3 | 833 | 8 | 8 | 106.7 | 106.7 | 120.0 |
| | 4 | 653 | 0 | 240 | 103.8 | 0.0 | 101.1 |
| | 5 | 975 | 23 | 143 | 96.0 | 96.0 | 93.7 |
| | 6 | 1275 | 75 | 60 | 106.7 | 98.5 | 93.7 |

## TRAFFIC DATA FOR COLUMBUS OVERLAP GAP

| Mic. # | Lane # | Volumes (veh/h) | | | Speeds (km/h) | | |
|---|---|---|---|---|---|---|---|
| | | A | MT | HT | A | MT | HT |
| 1 - 5 | 1 | 820 | 30 | 40 | 89.5 | 87.2 | 87.2 |
| | 2 | 770 | 10 | 140 | 91.9 | 85.0 | 85.0 |
| | 3 | 390 | 0 | 0 | 94.1 | 0.0 | 0.0 |
| | 4 | 500 | 20 | 40 | 87.2 | 89.6 | 85.0 |
| | 5 | 620 | 40 | 240 | 87.2 | 87.2 | 85.0 |
| | 6 | 280 | 30 | 70 | 94.5 | 91.9 | 85.0 |
| 6 - 10 | 1 | 588 | 0 | 60 | 89.5 | 0.0 | 87.2 |
| | 2 | 744 | 12 | 132 | 91.9 | 85.0 | 85.0 |
| | 3 | 588 | 24 | 12 | 94.1 | 86.1 | 94.5 |
| | 4 | 396 | 36 | 0 | 87.2 | 89.6 | 0.0 |
| | 5 | 720 | 60 | 204 | 87.2 | 87.2 | 85.0 |
| | 6 | 372 | 12 | 132 | 94.5 | 91.9 | 85.0 |
| 11 - 15 | 1 | 780 | 43 | 129 | 89.5 | 87.2 | 87.2 |
| | 2 | 857 | 17 | 189 | 91.9 | 85.0 | 85.0 |
| | 3 | 634 | 0 | 9 | 94.1 | 0.0 | 94.5 |
| | 4 | 609 | 0 | 17 | 87.2 | 0.0 | 85.0 |
| | 5 | 754 | 43 | 180 | 87.2 | 87.2 | 85.0 |
| | 6 | 420 | 51 | 120 | 94.5 | 91.9 | 85.0 |
| 16 - 20 | 1 | 732 | 24 | 96 | 89.5 | 87.2 | 87.2 |
| | 2 | 696 | 48 | 120 | 91.9 | 85.0 | 85.0 |
| | 3 | 660 | 12 | 0 | 94.1 | 86.1 | 0.0 |
| | 4 | 624 | 24 | 36 | 87.2 | 89.6 | 85.0 |
| | 5 | 972 | 48 | 240 | 87.2 | 87.2 | 85.0 |
| | 6 | 456 | 24 | 132 | 94.5 | 91.9 | 85.0 |
| 21 - 25 | 1 | 1008 | 12 | 72 | 89.5 | 87.2 | 87.2 |
| | 2 | 852 | 12 | 204 | 91.9 | 85.0 | 85.0 |
| | 3 | 672 | 24 | 0 | 94.1 | 86.1 | 0.0 |
| | 4 | 528 | 24 | 36 | 87.2 | 89.6 | 85.0 |
| | 5 | 756 | 36 | 288 | 87.2 | 87.2 | 85.0 |
| | 6 | 468 | 12 | 156 | 94.5 | 91.9 | 85.0 |
| 26 - 30 | 1 | 1008 | 12 | 72 | 89.5 | 87.2 | 87.2 |
| | 2 | 900 | 0 | 180 | 91.9 | 0.0 | 85.0 |
| | 3 | 1068 | 0 | 12 | 94.1 | 0.0 | 94.5 |
| | 4 | 636 | 0 | 12 | 87.2 | 0.0 | 85.0 |
| | 5 | 840 | 36 | 180 | 87.2 | 87.2 | 85.0 |
| | 6 | 432 | 12 | 108 | 94.5 | 91.9 | 85.0 |

## TRAFFIC DATA FOR DAYTON OVERLAP GAP

| Mic. # | Lane # | A | MT | HT | A | MT | HT |
|---|---|---|---|---|---|---|---|
| 1 - 5 | 1 | 990 | 30 | 40 | 96.0 | 93.7 | 91.4 |
| | 2 | 510 | 20 | 40 | 101.1 | 101.1 | 93.7 |
| | 3 | 170 | 0 | 0 | 106.7 | 0.0 | 0.0 |
| | 4 | 50 | 0 | 0 | 113.0 | 0.0 | 0.0 |
| | 5 | 540 | 0 | 30 | 109.7 | 0.0 | 98.5 |
| | 6 | 720 | 50 | 40 | 106.7 | 109.7 | 101.1 |
| 6 - 10 | 1 | 880 | 0 | 48 | 96.0 | 0.0 | 91.4 |
| | 2 | 576 | 0 | 24 | 101.1 | 0.0 | 93.7 |
| | 3 | 108 | 0 | 0 | 106.7 | 0.0 | 0.0 |
| | 4 | 144 | 0 | 0 | 113.0 | 0.0 | 0.0 |
| | 5 | 540 | 0 | 24 | 109.7 | 0.0 | 98.5 |
| | 6 | 624 | 0 | 60 | 106.7 | 0.0 | 101.1 |
| 11 - 15 | 1 | 1110 | 60 | 60 | 96.0 | 93.7 | 91.4 |
| | 2 | 560 | 20 | 40 | 101.1 | 101.1 | 93.7 |
| | 3 | 130 | 0 | 0 | 106.7 | 0.0 | 0.0 |
| | 4 | 160 | 0 | 0 | 113.0 | 0.0 | 0.0 |
| | 5 | 730 | 0 | 10 | 109.7 | 0.0 | 98.5 |
| | 6 | 700 | 0 | 80 | 106.7 | 0.0 | 101.1 |
| 16 - 20 | 1 | 930 | 10 | 60 | 96.0 | 93.7 | 91.4 |
| | 2 | 636 | 12 | 48 | 101.1 | 101.1 | 93.7 |
| | 3 | 120 | 0 | 0 | 106.7 | 0.0 | 0.0 |
| | 4 | 48 | 0 | 0 | 113.0 | 0.0 | 0.0 |
| | 5 | 468 | 0 | 24 | 109.7 | 0.0 | 98.5 |
| | 6 | 696 | 12 | 72 | 106.7 | 109.7 | 101.1 |
| 21 - 25 | 1 | 1130 | 70 | 70 | 96.0 | 93.7 | 91.4 |
| | 2 | 610 | 10 | 20 | 101.1 | 101.1 | 93.7 |
| | 3 | 70 | 0 | 0 | 106.7 | 0.0 | 0.0 |
| | 4 | 90 | 0 | 0 | 113.0 | 0.0 | 0.0 |
| | 5 | 590 | 30 | 20 | 109.7 | 98.5 | 98.5 |
| | 6 | 710 | 30 | 50 | 106.7 | 109.7 | 101.1 |
| 26 - 30 | 1 | 828 | 48 | 60 | 96.0 | 93.7 | 91.4 |
| | 2 | 444 | 12 | 60 | 101.1 | 101.1 | 93.7 |
| | 3 | 168 | 0 | 12 | 106.7 | 0.0 | 96.0 |
| | 4 | 48 | 0 | 0 | 113.0 | 0.0 | 0.0 |
| | 5 | 760 | 12 | 12 | 109.7 | 98.5 | 98.5 |
| | 6 | 852 | 48 | 60 | 106.7 | 109.7 | 101.1 |

# APPENDIX C

# GEOMETRY OF OVERLAP GAP FIELD MEASUREMENT SITES

## SITE GEOMETRY FOR CINCINNATI OVERLAP GAP #1

Noise Barriers

| Barrier | X1 (m) | Y1 (m) | X2 (m) | Y2 (m) | Bottom Elevation (m) | Top Elevation (m) |
|---|---|---|---|---|---|---|
| Single | 1500 | 2000 | 2500 | 2000 | 251.3 | 256.3 |
| Far | 1500 | 2000 | 2000 | 2000 | 251.3 | 256.3 |
| Near | 1967.5 | 1984.4 | 2500 | 1984.4 | 250.5 | 256.6 |

Overlap Length: 32.5 m
Overlap Width: 15.6 m

Traffic data recorded on Deerfield Road overpass facing north

Roadways

| Roadway | X1 (m) | Y1 (m) | X2 (m) | Y2 (m) | Elevation (m) |
|---|---|---|---|---|---|
| 1 | 1500 | 2005.5 | 2500 | 2005.5 | 251.3 |
| 2 | 1500 | 2009.1 | 2500 | 2009.1 | 251.3 |
| 3 | 1500 | 2012.8 | 2500 | 2012.8 | 251.3 |
| 4 | 1500 | 2027.4 | 2500 | 2027.4 | 251.3 |
| 5 | 1500 | 2031.1 | 2500 | 2031.1 | 251.3 |
| 6 | 1500 | 2034.7 | 2500 | 2034.7 | 251.3 |

Receivers

| Receiver | X (m) | Y (m) | Elevation (m) |
|---|---|---|---|
| 1 | 1998.5 | 1994.0 | 252.7 |
| 2 | 1989.5 | 1994.0 | 252.6 |
| 3 | 1985.0 | 1994.0 | 254.5 |
| 4 | 1980.5 | 1994.0 | 252.7 |
| 5 | 1971.5 | 1994.0 | 252.8 |
| 6 | 1962.5 | 1994.0 | 252.5 |
| 7 | 1953.5 | 1994.0 | 252.4 |
| 8 | 1949.0 | 1994.0 | 254.3 |
| 9 | 1944.5 | 1994.0 | 252.5 |
| 10 | 1935.5 | 1994.0 | 252.6 |
| 11 | 1998.5 | 1977.5 | 253.7 |
| 12 | 1989.5 | 1977.5 | 253.6 |
| 13 | 1985.0 | 1977.5 | 255.4 |
| 14 | 1980.5 | 1977.5 | 253.6 |
| 15 | 1971.5 | 1977.5 | 253.6 |
| 16 | 1962.5 | 1977.5 | 253.2 |
| 17 | 1953.5 | 1977.5 | 253.1 |
| 18 | 1949.0 | 1977.5 | 255.0 |
| 19 | 1944.5 | 1977.5 | 253.2 |
| 20 | 1935.5 | 1977.5 | 253.2 |
| 21 | 1926.5 | 1977.5 | 252.8 |
| 22 | 1917.5 | 1977.5 | 252.7 |
| 23 | 1913.0 | 1977.5 | 254.7 |
| 24 | 1908.5 | 1977.5 | 252.9 |
| 25 | 1899.5 | 1977.5 | 253.0 |
| 26 | 1969.0 | 1962.5 | 254.6 |
| 27 | 1962.5 | 1962.5 | 254.4 |
| 28 | 1944.5 | 1962.5 | 256.0 |
| 29 | 1926.5 | 1962.5 | 253.9 |
| 30 | 1908.5 | 1962.5 | 253.7 |

## SITE GEOMETRY FOR CINCINNATI OVERLAP GAP #2

Noise Barriers

| Barrier | X1 (m) | Y1 (m) | X2 (m) | Y2 (m) | Bottom Elevation (m) | Top Elevation (m) |
|---|---|---|---|---|---|---|
| Single | 1500 | 2000 | 2500 | 2000 | 246.1 | 251.2 |
| Far | 1500 | 2000 | 2000 | 2000 | 246.1 | 251.2 |
| Near | 1972 | 1982 | 2500 | 1982 | 246.3 | 252.1 |

Overlap Length: 28.0 m
Overlap Width: 18.0 m

Traffic data recorded on Kugler Mill Road overpass facing north

Roadways

| Roadway | X1 (m) | Y1 (m) | X2 (m) | Y2 (m) | Elevation (m) |
|---|---|---|---|---|---|
| 1 | 1500 | 2005.5 | 2500 | 2005.5 | 246.1 |
| 2 | 1500 | 2009.1 | 2500 | 2009.1 | 246.1 |
| 3 | 1500 | 2012.8 | 2500 | 2012.8 | 246.1 |
| 4 | 1500 | 2027.4 | 2500 | 2027.4 | 246.1 |
| 5 | 1500 | 2031.1 | 2500 | 2031.1 | 246.1 |
| 6 | 1500 | 2034.7 | 2500 | 2034.7 | 246.1 |

Receivers

| Receiver | X (m) | Y (m) | Elevation (m) |
|---|---|---|---|
| 1 | 1998.5 | 1991.0 | 249.1 |
| 2 | 1989.5 | 1991.0 | 249.1 |
| 3 | 1985.0 | 1991.0 | 251.0 |
| 4 | 1980.5 | 1991.0 | 249.2 |
| 5 | 1971.5 | 1991.0 | 249.1 |
| 6 | 1962.5 | 1991.0 | 248.5 |
| 7 | 1953.5 | 1991.0 | 248.2 |
| 8 | 1949.0 | 1991.0 | 249.9 |
| 9 | 1944.5 | 1991.0 | 247.9 |
| 10 | 1998.5 | 1976.5 | 250.0 |
| 11 | 1989.5 | 1976.5 | 249.7 |
| 12 | 1985.0 | 1976.5 | 251.5 |
| 13 | 1980.5 | 1976.5 | 249.5 |
| 14 | 1971.5 | 1976.5 | 249.3 |
| 15 | 1962.5 | 1976.5 | 248.6 |
| 16 | 1953.5 | 1976.5 | 248.2 |
| 17 | 1949.0 | 1976.5 | 249.9 |
| 18 | 1944.5 | 1976.5 | 247.9 |
| 19 | 1935.5 | 1976.5 | 247.7 |
| 20 | 1980.5 | 1962.5 | 249.1 |
| 21 | 1962.5 | 1962.5 | 248.4 |
| 22 | 1953.5 | 1962.5 | 250.0 |
| 23 | 1944.5 | 1962.5 | 247.9 |
| 24 | 1926.5 | 1962.5 | 247.2 |

## SITE GEOMETRY FOR COLUMBUS OVERLAP GAP

Noise Barriers

| Barrier | X1 (m) | Y1 (m) | X2 (m) | Y2 (m) | Bottom Elevation (m) | Top Elevation (m) |
|---|---|---|---|---|---|---|
| Single | 1500 | 2000 | 2500 | 2000 | 274.9 | 281.0 |
| Far | 2000 | 2000 | 2500 | 2000 | 274.9 | 281.0 |
| Near | 1500 | 1990.9 | 2030.5 | 1990.9 | 274.3 | 280.7 |

Overlap Length: 30.5 m
Overlap Width: 9.1 m

Traffic data recorded on Park Road overpass facing south

| Roadway | X1 (m) | Y1 (m) | X2 (m) | Y2 (m) | Elevation (m) |
|---|---|---|---|---|---|
| 1 | 1500 | 2009.3 | 2500 | 2009.3 | 276.2 |
| 2 | 1500 | 2013.0 | 2500 | 2013.0 | 276.2 |
| 3 | 1500 | 2016.6 | 2500 | 2016.6 | 276.2 |
| 4 | 1500 | 2038.8 | 2500 | 2038.8 | 276.1 |
| 5 | 1500 | 2042.5 | 2500 | 2042.5 | 276.1 |
| 6 | 1500 | 2046.1 | 2500 | 2046.1 | 276.1 |

Receivers

| Receiver | X (m) | Y (m) | Elevation (m) |
|---|---|---|---|
| 1 | 2001.5 | 1996.5 | 278.1 |
| 2 | 2010.5 | 1996.5 | 278.4 |
| 3 | 2015.0 | 1996.5 | 280.5 |
| 4 | 2019.5 | 1996.5 | 278.8 |
| 5 | 2028.5 | 1996.5 | 278.9 |
| 6 | 2037.5 | 1996.5 | 278.5 |
| 7 | 2046.5 | 1996.5 | 278.5 |
| 8 | 2051.0 | 1996.5 | 280.4 |
| 9 | 2055.5 | 1996.5 | 278.6 |
| 10 | 2064.5 | 1996.5 | 278.9 |
| 11 | 2001.5 | 1986.5 | 277.4 |
| 12 | 2010.5 | 1986.5 | 277.4 |
| 13 | 2015.0 | 1986.5 | 279.3 |
| 14 | 2019.5 | 1986.5 | 277.5 |
| 15 | 2028.5 | 1984.7 | 277.6 |
| 16 | 2037.5 | 1986.5 | 277.5 |
| 17 | 2046.5 | 1986.5 | 277.5 |
| 18 | 2051.0 | 1986.5 | 279.4 |
| 19 | 2055.5 | 1986.5 | 277.7 |
| 20 | 2064.5 | 1986.5 | 277.8 |
| 21 | 2073.5 | 1986.5 | 277.5 |
| 22 | 2082.5 | 1986.5 | 277.5 |
| 23 | 2087.0 | 1986.5 | 279.4 |
| 24 | 2091.5 | 1986.5 | 277.7 |
| 25 | 2100.5 | 1986.5 | 277.7 |
| 26 | 2015.0 | 1976.5 | 277.3 |
| 27 | 2046.5 | 1976.5 | 277.4 |
| 28 | 2064.5 | 1976.5 | 279.3 |
| 29 | 2091.5 | 1976.5 | 277.6 |
| 30 | 2100.5 | 1976.5 | 277.7 |

## SITE GEOMETRY FOR DAYTON OVERLAP GAP

Noise Barriers

| Barrier | X1 (m) | Y1 (m) | X2 (m) | Y2 (m) | Bottom Elevation (m) | Top Elevation (m) |
|---|---|---|---|---|---|---|
| Single | 1500 | 2000 | 2500 | 2000 | 275.1 | 277.2 |
| Far | 1500 | 2000 | 2000 | 2000 | 275.1 | 277.2 |
| Near | 1978.7 | 1992.7 | 2500 | 1992.7 | 275.2 | 279.2 |

Overlap Length: 21.3 m
Overlap Width: 7.3 m

Traffic data recorded on McEwen Road overpass facing west

Roadways

| Roadway | X1 (m) | Y1 (m) | X2 (m) | Y2 (m) | Elevation (m) |
|---|---|---|---|---|---|
| 1 | 1500 | 2011.8 | 2500 | 2011.8 | 275.6 |
| 2 | 1500 | 2015.5 | 2500 | 2015.5 | 275.6 |
| 3 | 1500 | 2019.1 | 2500 | 2019.1 | 275.6 |
| 4 | 1500 | 2041.2 | 2500 | 2041.2 | 275.5 |
| 5 | 1500 | 2044.9 | 2500 | 2044.9 | 275.5 |
| 6 | 1500 | 2048.5 | 2500 | 2048.5 | 275.5 |

Receivers

| Receiver | X (m) | Y (m) | Elevation (m) |
|---|---|---|---|
| 1 | 1998.5 | 1996.2 | 276.4 |
| 2 | 1992.5 | 1996.2 | 276.8 |
| 3 | 1989.5 | 1996.2 | 276.3 |
| 4 | 1986.5 | 1996.2 | 276.9 |
| 5 | 1980.5 | 1996.2 | 277.0 |
| 6 | 1974.5 | 1995.2 | 276.7 |
| 7 | 1968.5 | 1996.2 | 276.3 |
| 8 | 1965.5 | 1996.2 | 276.1 |
| 9 | 1962.5 | 1996.2 | 276.7 |
| 10 | 1956.5 | 1996.2 | 276.6 |
| 11 | 1998.5 | 1987.2 | 277.4 |
| 12 | 1992.5 | 1987.2 | 277.0 |
| 13 | 1989.5 | 1987.2 | 277.1 |
| 14 | 1986.5 | 1987.2 | 277.4 |
| 15 | 1980.5 | 1987.2 | 276.7 |
| 16 | 1974.5 | 1987.2 | 276.8 |
| 17 | 1968.5 | 1987.2 | 276.8 |
| 18 | 1965.5 | 1987.2 | 276.4 |
| 19 | 1962.5 | 1987.2 | 276.5 |
| 20 | 1956.5 | 1987.2 | 276.7 |
| 21 | 1998.5 | 1979.2 | 277.0 |
| 22 | 1992.5 | 1979.2 | 276.9 |
| 23 | 1989.5 | 1979.2 | 277.0 |
| 24 | 1986.5 | 1979.2 | 277.1 |
| 25 | 1980.5 | 1979.2 | 276.7 |
| 26 | 1974.5 | 1979.2 | 276.4 |
| 27 | 1968.5 | 1979.2 | 276.7 |
| 28 | 1965.5 | 1979.2 | 276.3 |
| 29 | 1962.5 | 1979.2 | 276.5 |
| 30 | 1956.5 | 1979.2 | 276.6 |

# APPENDIX D

# FIELD MEASUREMENTS AND GAP MODEL RESULTS - VERSION 1.0

## CINCINNATI OVERLAP GAP #1 RESULTS - VERSION 1.0

| | | GAP | | |
|---|---|---|---|---|
| Mic. # | Field Measurements | Single Barrier | Overlap Barrier | Overlap - Field |
| 1 | 80.4 | 66.2 | 80.8 | 0.4 |
| 2 | 77.0 | 66.1 | 79.0 | 2.0 |
| 3 | 79.0 | 68.9 | 78.7 | -0.3 |
| 4 | 76.2 | 66.2 | 78.1 | 1.9 |
| 5 | 75.0 | 66.3 | 77.4 | 2.4 |
| 6 | 73.3 | 66.0 | 76.7 | 3.4 |
| 7 | 71.9 | 65.9 | 75.4 | 3.5 |
| 8 | 73.2 | 68.5 | 75.2 | 2.0 |
| 9 | 71.4 | 66.0 | 74.2 | 2.8 |
| 10 | 70.7 | 66.1 | 73.2 | 2.5 |
| 11 | 63.3 | 66.2 | 65.4 | 2.1 |
| 12 | 62.9 | 66.1 | 65.4 | 2.5 |
| 13 | 65.3 | 67.4 | 67.7 | 2.4 |
| 14 | 63.7 | 66.1 | 65.6 | 1.9 |
| 15 | 65.0 | 66.1 | 65.8 | 0.8 |
| 16 | 65.6 | 64.9 | 67.1 | 1.5 |
| 17 | 66.2 | 64.8 | 69.4 | 3.2 |
| 18 | 68.6 | 66.5 | 70.5 | 1.9 |
| 19 | 67.1 | 64.9 | 70.0 | 2.9 |
| 20 | 66.9 | 64.9 | 69.9 | 3.0 |
| 21 | 69.8 | 64.6 | 70.0 | 0.2 |
| 22 | 68.9 | 64.5 | 69.8 | 0.9 |
| 23 | 70.3 | 66.1 | 70.1 | -0.2 |
| 24 | 68.7 | 64.7 | 69.5 | 0.8 |
| 25 | 68.2 | 64.8 | 69.3 | 1.1 |
| 26 | 64.1 | 66.6 | 67.1 | 3.0 |
| 27 | 64.2 | 66.5 | 67.2 | 3.0 |
| 28 | 66.7 | 67.1 | 69.7 | 3.0 |
| 29 | 65.6 | 66.2 | 69.5 | 3.9 |
| 30 | 66.3 | 66.1 | 69.4 | 3.1 |
| | | | Avg. Difference | 2.1 |

All sound levels are in units of dBA

## CINCINNATI OVERLAP GAP #2 RESULTS - VERSION 1.0

| | | GAP | | |
|---|---|---|---|---|
| Mic. # | Field Measurements | Single Barrier | Overlap Barrier | Overlap - Field |
| 1 | 79.9 | 67.8 | 79.8 | -0.2 |
| 2 | 78.1 | 67.8 | 78.4 | 0.3 |
| 3 | 79.0 | 69.9 | 78.2 | -0.8 |
| 4 | 76.7 | 68.0 | 77.6 | 0.9 |
| 5 | 75.3 | 67.8 | 76.9 | 1.6 |
| 6 | 74.0 | 65.8 | 74.5 | 0.5 |
| 7 | 71.8 | 65.3 | 73.2 | 1.4 |
| 8 | 72.6 | 67.6 | 73.1 | 0.5 |
| 9 | 70.2 | 65.0 | 72.1 | 1.9 |
| 10 | 64.9 | 66.3 | 65.4 | 0.4 |
| 11 | 64.8 | 66.1 | 65.3 | 0.5 |
| 12 | 70.0 | 66.7 | 66.7 | -3.3 |
| 13 | 65.6 | 66.0 | 65.2 | -0.4 |
| 14 | 67.7 | 65.8 | 65.2 | -2.5 |
| 15 | 68.9 | 65.6 | 70.1 | 1.2 |
| 16 | 69.3 | 65.2 | 71.0 | 1.7 |
| 17 | 70.7 | 66.6 | 71.4 | 0.7 |
| 18 | 67.8 | 65.0 | 71.0 | 3.2 |
| 19 | 66.9 | 64.8 | 70.6 | 3.7 |
| 20 | 63.6 | 67.0 | 66.6 | 3.0 |
| 21 | 64.4 | 66.5 | 67.6 | 3.2 |
| 22 | 66.0 | 67.5 | 69.8 | 3.8 |
| 23 | 64.3 | 66.1 | 69.5 | 5.2 |
| 24 | 63.3 | 65.5 | 69.7 | 6.4 |
| | | | Avg. Difference | 1.4 |

All sound levels are in units of dBA

## COLUMBUS OVERLAP GAP RESULTS - VERSION 1.0

| | | GAP | | |
|---|---|---|---|---|
| Mic. # | Field Measurements | Single Barrier | Overlap Barrier | Overlap - Field |
| 1 | 78.0 | 63.5 | 78.0 | 0.0 |
| 2 | 74.9 | 64.1 | 76.3 | 1.4 |
| 3 | 77.7 | 69.5 | 76.4 | -1.3 |
| 4 | 72.6 | 65.0 | 75.4 | 2.8 |
| 5 | 70.3 | 65.3 | 74.8 | 4.5 |
| 6 | 69.3 | 64.5 | 73.4 | 4.1 |
| 7 | 69.6 | 64.5 | 71.7 | 2.1 |
| 8 | 70.2 | 69.4 | 72.6 | 2.3 |
| 9 | 68.5 | 64.7 | 70.4 | 1.9 |
| 10 | 68.1 | 65.5 | 69.7 | 1.6 |
| 11 | 65.9 | 65.4 | 64.3 | -1.6 |
| 12 | 66.7 | 65.4 | 64.7 | -2.0 |
| 13 | 68.9 | 68.1 | 68.3 | -0.7 |
| 14 | 66.1 | 65.5 | 65.1 | -1.0 |
| 15 | 67.1 | 65.6 | 65.5 | -1.6 |
| 16 | 68.1 | 65.0 | 69.3 | 1.2 |
| 17 | 69.1 | 65.0 | 70.0 | 0.9 |
| 18 | 69.4 | 67.8 | 71.2 | 1.8 |
| 19 | 68.0 | 65.3 | 70.0 | 2.0 |
| 20 | 67.9 | 65.4 | 69.6 | 1.7 |
| 21 | 66.9 | 65.6 | 69.7 | 2.8 |
| 22 | 67.5 | 65.6 | 69.3 | 1.8 |
| 23 | 68.1 | 68.5 | 70.6 | 2.5 |
| 24 | 66.5 | 65.9 | 69.2 | 2.7 |
| 25 | 66.6 | 65.9 | 68.9 | 2.3 |
| 26 | 66.6 | 64.5 | 64.6 | -2.0 |
| 27 | 67.6 | 64.6 | 67.2 | -0.4 |
| 28 | 67.9 | 66.7 | 69.0 | 1.1 |
| 29 | 66.2 | 64.8 | 67.4 | 1.2 |
| 30 | 66.4 | 65.0 | 67.3 | 0.9 |
| | | | Avg. Difference | 1.1 |

All sound levels are in units of dBA

## DAYTON OVERLAP GAP RESULTS - VERSION 1.0

| | | GAP | | |
|---|---|---|---|---|
| Mic. # | Field Measurements | Single Barrier | Overlap Barrier | Overlap - Field |
| 1 | 76.0 | 68.8 | 76.2 | 0.2 |
| 2 | 74.6 | 70.1 | 75.5 | 0.9 |
| 3 | 73.1 | 68.4 | 74.8 | 1.7 |
| 4 | 73.3 | 70.4 | 74.8 | 1.5 |
| 5 | 71.8 | 70.6 | 74.3 | 2.5 |
| 6 | 69.7 | 69.0 | 72.4 | 2.7 |
| 7 | 68.3 | 67.6 | 71.2 | 2.9 |
| 8 | 67.8 | 66.9 | 70.3 | 2.5 |
| 9 | 68.2 | 69.0 | 70.9 | 2.7 |
| 10 | 67.8 | 68.7 | 70.3 | 2.5 |
| 11 | 64.3 | 69.9 | 67.9 | 3.6 |
| 12 | 63.7 | 69.8 | 68.5 | 4.8 |
| 13 | 64.4 | 69.9 | 68.8 | 4.4 |
| 14 | 66.2 | 69.9 | 69.0 | 2.8 |
| 15 | 65.5 | 69.6 | 68.8 | 3.3 |
| 16 | 66.9 | 69.3 | 69.1 | 2.2 |
| 17 | 67.1 | 69.3 | 69.9 | 2.8 |
| 18 | 66.8 | 68.8 | 69.9 | 3.1 |
| 19 | 67.3 | 69.0 | 70.0 | 2.7 |
| 20 | 68.0 | 69.2 | 70.3 | 2.3 |
| 21 | 64.1 | 68.7 | 67.0 | 2.9 |
| 22 | 64.0 | 68.6 | 67.3 | 3.3 |
| 23 | 64.6 | 68.7 | 67.5 | 2.9 |
| 24 | 65.0 | 68.7 | 67.7 | 2.7 |
| 25 | 65.2 | 68.5 | 67.6 | 2.4 |
| 26 | 65.4 | 68.7 | 68.0 | 2.6 |
| 27 | 66.1 | 69.0 | 68.8 | 2.7 |
| 28 | 65.9 | 68.6 | 68.6 | 2.7 |
| 29 | 66.7 | 68.8 | 69.0 | 2.3 |
| 30 | 67.2 | 68.9 | 69.2 | 2.0 |
| | | | Avg. Difference | 2.6 |

All sound levels are in units of dBA

# APPENDIX E

# FIELD MEASUREMENTS AND GAP MODEL RESULTS - VERSION 2.0

## CINCINNATI OVERLAP GAP #1 RESULTS - VERSION 2.0

| Mic. # | Field Measurements | GAP | | Overlap - Field |
|---|---|---|---|---|
| | | Single Barrier | Overlap Barrier | |
| 1 | 80.4 | 63.6 | 79.2 | -1.2 |
| 2 | 77.0 | 63.6 | 77.4 | 0.4 |
| 3 | 79.0 | 65.7 | 77.0 | -2.0 |
| 4 | 76.2 | 63.6 | 76.5 | 0.3 |
| 5 | 75.0 | 63.7 | 75.8 | 0.8 |
| 6 | 73.3 | 63.7 | 75.1 | 1.8 |
| 7 | 71.9 | 63.6 | 73.8 | 1.9 |
| 8 | 73.2 | 65.7 | 73.5 | 0.3 |
| 9 | 71.4 | 63.7 | 72.6 | 1.2 |
| 10 | 70.7 | 63.7 | 71.6 | 0.8 |
| 11 | 63.3 | 64.1 | 63.3 | 0.0 |
| 12 | 62.9 | 64.0 | 63.4 | 0.5 |
| 13 | 65.3 | 65.2 | 65.5 | 0.2 |
| 14 | 63.7 | 64.0 | 63.6 | -0.1 |
| 15 | 65.0 | 64.0 | 63.7 | -1.3 |
| 16 | 65.6 | 62.4 | 65.3 | -0.3 |
| 17 | 66.2 | 62.4 | 68.0 | 1.8 |
| 18 | 68.6 | 63.9 | 69.0 | 0.4 |
| 19 | 67.1 | 62.4 | 68.7 | 1.6 |
| 20 | 66.9 | 62.4 | 68.6 | 1.7 |
| 21 | 69.8 | 62.5 | 68.8 | -1.0 |
| 22 | 68.9 | 62.4 | 68.6 | -0.3 |
| 23 | 70.3 | 63.8 | 68.7 | -1.6 |
| 24 | 68.7 | 62.6 | 68.2 | -0.5 |
| 25 | 68.2 | 62.6 | 68.1 | -0.1 |
| 26 | 64.1 | 64.0 | 64.4 | 0.3 |
| 27 | 64.2 | 63.9 | 64.4 | 0.1 |
| 28 | 66.7 | 64.4 | 67.7 | 1.0 |
| 29 | 65.6 | 63.6 | 67.7 | 2.1 |
| 30 | 66.3 | 63.5 | 67.7 | 1.4 |
| | | | Avg. Difference | 0.3 |

All sound levels are in units of dBA

## CINCINNATI OVERLAP GAP #2 RESULTS - VERSION 2.0

| Mic. # | Field Measurements | GAP | | Overlap - Field |
|---|---|---|---|---|
| | | Single Barrier | Overlap Barrier | |
| 1 | 79.9 | 66.0 | 78.8 | -1.1 |
| 2 | 78.1 | 66.0 | 77.5 | -0.6 |
| 3 | 79.0 | 68.0 | 77.2 | -1.8 |
| 4 | 76.7 | 66.2 | 76.6 | -0.1 |
| 5 | 75.3 | 66.0 | 76.0 | 0.7 |
| 6 | 74.0 | 64.1 | 73.6 | -0.4 |
| 7 | 71.8 | 63.8 | 72.3 | 0.5 |
| 8 | 72.6 | 65.8 | 72.1 | -0.5 |
| 9 | 70.2 | 63.4 | 71.2 | 1.0 |
| 10 | 64.9 | 64.5 | 63.5 | -1.4 |
| 11 | 64.8 | 64.3 | 63.4 | -1.4 |
| 12 | 70.0 | 64.9 | 64.8 | -5.2 |
| 13 | 65.6 | 64.2 | 63.4 | -2.2 |
| 14 | 67.7 | 64.0 | 63.3 | -4.4 |
| 15 | 68.9 | 63.9 | 69.1 | 0.1 |
| 16 | 69.3 | 63.5 | 70.1 | 0.8 |
| 17 | 70.7 | 64.9 | 70.4 | -0.3 |
| 18 | 67.8 | 63.3 | 70.0 | 2.2 |
| 19 | 66.9 | 63.1 | 69.7 | 2.8 |
| 20 | 63.6 | 65.1 | 64.7 | 1.1 |
| 21 | 64.4 | 64.6 | 66.0 | 1.6 |
| 22 | 66.0 | 65.5 | 68.3 | 2.3 |
| 23 | 64.3 | 64.2 | 68.2 | 3.9 |
| 24 | 63.3 | 63.7 | 68.5 | 5.2 |
| | | | Avg. Difference | 0.1 |

All sound levels are in units of dBA

## COLUMBUS OVERLAP GAP RESULTS - VERSION 2.0

| | | GAP | | |
|---|---|---|---|---|
| Mic. # | Field Measurements | Single Barrier | Overlap Barrier | Overlap - Field |
| 1 | 78.0 | 62.9 | 77.7 | -0.3 |
| 2 | 74.9 | 63.5 | 76.0 | 1.1 |
| 3 | 77.7 | 68.5 | 76.0 | -1.7 |
| 4 | 72.6 | 64.3 | 75.1 | 2.5 |
| 5 | 70.3 | 64.5 | 74.4 | 4.1 |
| 6 | 69.3 | 63.8 | 73.1 | 3.8 |
| 7 | 69.6 | 63.8 | 71.3 | 1.7 |
| 8 | 70.2 | 68.4 | 71.9 | 1.7 |
| 9 | 68.5 | 64.0 | 70.0 | 1.5 |
| 10 | 68.1 | 64.7 | 69.2 | 1.1 |
| 11 | 65.9 | 64.5 | 63.6 | -2.3 |
| 12 | 66.7 | 64.5 | 64.0 | -2.7 |
| 13 | 68.9 | 67.0 | 67.2 | -1.7 |
| 14 | 66.1 | 64.7 | 64.3 | -1.8 |
| 15 | 67.1 | 64.8 | 64.7 | -2.4 |
| 16 | 68.1 | 64.1 | 68.8 | 0.7 |
| 17 | 69.1 | 64.1 | 69.6 | 0.5 |
| 18 | 69.4 | 66.8 | 70.5 | 1.1 |
| 19 | 68.0 | 64.4 | 69.6 | 1.6 |
| 20 | 67.9 | 64.5 | 69.1 | 1.2 |
| 21 | 66.9 | 64.8 | 69.3 | 2.4 |
| 22 | 67.5 | 64.8 | 68.9 | 1.4 |
| 23 | 68.1 | 67.5 | 69.9 | 1.8 |
| 24 | 66.5 | 65.1 | 68.7 | 2.2 |
| 25 | 66.6 | 65.1 | 68.4 | 1.8 |
| 26 | 66.6 | 63.6 | 63.6 | -3.0 |
| 27 | 67.6 | 63.7 | 66.4 | -1.2 |
| 28 | 67.9 | 65.7 | 68.2 | 0.3 |
| 29 | 66.2 | 63.9 | 66.7 | 0.5 |
| 30 | 66.4 | 64.0 | 66.6 | 0.2 |
| | | | Avg. Difference | 0.5 |

All sound levels are in units of dBA

## DAYTON OVERLAP GAP RESULTS - VERSION 2.0

| Mic. # | Field Measurements | GAP | | |
|---|---|---|---|---|
| | | Single Barrier | Overlap Barrier | Overlap - Field |
| 1 | 76.0 | 66.7 | 75.3 | -0.8 |
| 2 | 74.6 | 68.2 | 74.4 | -0.3 |
| 3 | 73.1 | 66.3 | 73.7 | 0.6 |
| 4 | 73.3 | 68.5 | 73.6 | 0.3 |
| 5 | 71.8 | 68.8 | 73.1 | 1.3 |
| 6 | 69.7 | 67.2 | 71.4 | 1.6 |
| 7 | 68.3 | 65.7 | 70.0 | 1.7 |
| 8 | 67.8 | 64.9 | 69.1 | 1.3 |
| 9 | 68.2 | 67.3 | 69.6 | 1.4 |
| 10 | 67.8 | 66.9 | 68.9 | 1.1 |
| 11 | 64.3 | 68.2 | 66.2 | 1.9 |
| 12 | 63.7 | 68.2 | 66.7 | 3.0 |
| 13 | 64.4 | 68.2 | 67.1 | 2.6 |
| 14 | 66.2 | 68.2 | 67.2 | 1.0 |
| 15 | 65.5 | 67.9 | 67.0 | 1.5 |
| 16 | 66.9 | 67.7 | 67.5 | 0.6 |
| 17 | 67.1 | 67.7 | 68.4 | 1.3 |
| 18 | 66.8 | 67.0 | 68.4 | 1.6 |
| 19 | 67.3 | 67.2 | 68.6 | 1.3 |
| 20 | 68.0 | 67.5 | 68.8 | 0.8 |
| 21 | 64.1 | 66.9 | 65.2 | 1.1 |
| 22 | 64.0 | 66.9 | 65.4 | 1.4 |
| 23 | 64.6 | 66.9 | 65.7 | 1.1 |
| 24 | 65.0 | 67.0 | 65.9 | 0.9 |
| 25 | 65.2 | 66.7 | 65.7 | 0.5 |
| 26 | 65.4 | 66.9 | 66.1 | 0.7 |
| 27 | 66.1 | 67.2 | 67.0 | 0.9 |
| 28 | 65.9 | 66.7 | 66.8 | 0.8 |
| 29 | 66.7 | 67.0 | 67.3 | 0.6 |
| 30 | 67.2 | 67.1 | 67.5 | 0.3 |
| | | | Avg. Difference | 1.1 |

All sound levels are in units of dBA

# APPENDIX F

# MODEL CALIBRATION DATA - VERSION 1.0

## RECEIVER CASE #1 CALIBRATION

| Site | Mic. # | Field Measurements | GAP Overlap Barrier | Overlap - Field | Average Difference |
|---|---|---|---|---|---|
| Cincinnati #1 | 11 | 63.3 | 65.4 | 2.1 | |
| Cincinnati #1 | 12 | 62.9 | 65.4 | 2.5 | |
| Cincinnati #1 | 13 | 65.3 | 67.7 | 2.4 | |
| Cincinnati #1 | 14 | 63.7 | 65.6 | 1.9 | |
| Cincinnati #1 | 15 | 65.0 | 65.8 | 0.8 | |
| Cincinnati #1 | 26 | 64.1 | 67.1 | 3.0 | 2.1 |
| Cincinnati #2 | 10 | 64.9 | 65.4 | 0.4 | |
| Cincinnati #2 | 11 | 64.8 | 65.3 | 0.5 | |
| Cincinnati #2 | 13 | 65.6 | 65.2 | -0.4 | |
| Cincinnati #2 | 20 | 63.6 | 66.6 | 3.0 | 0.9 |
| Columbus | 11 | 65.9 | 64.3 | -1.6 | |
| Columbus | 12 | 66.7 | 64.7 | -2.0 | |
| Columbus | 13 | 68.9 | 68.3 | -0.7 | |
| Columbus | 14 | 66.1 | 65.1 | -1.0 | |
| Columbus | 15 | 67.1 | 65.5 | -1.6 | |
| Columbus | 26 | 66.6 | 64.6 | -2.0 | -1.5 |
| Dayton | 11 | 64.3 | 67.9 | 3.6 | |
| Dayton | 12 | 63.7 | 68.5 | 4.8 | |
| Dayton | 13 | 64.4 | 68.8 | 4.4 | |
| Dayton | 14 | 66.2 | 69.0 | 2.8 | |
| Dayton | 15 | 65.5 | 68.8 | 3.3 | |
| Dayton | 21 | 64.1 | 67.0 | 2.9 | |
| Dayton | 22 | 64.0 | 67.3 | 3.3 | |
| Dayton | 23 | 64.6 | 67.5 | 2.9 | |
| Dayton | 24 | 65.0 | 67.7 | 2.7 | |
| Dayton | 25 | 65.2 | 67.6 | 2.4 | 3.3 |
| | | | | Calibration factor | 1.2 |

All sound levels are in units of dBA

## RECEIVER CASE #2 CALIBRATION

| Site | Mic. # | Field Measurements | GAP Overlap Barrier | Overlap - Field | Average Difference |
|---|---|---|---|---|---|
| Cincinnati #1 | 1 | 80.4 | 80.8 | 0.4 | |
| Cincinnati #1 | 2 | 77.0 | 79.0 | 2.0 | |
| Cincinnati #1 | 3 | 79.0 | 78.7 | -0.3 | |
| Cincinnati #1 | 4 | 76.2 | 78.1 | 1.9 | |
| Cincinnati #1 | 5 | 75.0 | 77.4 | 2.4 | 1.3 |
| Cincinnati #2 | 1 | 79.9 | 79.8 | -0.2 | |
| Cincinnati #2 | 2 | 78.1 | 78.4 | 0.3 | |
| Cincinnati #2 | 3 | 79.0 | 78.2 | -0.8 | |
| Cincinnati #2 | 4 | 76.7 | 77.6 | 0.9 | 0.1 |
| Columbus | 1 | 78.0 | 78.0 | 0.0 | |
| Columbus | 2 | 74.9 | 76.3 | 1.4 | |
| Columbus | 3 | 77.7 | 76.4 | -1.3 | |
| Columbus | 4 | 72.6 | 75.4 | 2.8 | |
| Columbus | 5 | 70.3 | 74.8 | 4.5 | 1.5 |
| Dayton | 1 | 76.0 | 76.2 | 0.2 | |
| Dayton | 2 | 74.6 | 75.5 | 0.9 | |
| Dayton | 3 | 73.1 | 74.8 | 1.7 | |
| Dayton | 4 | 73.3 | 74.8 | 1.5 | |
| Dayton | 5 | 71.8 | 74.3 | 2.5 | 1.3 |
| | | | | Calibration factor | 1.0 |

All sound levels are in units of dBA

## RECEIVER CASE #3 CALIBRATION

| Site | Mic. # | Field Measurements | GAP Overlap Barrier | Overlap - Field | Average Difference |
|---|---|---|---|---|---|
| Cincinnati #1 | 6 | 73.3 | 76.7 | 3.4 | |
| Cincinnati #1 | 7 | 71.9 | 75.4 | 3.5 | |
| Cincinnati #1 | 8 | 73.2 | 75.2 | 2.0 | |
| Cincinnati #1 | 9 | 71.4 | 74.2 | 2.8 | |
| Cincinnati #1 | 10 | 70.7 | 73.2 | 2.5 | 2.9 |
| Cincinnati #2 | 5 | 75.3 | 76.9 | 1.6 | |
| Cincinnati #2 | 6 | 74.0 | 74.5 | 0.5 | |
| Cincinnati #2 | 7 | 71.8 | 73.2 | 1.4 | |
| Cincinnati #2 | 8 | 72.6 | 73.1 | 0.5 | |
| Cincinnati #2 | 9 | 70.2 | 72.1 | 1.9 | 1.2 |
| Columbus | 6 | 69.3 | 73.4 | 4.1 | |
| Columbus | 7 | 69.6 | 71.7 | 2.1 | |
| Columbus | 8 | 70.2 | 72.6 | 2.3 | |
| Columbus | 9 | 68.5 | 70.4 | 1.9 | |
| Columbus | 10 | 68.1 | 69.7 | 1.6 | 2.4 |
| Dayton | 6 | 69.7 | 72.4 | 2.7 | |
| Dayton | 7 | 68.3 | 71.2 | 2.9 | |
| Dayton | 8 | 67.8 | 70.3 | 2.5 | |
| Dayton | 9 | 68.2 | 70.9 | 2.7 | |
| Dayton | 10 | 67.8 | 70.3 | 2.5 | 2.7 |
| | | | | Calibration factor | 2.3 |

All sound levels are in units of dBA

## RECEIVER CASE #4 CALIBRATION

| Site | Mic. # | Field Measurements | GAP Overlap Barrier | Overlap - Field | Average Difference |
|---|---|---|---|---|---|
| Cincinnati #1 | 16 | 65.6 | 67.1 | 1.5 | |
| Cincinnati #1 | 17 | 66.2 | 69.4 | 3.2 | |
| Cincinnati #1 | 27 | 64.2 | 67.2 | 3.0 | |
| Cincinnati #1 | 28 | 66.7 | 69.7 | 3.0 | |
| Cincinnati #1 | 29 | 65.6 | 69.5 | 3.9 | 2.9 |
| Cincinnati #2 | 21 | 64.4 | 67.6 | 3.2 | |
| Cincinnati #2 | 22 | 66.0 | 69.8 | 3.8 | 3.5 |
| Columbus | 16 | 68.1 | 69.3 | 1.2 | |
| Columbus | 27 | 67.6 | 67.2 | -0.4 | |
| Columbus | 28 | 67.9 | 69.0 | 1.1 | 0.6 |
| Dayton | 16 | 66.9 | 69.1 | 2.2 | |
| Dayton | 17 | 67.1 | 69.9 | 2.8 | |
| Dayton | 18 | 66.8 | 69.9 | 3.1 | |
| Dayton | 26 | 65.4 | 68.0 | 2.6 | |
| Dayton | 27 | 66.1 | 68.8 | 2.7 | |
| Dayton | 28 | 65.9 | 68.6 | 2.7 | |
| Dayton | 29 | 66.7 | 69.0 | 2.3 | |
| Dayton | 30 | 67.2 | 69.2 | 2.0 | 2.6 |
| | | | | Calibration factor | 2.4 |

All sound levels are in units of dBA

## RECEIVER CASE #5 CALIBRATION

| Site | Mic. # | Field Measurements | GAP Overlap Barrier | Overlap - Field | Average Difference |
|---|---|---|---|---|---|
| Cincinnati #1 | 18 | 68.6 | 70.5 | 1.9 | |
| Cincinnati #1 | 19 | 67.1 | 70.0 | 2.9 | |
| Cincinnati #1 | 20 | 66.9 | 69.9 | 3.0 | |
| Cincinnati #1 | 21 | 69.8 | 70.0 | 0.2 | |
| Cincinnati #1 | 22 | 68.9 | 69.8 | 0.9 | |
| Cincinnati #1 | 23 | 70.3 | 70.1 | -0.2 | |
| Cincinnati #1 | 24 | 68.7 | 69.5 | 0.8 | |
| Cincinnati #1 | 25 | 68.2 | 69.3 | 1.1 | |
| Cincinnati #1 | 30 | 66.3 | 69.4 | 3.1 | 1.5 |
| Cincinnati #2 | 15 | 68.9 | 70.1 | 1.2 | |
| Cincinnati #2 | 16 | 69.3 | 71.0 | 1.7 | |
| Cincinnati #2 | 17 | 70.7 | 71.4 | 0.7 | |
| Cincinnati #2 | 18 | 67.8 | 71.0 | 3.2 | |
| Cincinnati #2 | 19 | 66.9 | 70.6 | 3.7 | 2.1 |
| Columbus | 17 | 69.1 | 70.0 | 0.9 | |
| Columbus | 18 | 69.4 | 71.2 | 1.8 | |
| Columbus | 19 | 68.0 | 70.0 | 2.0 | |
| Columbus | 20 | 67.9 | 69.6 | 1.7 | |
| Columbus | 21 | 66.9 | 69.7 | 2.8 | |
| Columbus | 22 | 67.5 | 69.3 | 1.8 | |
| Columbus | 23 | 68.1 | 70.6 | 2.5 | |
| Columbus | 24 | 66.5 | 69.2 | 2.7 | |
| Columbus | 25 | 66.6 | 68.9 | 2.3 | |
| Columbus | 29 | 66.2 | 67.4 | 1.2 | |
| Columbus | 30 | 66.4 | 67.3 | 0.9 | 1.9 |
| Dayton | 19 | 67.3 | 70.0 | 2.7 | |
| Dayton | 20 | 68.0 | 70.3 | 2.3 | 2.5 |
| | | | | Calibration factor | 2.0 |

All sound levels are in units of dBA

# APPENDIX G

# CALIBRATED MODEL RESULTS - VERSION 1.0

## CINCINNATI OVERLAP GAP #1 CALIBRATED RESULTS

| | | GAP | | |
|---|---|---|---|---|
| Mic. # | Field Measurements | Single Barrier | Overlap Barrier | Overlap - Field |
| 1 | 80.4 | 66.2 | 79.8 | -0.6 |
| 2 | 77.0 | 66.1 | 78.0 | 1.0 |
| 3 | 79.0 | 68.9 | 77.7 | -1.3 |
| 4 | 76.2 | 66.2 | 77.1 | 0.9 |
| 5 | 75.0 | 66.3 | 76.4 | 1.4 |
| 6 | 73.3 | 66.0 | 74.4 | 1.1 |
| 7 | 71.9 | 65.9 | 73.1 | 1.2 |
| 8 | 73.2 | 68.5 | 72.9 | -0.3 |
| 9 | 71.4 | 66.0 | 71.9 | 0.5 |
| 10 | 70.7 | 66.1 | 70.9 | 0.2 |
| 11 | 63.3 | 66.2 | 64.2 | 0.9 |
| 12 | 62.9 | 66.1 | 64.2 | 1.3 |
| 13 | 65.3 | 67.4 | 66.5 | 1.2 |
| 14 | 63.7 | 66.1 | 64.4 | 0.7 |
| 15 | 65.0 | 66.1 | 64.6 | -0.5 |
| 16 | 65.6 | 64.9 | 64.7 | -0.9 |
| 17 | 66.2 | 64.8 | 67.0 | 0.8 |
| 18 | 68.6 | 66.5 | 68.5 | -0.1 |
| 19 | 67.1 | 64.9 | 68.0 | 0.9 |
| 20 | 66.9 | 64.9 | 67.9 | 1.0 |
| 21 | 69.8 | 64.6 | 68.0 | -1.8 |
| 22 | 68.9 | 64.5 | 67.8 | -1.1 |
| 23 | 70.3 | 66.1 | 68.1 | -2.2 |
| 24 | 68.7 | 64.7 | 67.5 | -1.2 |
| 25 | 68.2 | 64.8 | 67.3 | -0.9 |
| 26 | 64.1 | 66.6 | 65.9 | 1.8 |
| 27 | 64.2 | 66.5 | 64.8 | 0.6 |
| 28 | 66.7 | 67.1 | 67.3 | 0.6 |
| 29 | 65.6 | 66.2 | 67.1 | 1.5 |
| 30 | 66.3 | 66.1 | 67.4 | 1.1 |
| | | | Avg. Difference | 0.3 |

All sound levels are in units of dBA

## CINCINNATI OVERLAP GAP #2 CALIBRATED RESULTS

| | | GAP | | |
|---|---|---|---|---|
| Mic. # | Field Measurements | Single Barrier | Overlap Barrier | Overlap - Field |
| 1 | 79.9 | 67.8 | 78.8 | -1.2 |
| 2 | 78.1 | 67.8 | 77.4 | -0.7 |
| 3 | 79.0 | 69.9 | 77.2 | -1.8 |
| 4 | 76.7 | 68.0 | 76.6 | -0.1 |
| 5 | 75.3 | 67.8 | 74.6 | -0.7 |
| 6 | 74.0 | 65.8 | 72.2 | -1.8 |
| 7 | 71.8 | 65.3 | 70.9 | -0.9 |
| 8 | 72.6 | 67.6 | 70.8 | -1.8 |
| 9 | 70.2 | 65.0 | 69.8 | -0.4 |
| 10 | 64.9 | 66.3 | 64.2 | -0.8 |
| 11 | 64.8 | 66.1 | 64.1 | -0.8 |
| 12 | 70.0 | 66.7 | 65.5 | -4.5 |
| 13 | 65.6 | 66.0 | 64.0 | -1.6 |
| 14 | 67.7 | 65.8 | 62.8 | -4.9 |
| 15 | 68.9 | 65.6 | 68.1 | -0.8 |
| 16 | 69.3 | 65.2 | 69.0 | -0.3 |
| 17 | 70.7 | 66.6 | 69.4 | -1.3 |
| 18 | 67.8 | 65.0 | 69.0 | 1.2 |
| 19 | 66.9 | 64.8 | 68.6 | 1.7 |
| 20 | 63.6 | 67.0 | 65.4 | 1.8 |
| 21 | 64.4 | 66.5 | 65.2 | 0.8 |
| 22 | 66.0 | 67.5 | 67.4 | 1.4 |
| 23 | 64.3 | 66.1 | 67.1 | 2.8 |
| 24 | 63.3 | 65.5 | 67.7 | 4.4 |
| | | | Avg. Difference | -0.4 |

All sound levels are in units of dBA

## COLUMBUS OVERLAP GAP CALIBRATED RESULTS

| | | GAP | | |
|---|---|---|---|---|
| Mic. # | Field Measurements | Single Barrier | Overlap Barrier | Overlap - Field |
| 1 | 78.0 | 63.5 | 77.0 | -1.0 |
| 2 | 74.9 | 64.1 | 75.3 | 0.4 |
| 3 | 77.7 | 69.5 | 75.4 | -2.3 |
| 4 | 72.6 | 65.0 | 74.4 | 1.8 |
| 5 | 70.3 | 65.3 | 73.8 | 3.5 |
| 6 | 69.3 | 64.5 | 71.1 | 1.8 |
| 7 | 69.6 | 64.5 | 69.4 | -0.3 |
| 8 | 70.2 | 69.4 | 70.3 | 0.0 |
| 9 | 68.5 | 64.7 | 68.1 | -0.4 |
| 10 | 68.1 | 65.5 | 67.4 | -0.7 |
| 11 | 65.9 | 65.4 | 63.1 | -2.8 |
| 12 | 66.7 | 65.4 | 63.5 | -3.2 |
| 13 | 68.9 | 68.1 | 67.1 | -1.9 |
| 14 | 66.1 | 65.5 | 63.9 | -2.2 |
| 15 | 67.1 | 65.6 | 64.3 | -2.8 |
| 16 | 68.1 | 65.0 | 66.9 | -1.2 |
| 17 | 69.1 | 65.0 | 68.0 | -1.1 |
| 18 | 69.4 | 67.8 | 69.2 | -0.3 |
| 19 | 68.0 | 65.3 | 68.0 | 0.0 |
| 20 | 67.9 | 65.4 | 67.6 | -0.3 |
| 21 | 66.9 | 65.6 | 67.7 | 0.8 |
| 22 | 67.5 | 65.6 | 67.3 | -0.2 |
| 23 | 68.1 | 68.5 | 68.6 | 0.5 |
| 24 | 66.5 | 65.9 | 67.2 | 0.7 |
| 25 | 66.6 | 65.9 | 66.9 | 0.3 |
| 26 | 66.6 | 64.5 | 63.4 | -3.2 |
| 27 | 67.6 | 64.6 | 64.8 | -2.8 |
| 28 | 67.9 | 66.7 | 66.6 | -1.3 |
| 29 | 66.2 | 64.8 | 65.4 | -0.8 |
| 30 | 66.4 | 65.0 | 65.3 | -1.1 |
| | | | Avg. Difference | -0.7 |

All sound levels are in units of dBA

## DAYTON OVERLAP GAP CALIBRATED RESULTS

| | | GAP | | |
|---|---|---|---|---|
| Mic. # | Field Measurements | Single Barrier | Overlap Barrier | Overlap - Field |
| 1 | 76.0 | 68.8 | 75.2 | -0.8 |
| 2 | 74.6 | 70.1 | 74.5 | -0.1 |
| 3 | 73.1 | 68.4 | 73.8 | 0.7 |
| 4 | 73.3 | 70.4 | 73.8 | 0.5 |
| 5 | 71.8 | 70.6 | 73.3 | 1.5 |
| 6 | 69.7 | 69.0 | 70.1 | 0.4 |
| 7 | 68.3 | 67.6 | 68.8 | 0.5 |
| 8 | 67.8 | 66.9 | 68.0 | 0.2 |
| 9 | 68.2 | 69.0 | 68.6 | 0.4 |
| 10 | 67.8 | 68.7 | 68.0 | 0.2 |
| 11 | 64.3 | 69.9 | 66.7 | 2.4 |
| 12 | 63.7 | 69.8 | 67.3 | 3.6 |
| 13 | 64.4 | 69.9 | 67.6 | 3.2 |
| 14 | 66.2 | 69.9 | 67.8 | 1.6 |
| 15 | 65.5 | 69.6 | 67.6 | 2.1 |
| 16 | 66.9 | 69.3 | 66.7 | -0.2 |
| 17 | 67.1 | 69.3 | 67.5 | 0.4 |
| 18 | 66.8 | 68.8 | 67.5 | 0.7 |
| 19 | 67.3 | 69.0 | 68.0 | 0.7 |
| 20 | 68.0 | 69.2 | 68.3 | 0.3 |
| 21 | 64.1 | 68.7 | 65.8 | 1.7 |
| 22 | 64.0 | 68.6 | 66.1 | 2.1 |
| 23 | 64.6 | 68.7 | 66.3 | 1.7 |
| 24 | 65.0 | 68.7 | 66.5 | 1.5 |
| 25 | 65.2 | 68.5 | 66.4 | 1.2 |
| 26 | 65.4 | 68.7 | 65.6 | 0.2 |
| 27 | 66.1 | 69.0 | 66.4 | 0.3 |
| 28 | 65.9 | 68.6 | 66.2 | 0.3 |
| 29 | 66.7 | 68.8 | 66.6 | -0.1 |
| 30 | 67.2 | 68.9 | 66.8 | -0.4 |
| | | | Avg. Difference | 0.9 |

All sound levels are in units of dBA

# APPENDIX H

# ABSORPTIVE BARRIER TESTING

## SITE GEOMETRY FOR CALIFORNIA OVERLAP GAP (ABSORPTIVE)

Noise Barriers

| Barrier | X1 (m) | Y1 (m) | X2 (m) | Y2 (m) | Bottom Elevation (m) | Top Elevation (m) |
|---|---|---|---|---|---|---|
| Single | 1500 | 2000 | 2500 | 2000 | 200 | 205.5 |
| Far | 1500 | 2000 | 2000 | 2000 | 200 | 205.5 |
| Near | 1992.7 | 1997 | 2500 | 1997 | 200 | 205.5 |

Overlap Length: 7.32 m
Overlap Width: 3.05 m

| Roadway | X1 (m) | Y1 (m) | X2 (m) | Y2 (m) | Elevation (m) |
|---|---|---|---|---|---|
| 1 | 1500 | 2007.3 | 2500 | 2007.3 | 200 |
| 2 | 1500 | 2011.0 | 2500 | 2011.0 | 200 |
| 3 | 1500 | 2014.6 | 2500 | 2014.6 | 200 |
| 4 | 1500 | 2018.3 | 2500 | 2018.3 | 200 |
| 5 | 1500 | 2029.3 | 2500 | 2029.3 | 200 |
| 6 | 1500 | 2032.9 | 2500 | 2032.9 | 200 |
| 7 | 1500 | 2036.6 | 2500 | 2036.6 | 200 |
| 8 | 1500 | 2040.2 | 2500 | 2040.2 | 200 |

Receivers

| Receiver | X (m) | Y (m) | Elevation (m) |
|---|---|---|---|
| 1 | 1982.6 | 1994.5 | 201.5 |
| 2 | 1982.6 | 1994.5 | 204.6 |
| 3 | 1990.2 | 1994.5 | 201.5 |

## TRAFFIC DATA FOR CALIFORNIA OVERLAP GAP (ABSORPTIVE)

| | | Volumes (veh/h) | | | Speeds (km/h) | | |
|---|---|---|---|---|---|---|---|
| Mic. # | Lane # | A | MT | HT | A | MT | HT |
| 1 - 3 | 1 | 797 | 40 | 15 | 57 | 57 | 57 |
| | 2 | 969 | 38 | 74 | 57 | 57 | 57 |
| | 3 | 686 | 29 | 7 | 57 | 57 | 57 |
| | 4 | 139 | 4 | 0 | 57 | 57 | 57 |
| | 5 | 357 | 8 | 1 | 57 | 57 | 57 |
| | 6 | 757 | 37 | 22 | 57 | 57 | 57 |
| | 7 | 702 | 55 | 97 | 57 | 57 | 57 |
| | 8 | 808 | 44 | 40 | 57 | 57 | 57 |

## CALIFORNIA OVERLAP GAP (ABSORPTIVE) RESULTS

**Before absorptive treatment**

| | | GAP | | |
|---|---|---|---|---|
| Mic. # | Field Measurements | Single Barrier | Overlap Barrier | Overlap - Field |
| 1 | 66.2 | 57.7 | 63.6 | -2.6 |
| 2 | 68.3 | 62.8 | 64.9 | -3.4 |
| 3 | 65.2 | 57.7 | 62.2 | -3.0 |
| | | | Avg. Difference | -3.0 |

All sound levels are in units of dBA

**After absorptive treatment (assume NRC=0.85)**

| | | GAP | | |
|---|---|---|---|---|
| Mic. # | Field Measurements | Single Barrier | Overlap Barrier | Overlap - Field |
| 1 | 63.0 | 57.7 | 60.7 | -2.3 |
| 2 | 64.4 | 62.8 | 63.0 | -1.4 |
| 3 | 61.9 | 57.7 | 55.6 | -6.3 |
| | | | Avg. Difference | -3.3 |

All sound levels are in units of dBA